Spring 2003

Factors Effecting Uptake and Visualization of Superparamagnetic Iron Oxide Particles by Macrophages: Relevance for Use in MRI Plaque Imaging

Walter John Rogers

Factors Effecting Uptake and Visualization of Superparamagnetic Iron Oxide Particles by Macrophages: Relevance for Use in MRI Plaque Imaging

A Dissertation presented to the Bayer School of Natural and Environmental Sciences of Duquesne University

As partial fulfillment of the requirements
for the degree of Doctor of Philosophy

by

Walter John Rogers

March 5, 2003

Abstract

Cardiovascular disease kills nearly 1 million Americans each year. While treatment at all levels has made significant advances over the past 3 decades, diagnosis is still limited to structural or hemodynamic changes associated with advanced disease. More than 60% of myocardial infarctions (MI) result from the rupture and associated acute thrombosis of atherosclerotic plaque that reduce lumen size by less that 50%. Ultra small superparamagnetic iron oxide particles (USPIO) have recently been proposed as a macrophage targeted magnetic resonance contrast agent. The goal of the present study was to determine if, and the extent to which, molecules known to alter macrophage metabolism significantly alter the extent to which USPIO's are internalized in these cells.

Murine macrophage cells (J774) known to be constitutively activated, were cultured in 8 well chamber slides. One group of 4 wells was treated for 24 hours with the test agent. Control and treated cells were then incubated for 4 hours with 0.0μL, 1.0 μL (11.2 μg Fe), 10.0 μL (112.0 μg Fe) and 100.0 μL (1.12 mg Fe) of stock USPIO (Feridex, Berlex labs). Cell density and iron uptake was quantified using spectral analysis of digital microscope images of fixed cells stained with acridine orange and counterstained with Prussian Blue.

Macrophage uptake of USPIO was significantly related to iron concentration (r^2= 0.992). However there was saturation of cell uptake at higher USPIO concentration. Uptake, (iron area/total image area) expressed as the percent, became significantly greater than background by 5 minutes (0.084$\pm$ 0.001% versus 0.045 $\pm$0.029%, p=0.028) and peaked at 4 hours. At low dose (10 and 20 ng/ml) Interleukin-4 did not affect cell uptake of USPIO. However at 40 ng/ml, IL-4 produced a significant increase in iron endocytosis at 1.12 mg Fe/ml (2-way ANOVA, p=0.032). Similarly, Human Interferon gamma (IFN-γ) had no effect at the 3 lower doses (10, 100, and 500 International Units (IU)/ml, corresponding to 0.5, 5.0, 25.0 and 50 ng/ml). Treatment with 1000 IU/ml resulted in an increase in cell uptake (2-way ANOVA, p=0.045).

To test the importance of serum proteins on endocytosis, a group of cells were cultured with and without 10% fetal bovine serum (FBS). Absence of FBS resulted in a substantial reduction in USPIO uptake ($p<0.001$). There was also a trend toward reduced cell density compared to control ($p=0.056$) which is likely the effect of the absence of growth factors in the FBS free cell cultures.

Cytochalsin-B depolarizes actin filaments within macrophage plasma membrane and thus inhibits membrane invagination and thus endocytosis. At a dose of 1.0 μg/ml it has been previously been shown to preferentially inhibit endocytosis of larger particles (> 300 nm) with little effect on small (< 300 nm). In the present study, USPIO uptake trended toward being reduced ($p=0.062$) indicating that although individual particle size was small (100-150 nm), the aggregation of these particles results in a larger effective size in terms of trans-membrane pathway.

The test USPIO was coated with a thin layer of dextran-10. The mannose receptor has broad affinity to polysaccharide moieties. To test the potential for this receptor to be involved in USPIO endocytosis the receptor was blocked with mannan. There was no significant inhibition of endocytosis ($p=0.188$) excluding this receptor as a major endocytotic pathway for the tested USPIO.

Both angiotensin converting enzyme inhibiting drugs and HMG-CoA reductase inhibiting medications are used widely for control of hypertension and lipid lowering therapy respectively. Cells were treated with Captopril at doses of 0.001, 0.01, 0.1 and 1.0mM. Even at the highest dose there was no difference between treated and control cells in terns of cell density or USPIO uptake. Treatment with the statin mevinolin resulted substantial inhibition of USPIO uptake at 1.0 and 17.5 μM ($p=0.004$ and $p<0.001$ respectively). In addition cell density was reduced at the higher dose compared to control ($p=0.033$) which is in agreement with this agents known macrophage anti-proliferative properties.

This study suggests that USPIO's enter macrophages via a number of different pathways including opsonification to serum proteins, scavenger receptors and fluid phase endocytosis. The effect of the actin blocking agent cytochalasin-B indicates that the size of USPIO aggregates rather than individual particles determine the rate of endocytosis.

Finally, these data provide evidence that substantial regulation of USPIO uptake occurs by both endogenous (cytokines) and exogenous agents (HMG Co-A reductase inhibitors). Mevinolin therapy may reduce the sensitivity for USPIO agents to detect the presence of macrophages in the vessel wall. Although it is beyond the scope of this study, it would be of interest to determine if mevinolin treated macrophages recover endocytotic capacity after treatment is withdrawn or whether the effect is permanent. If USPIO enhanced MRI can detect macrophage loss of function, and if this effect is related to inflammation or plaque stability, MRI could have a role in determining the effectiveness of statin as well as other drug therapies aimed at treating atherosclerotic disease.

Dedication

This thesis is dedicated to the memory of my parents.

Acknowledgements

I have been quite fortunate to have a number of true mentors and gifted associates during my training. Lewis Becker, MD, was my first, and perhaps most influential mentor at Johns Hopkins. His high standards for scientific investigation and enthusiastic guidance were invaluable. Myron Weisfeldt, MD provided a model for scientific inquiry, without bounds. Recruiting me into the cardiac MRI group at JHU established the direction of my academic career. His “hands on” leadership and vision are rare by any standards. While at Hopkins I had the good fortune to work with Edward Shapiro, MD. Together we learned the potential of MRI in cardiology. His gentleness and generosity will always be appreciated. I must thank James Weiss, MD for his positive encouragement through many revisions of many manuscripts. Elias Zerhouni and William Brody, PhD, MD, taught me the entrepreneurial side of research. Both showed genuine interest in seeing me succeed and went out of their way on countless occasions.

While at Allegheny General, I spent many enjoyable early and late hours working with Christopher Kramer, MD as we began applying MRI to “real” patients. I am grateful to Yong-Jian Geng, MD, PhD and Alana Majors, PhD for inviting me into their labs and providing mentorship while I began to “retrain” in Vascular Biology. I must acknowledge the personal support of Robert WW Biederman, MD. Dr. Biederman is a rare classical scientist. I thank him for countless discussions on topics of medicine, philosophy and world history. I must express special appreciation to the faculty at Duquesne University Department of Chemistry and Biochemistry for accepting me into their program after the bankruptcy at MCP-Hahnemann closed my program. They have gone out of their way to make me feel part of their school. Finally, I must thank my wife Peggy and my children Brittany and Andrew for their support over many years and locations of my graduate studies.

Table of Contents

Chapter V

Discussion

List of Figures

List of Tables

Acronyms

(listed in order of occurrence)

MI : myocardial infarction

(U)SPIO : (ultra-small) superparamagnetic iron oxide

IL : interleuken

IFN-γ : interferon gamma

FBS : fetal bovine serum

HMG-CoA : 3-hydroxy-3-methyl-glutaryl coenzyme reductase

MR(I) : magnetic resonance (imaging)

VCAM-1 : vascular cell adhesion molecule-1

MCP-1 : monocyte chemoattractant protein-1

M-CSF : macrophage-colony stimulating factor

oxLDL : oxidized low density lipoprotein

TNF-α : tumor necrosis factor-α

TGF-β : transforming factor-β

FGF : fibroblast growth factor

PDGF : platelet-derived growth factor

MMP: matrix metalloproteinase

tPA : tissue plasminogen activator

uPA : urokinase plasminogen activator

Fc : (crystallizable) fragment

IgE : immunoglobulin E

B_0 : static magnetic field

γ : gyromagnetic ratio

T : tesla (10,000 gauss)

rf : radio frequency

T1 : longitudinal magnetic relaxation time

T2 : transverse relaxation time

Gd-DTPA : gadolinium (III)-diethyltriaminepentaacetic acid

MION : monocrystalline iron oxide

MSM : starch coated iron oxide

DSM : crosslinked starch-coated iron oxide

FTIS : fourier transform infrared spectroscopy

XPS : x-ray photelectronic spectroscopy

SSIMS : static secondary iron mass spectroscopy

EMU : electromagnetic units

RES : reticuloendothelial system

MHC : major histocompatibility complex

NO : nitrous oxide

iNOS: inducible nitrous oxide synthase

ScR : scavenger receptor

LOX : lectin-like receptor

mRNA : messenger ribonucleic acid

AcLDL : acetylated low density lipoprotein

WHHL : Watanabe hereditable hyperlipidemic

RAM-11 : anti-rabbit monocyte/macrophage antibody

EDTA : Ethylenediamine Tetraacetic Acid

PBS : phosphate buffered saline

DMEM : Dulbecco's modified Eagle's medium

GE : general electric

ANOVA : analysis of variance

TR : time to repetition

TE : time to echo

SE : spin echo

TI : time to inversion

FSE : fast spin echo

R : regression

DF : degrees of freedom

SS : sum of squares

MS : mean square

NS : non-significant P-value

Introduction

Macrophages as Markers of Atherosclerosis

Until recently atherosclerosis was considered a bland lipid storage disease. Data from basic research, pathologic analysis and clinical epidemiological studies have shown that atherosclerosis is intrinsically an inflammatory disease[1,2]. As such, the initiation and progression of this disease are controlled by immune response mechanisms[3] In general, inflammation is a defense reaction caused by tissue damage, or infection, characterized by redness, heat, swelling, and pain. The primary objective of inflammation is to localize and eradicate the irritant and repair the surrounding tissue. For the survival of the host, inflammation is a necessary and beneficial process. The inflammatory response involves three major stages: first, dilation of capillaries to increase blood flow; second, microvascular structural changes and escape of plasma proteins from the bloodstream; and third, leukocyte transmigration through endothelium and accumulation at the site of injury. It is this normal response to injury which initiates the atherosclerotic cascade within the vessel wall. Normal vascular endothelium does not support binding of leukocytes (including monocytes). However regardless of the form of “injury (hyperlipidemia[4], hypertension[5] , even low laminar sheer stress[6]) endothelial cells begin to express adhesion molecules, such as vascular cell adhesion molecule-1 (VCAM-1) that bind to various classes of leukocytes initiating the capture of monocytes and T-lymphocytes as shown in figure 1[7] Once attached to the endothelium, leukocytes migrate across

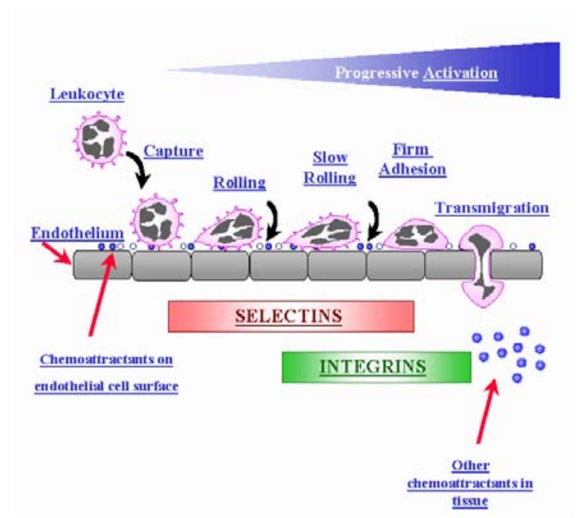

Figure 1: Cartoon illustrating leukocyte adhesion and endothelial transmigration.

endothelium if an exogenous chemo-attractant is present within the intima. Chemoattractant cytokines or chemokines are small disulphide-linked polypeptides, typically of 60–70 amino acids in length, and are potent chemoattractants for leukocytes such as T cells, natural killer (NK) cells, monocytes and macrophages.[8] Monocyte chemo-attractant protein-1 (MCP-1) is one member of this family[9]. Chemokines mediate their effects via interaction with specific chemokine receptors expressed on a wide range of cell types. Binding of a chemokine to its specific receptor on the cell surface leads to the generation of an intracellular signal via a $G\alpha_I$-containing G-protein complex and this results in cell chemotaxis towards the source of the chemokine. Thus the entry of monocytes into the vessel wall depends on the interaction between adhesion molecules on the surface of endothelial cells and their counter ligands on monocytes. Once resident in the arterial wall, the blood-derived inflammatory cells participate in and perpetuate a local inflammatory response. Monocyte differentiation into macrophages is achieved by MCP-1, and macrophage colony-stimulating factor[10] (M-CSF). Macrophage activation and the accompanying phenotypic change in function is achieved through scavenger receptors by oxidized lipoproteins (oxLDL) [11]

About 50% of infants in the first 6 months of life have regions within the coronary arteries containing lipids and macrophages[12]. It is unclear whether these regions represent pre-atheroma and will go on to produce overt atherosclerotic lesions. Lesion progression may result in multiple morphologies [13] [14] and advanced lesions vary with respect to the proportion of lipids, thrombus, calcium and connective tissue. However inflammatory cells including macrophages are present in all lesions. Thus macrophages provide both a sensitive (in that they are present in very early lesions) as well as specific (they are not found in normal vessel wall) marker for atherosclerosis.

Macrophage Biology

Macrophages are derived from bone marrow stem cells (promonocytes and promyelocytes). These precursor cells have little synthetic capacity and are not capable of cell division. They make up about 2-10% of the peripheral white blood cells. They have a mean diameter of 15-20 μm. After they are released into the blood as monocytes they may circulate for 1-2 days prior to migrating into tissues and differentiating into macrophages. Macrophages can survive for months within the tissue. Macrophages express different phenotypes including differences in phagocytic capacity and cytokine production and surface receptor expression based of the stimulus provided by the surrounding tissue. Macrophages are responsible for tissue remodeling during development and wound repair. They produce numerous cytokines, growth factors and proteases that aid the remodeling of the extravascular matrix and stimulate the recruitment of other cell types such as fibroblasts and smooth muscle cells. Again the mechanisms that are appropriate for wound healing have detrimental effects when they occur within the vascular media. Key cytokines produced by macrophages include interleukin 1β (IL-1β), tumor necrosis factor-α (TNF-α), IL-10, IL-12 and transforming factor β (TGF-β)[15]. Macrophage-derived growth factors that have significant effect on the progression of atherosclerosis include fibroblast growth factors (FGF's), platelet-derived growth factors (PDGF), which is a potent stimulator of smooth muscle cell growth, migration and differentiation. In addition to these processes which have the effect of initiating vessel wall thickening and stimulating a fibrotic, synthetic stimulus in smooth muscle cells, macrophages also secrete other materials which degrade and weaken the extravascular matrix within the forming fibrous plaque. Specifically, members of the matrix metalloproteinase (MMP) family of zinc-containing endopeptidases. Histochemical and genetic studies have shown an association of MMP-1, MMP-2, MMP-3 and MMP-9 in destabilization of atherosclerotic plaque[16], [17]. Activated macrophages also secrete tissue plasminogen activator (tPA) and urokinase plasminogen activator (uPA). Both of these products act to degrade fibrin and are thus involved in natural blood clot dissolution[18].

Mechanisms of Endocytosis in Macrophages

Macrophages have evolved a number of mechanisms to internalize particles [19] and solutes[46]. The 2 major methods are phagocytosis and endocytosis. Endocytosis has 2 subgroups: fluid phase pinocytosis which does not involve surface receptors and, receptor-mediated endocytosis [20]. Pinocytosis usually refers to the uptake of fluids and solutes by small vesicles (≤ 150 nm) and in some cases is a constitutive process. Receptor-mediated endocytosis [21] is the specific process by which macromolecules, viruses and small particles enter cells. Both pinocytosis and receptor mediated endocytosis use a clathrin-based mechanism and usually occur independently of actin polymerization. Phagocytosis involves the uptake of large particles (>0.5 µm) by means of an actin-dependent mechanism. Feridex, the iron particle under investigation in the present study has an individual size of about 100 nm

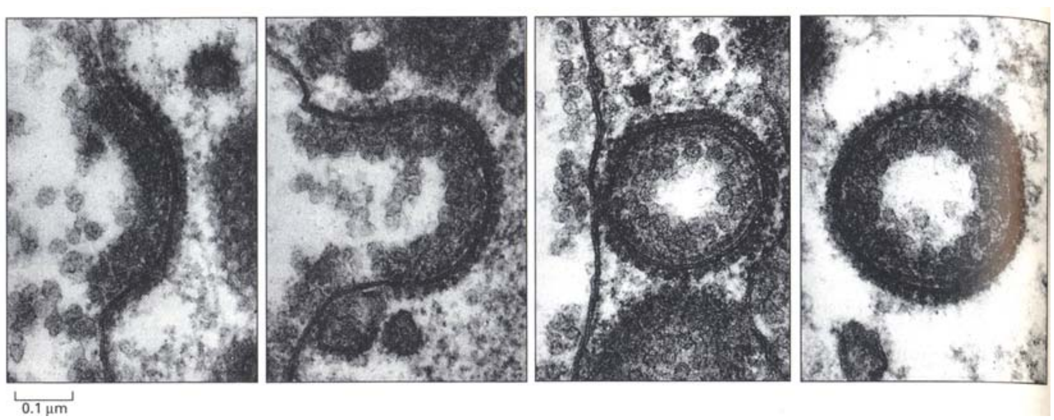

Figure 2: Electron micrograph showing stages of endocytosis from receptor migration to vescicle formation and separation. (from Endocytosis, edited by Ira Pastan and Mark Willingham, Plenum Press, 1985.)

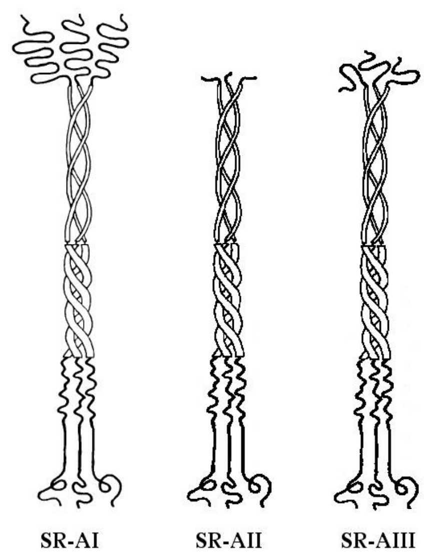

Figure 3: Structure of 3 members of the class A scavenger receptor family. From web page of Dr. Siamon Gordon, dunn1.path.ox.ac.uk/~cholt/sgMSR.html)

but is usually found as aggregates of multiple particles. The above electron micrograph (figure 2) shows the process of endocytosis. Whether ingesting fluid, small particles or larger particles, the endocytotic part of the cycle usually begins at specialized regions of the plasma membrane called clathrin-coated pits, which occupy about 2% of the total membrane surface area. Clathrin-coated pits are rapidly endocytosed, with a life-time of about 1 minute. This constitutive, but regulated, vesicle formation is one method by which the surrounding environment is sampled, and will likely be one route by which Feridex particles are internalized. Clatherin is a fibrous protein containing a heavy chain (180,00 mw) and several light chains (20,000-40,000 mw). These molecules form a cage-like lattice around the entire vesicle. The purified protein is a triskeleton; a three armed trimer. When polymerized, the coated pit becomes a coated vesicle and pinches off into the cytoplasm.

In addition to constitutive pinocytosis, macrophages have a mechanism for recognizing specific cell surface structure and thereby concentrating extracellular molecules via the clathrin-coated pits. Trans-membrane proteins concentrated in the coated pits include Scavenger (the structure of 3 variations is shown in figure 3[22]), mannose, compliment and receptors for the Fc-portion of immunoglobulin IgG (Fc-receptors). Scavenger receptors are defined by their ability to endocytose modified forms of low density lipoprotein (LDL). This class of receptors was first described by Goldstein and Brown in 1979[23]. In contrast to receptor-mediated endocytosis of unmodified LDL, which is regulated via a concentration dependent negative feedback system, scavenger receptors internalize modified LDL's without regulation and result in creation of foam cells containing large amounts of cholesterol. At least eight macrophage expressed scavenger receptors have been identified using molecular cloning. They differ in structure, and can internalize a broad range of ligands. There is great diversity as to the receptor recognized ligands and include toxins and lectins, viruses, proteins and antibodies such as transferrin, LDL, and IgE. Also hormones and growth factors are internalized via receptor-mediated endocytosis including insulin, glucagons, and platelet derived growth hormone.[24]

Magnetic Resonance Imaging

While magnetic resonance imaging (MRI) is a relatively recent development (introduced by Paul Lauterbur in 1973), the spectroscopic method upon which it is based was discovered in 1946. It is important to appreciate that the physical and biochemical structure information is still available using the MRI technique.

When certain nuclei are placed in a static magnetic field (designated B_0) they have, under proper conditions, the ability to absorb and reradiate electromagnetic energy. This "resonance" characteristic is the basis for signals generated in nuclear magnetic resonance spectroscopy and imaging. In order for the nuclei to interact with the magnetic field they themselves behave as small bar magnets. This property is limited to nuclei with an odd number of neutrons and protons defined as "spin". "Spin" is a fundamental property of nature like electrical charge or mass. Spin comes in multiples of 1/2 and can be + or -. Protons, electrons, and neutrons possess spin. Individual unpaired electrons, protons, and neutrons each possesses a spin of 1/2. In nuclear magnetic resonance, it is unpaired nuclear spins that are of importance. There are numerous elements in the periodic table that meet the basic requirements for investigation using magnetic resonance. However only a limited group exist in biological systems in sufficient abundance to permit detection. The table below lists the 7 most commonly investigated nuclei. The precession (Larmor) frequency is given as $\gamma B_0/2\pi$. Where the gyromagnetc ratio (γ) is the constant associated with a given nuclei. B_0 is the static magnetic field strength and is expressed as MHz/T where T is Tesla equivalent to a magnetic field of 10,000 gauss.

Table 1: List of 7 common nuclei used in magnetic resonance.

NUCLEI	UNPAIRED PROTONS	UNPAIRED NEUTRONS	NET SPIN	γ(MHZ/T)
^1H	1	0	1/2	42.58
^2H	1	1	1	6.54

^{31}P	0	1	1/2	17.25
^{23}Na	0	1	3/2	11.27
^{14}N	1	1	1	3.08
^{13}C	0	1	1/2	10.71
^{19}F	0	1	1/2	40.08

Due to the high concentration of hydrogen protons in biological structures, clinical imaging is nearly exclusively based on the hydrogen nuclei. In the magnetic field, the nuclei align with the magnetic field. Due to their gyroscopic properties, the spins rotate or precess around their axis and around the direction B_0 at a small off axis angle. Based on a net spin value of ½, hydrogen can exist in 2 energy states ½ and –½. By adding energy at the resonant or Larmor frequency, spins may transition from the low to high energy state. Energy is released into the local environment when they return to the low energy state. It is the efficiency with which this energy can be released and the local nuclei concentration that determines image contrast in acquired image data.

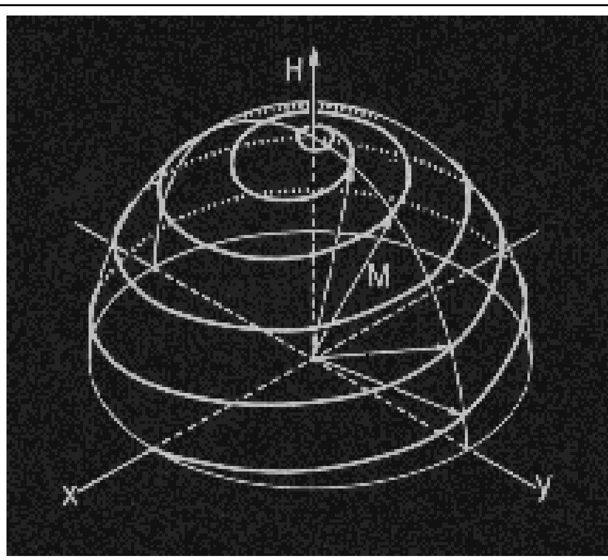

Figure 4: Schematic displaying 3D relaxation trajectory for the net magnetization vector (M).

The standard notation for displaying the net magnetic vector under investigation indicates the direction of the B_0 field along the +z-direction (designated *H* in figure 4), and the direction of the net magnetization vector (*M*) at equilibrium also in the +z-direction. Radio-frequency (rf) energy applied to the system results in rotation of *M* into the x-y plane or into the –z direction. Figure 4 displays the vectors trajectory after application of sufficient rf energy (at the Larmor frequency) to rotate the vector into the x-y plane. Two components of “relaxation” to equilibrium exist. Immediately after the rf is applied (then turned off), the vector is rotated into the x-y plane and does not contain a z-component. Relaxation results in progressive return of the z-component and rotation around the z–axis. The rate of longitudinal component recovery is designated T1. T1 depends on how efficiently energy is transferred from the resonant nuclei to the rest of the lattice via random thermal collisions between the molecules. The vector displayed in figure 4 is made up of individual vectors that will have different rates of relaxation depending on their local environment (i.e. water versus lipids). Immediately after the rf pulse they are all in the same x-y position but rapidly move out-of-phase. T2 is a measure of the rate of decay of coherence among nuclei.

Table 2: comparison of T1 and T2 relaxation times for biological tissues at 0.5T and 1.5T

Tissue	T2 (msec)	T1(msec) at 0.5T	T1(msec) at 1.5T
Adipose	80	210	260
Liver	42	350	500
Muscle	45	550	870
White Matter	90	500	780
Grey Matter	100	650	920
CSF	160	1800	2400

The above table shows the difference in T1 and T2 among different tissues. It can also be seen that T1 is field strength dependent and increases with increasing B_0. T2 is independent of B_0.

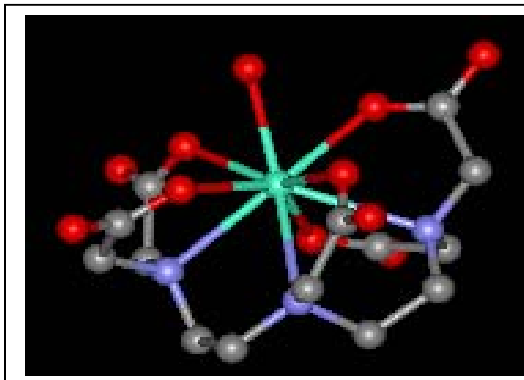

Figure 5: Chemical structure of the most common clinically used contrast agent: Gd-DTPA

MRI Contrast Agents

Effective MRI contrast agent fall into 3 general classes: 1) *Relaxation rate enhancers* (T1 and, or T2); 2) *Resonant frequency shift agents*, or 3) *Magnetic susceptibility agents*, in such a way as to result in an observable change in local signal when imaged with the appropriate pulse sequence. The contrast agent most widely used in MRI is a low molecular weight gadolinium agent. Figure 5[25] displays the superimposition of minimized crystal structures (green) and the Genetic Algorithm predicted conformation (magenta). Gadolinium was discovered by J. C. G. de Marignac in 1880, who named the metal for Finnish geologist, J. Gadolin. This agent is a relaxation agent and is distributed primarily by blood flow alone providing no information regarding inflammation or the distribution of specific cell types.

Metal ions such as Dy^{3+}, Ho^{3+} and Eu^{2+} have significant unpaired electron spins, rapid electron spin relaxation characteristics and exhibit little effect of relaxation properties but result in a substantial shift of resonant frequency.

There are a number of iron oxide particles undergoing phase II or III clinical trials. There is but a single iron agent approved by the FDA. It is approved for use as a liver MRI contrast agent and marketed under the trade name Feridex (Berlex labs, Wayne NJ). While the primary indication for these agents is a liver contrast agent, there are preliminary reports that they may identify sites of atherosclerosis by means of labeling macrophages. In that these iron agents represent a "process specific" contrast agent, it is critical that macrophages be characterized regarding endocytotic route, (i.e. is this a receptor mediated phagocytosis?) and factors regulating the extent and rate of particle phagocytosis. If uptake of particles varies significantly based on endogenous and or exogenous factors, interpretation of MR images produced after particle administration must take this into account.

Mechanism of Magnetic Resonance Signal Alteration by Iron Oxide

Table 3 adapted from "Principles of MRI Contrast Enhancement" R.C. Brasch [26] shows electron sub-shell configurations for first-transition-series ions with corresponding spin quantum numbers. Generally the greater the number of

Table 3: Electron sub-shell configurations for transition metals with potential for use as MRI contrast agents

Transition Series	Electron Subshell	Spin Maximum
VO^{+2}	$3d^1$	1/2
Ti^{+2}	$3d^2$	1
Cr^{+3}	$3d^3$	3/2
Cr^{+2}, Mn^{+3}	$3d^4$	2
Mn^{+2}, $\mathbf{Fe^{+3}}$	$3d^5$	5/2
$\mathbf{Fe^{+2}}$, Co^{+3}	$3d^6$	2
Co^{+2}, Ni^{+3}	$3d^7$	3/2
Ni^{+2}, Cu^{+3}	$3d^8$	1
Cu^{+2}	$3d^9$	1/2

unpaired electrons the stronger the paramagnetic behavior and the greater the T1 and T2 shortening effect. In addition, the distance between the paramagnetic center and the protons affected, the tumbling motions of the paramagnet and the protons, and the rate of electron spin relaxation all combine to define the degree of T1 and T2 shortening and the final effect on signal [27].

These metal ions reversibly bind a number of water molecules in their inner hydration sphere and exert their relaxivity effect. Unpaired electrons have magnetic dipoles that respond to an external magnetic field much the same way as a bar magnet. Paramagnetisim is characterized by the independent action of individual molecular magnetic moments. Feridex contains Fe^{3+} and Fe^{2+} in a 2:1 ratio. Fe^{3+} contains 5 unpaired electrons. The general formula is $Fe^{3+}O_3Fe^{2+}O$.

Superparamagnetism can arise if the crystal containing regions of unpaired spins is sufficiently large that it can be considered as a thermodynamically independent, single-domain particle [28]. Such a particle has a net magnetic dipole that is large or larger, compared to the sum of its individual unpaired electrons.

The T1 and T2 shortening arises as a consequence of interactions between the unpaired electrons of the para or superparamagnetic species and the hydrogen nuclei of water molecules. These interactions result in transfer of energy from the water molecules to their surrounding environment.

Table 4: Current iron particles under investigation for use in MRI

Specific Iron Particle	**Diameter**
Monocrystalline iron oxide (MION)	overall:21 nm, core: 4-5 nm
Superparamagnetic iron oxide particles	72 nm
Magnetite albumin	1-5 μm
Ultra Small Particles of Iron Oxide	18 nm
Dextran coated Fe^3O^4 (Feridex)	27-30 nm
Starch coated iron oxide (MSM)	0.1-0.5 μm
Crosslinked starch coated iron oxide (DSM)	1.0-1.8 μm

<u>Description of specific particle</u>

The specific material used in this study is sold under the brand name Feridex and marketed by Berlex laboratories. It is packaged as a sterile aqueous colloid of superparamagnetic iron oxide associated with dextran. Chemically Feridex is a

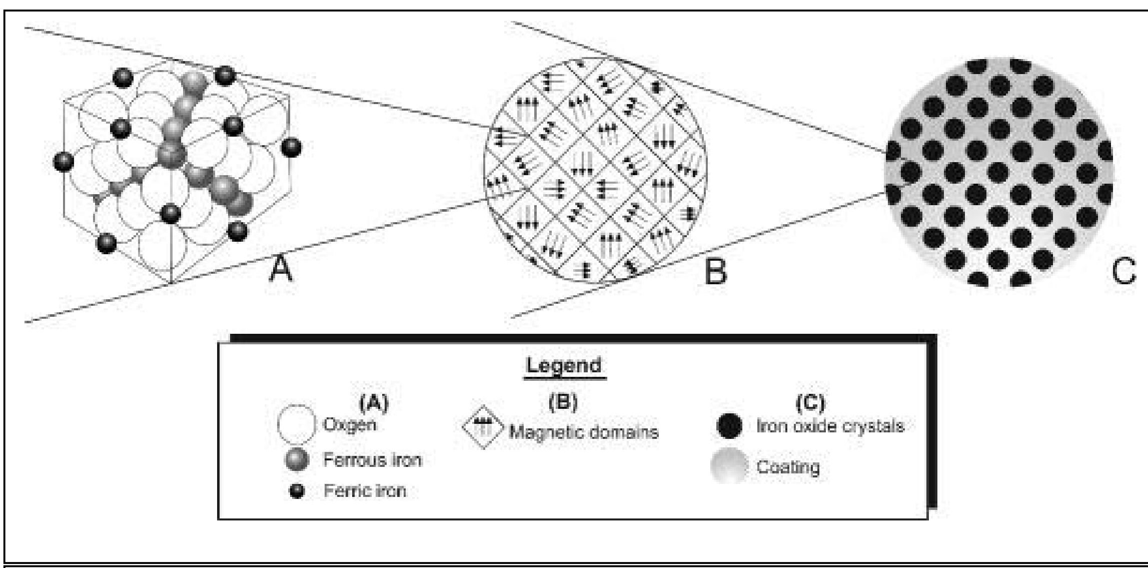

Figure 6 : Scematic representation of (A) crystal structure for SPIO, (B) presence of multiple random magnetic domains within crystal, (C) SPIO particle with multiple crystals in black and coating in grey.

Once internalized into a macrophage, particles follow an intracellular transport pathway from endosomes to lysosomes. Thus particles are exposed to a gradually decreasing pH as low as 4.5.[32] In order to determine the eventual biological fate of injected iron nanoparticles, Skotland et al.[33] tested the effect of incubating iron nanoparticles at a pH of 4.5 to 5.0 in the presence of dicarboxylic acid citrate to determine if iron particles are solubilized. At a pH of 4.5 iron was fully solubilized by 10 days. In less acidic environments this time increased significantly to 22 days at a pH of 5.0. In the same study, distribution of ^{59}Fe particles was distributed 73% in the liver, 18% in the bone marrow and 5% in the spleen of rats 8 hours after administration. It was postulated that after iron is solubilized in the lysosome it traverses the cytosol, eventually making it to the mitochondria where it is used for heme synthesis.

Surface Properties of Feridex Material

In addition to size and particle charge, the properties of the coating on the iron oxide particles will influence the mode and extent of uptake by macrophages and other phagocytic cells. Jung [34] compared SPIO colloids consisting of nonstoichiometric magnetite crystalline cores coated with dextran T-10 (brand name Feridex, of the class ferumoxides), Ferumoxtran (also coated with T-10 dextran but using a different method and ferumoxsil (coated with siloxane). Review will be limited to ferumoxides (Feridex).

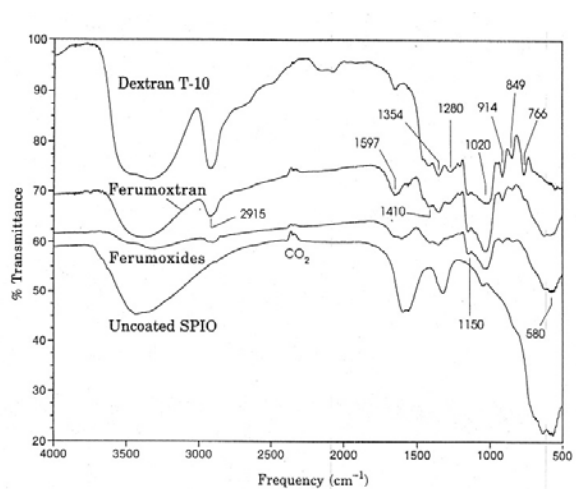

Figure 7: Fourier Transform Infrared Spectroscopy of Feridex showing presence of adsorbed Dextran-10

In the work by Jung et al.[34] Fourier transform infrared spectroscopy (FTIS) was measured with different nonoparticle types mixed with KBr, ground with an agate mortar and pestle and dried for 1 hour at 110 degrees C. Spectra were acquired over the range of 400 to 4000 $^{-1}$

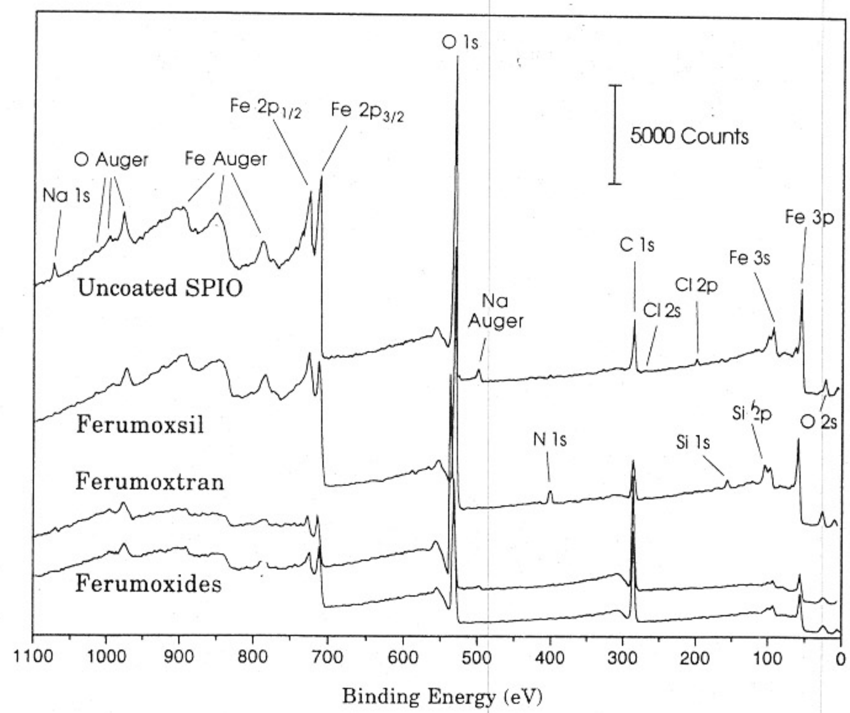

Figure 8: X-ray Photoelectronic Spectroscopy of Feridex showing x-ray attenuation (750-1000 eV) associated with surface layers of dextran

cm. All spectra were ratioed against KBr. Figure 7 shows a graph of the spectra plotting % Transmission versus Frequency. Spectra were displayed vertically for clarity. For comparison, spectra from uncoated particles and pure dextran T-10 are included.

Wavelength specific "bands" showed the presence of adsorbed dextran T-10. Bands of reduced transmission (ferumoxide) at ≈ 3400 cm^{-1} and ≈ 1600 cm^{-1} resulted from νO-H stretching and deformation modes of dextran hydroxyl groups and physisorbed water. νC-H and δC-H vibrational modes are seen as dips in the %transmission at ≈ 2900 cm^{-1} and 1250-1460 cm^{-1}. νC-O vibrations are seen as regions of reduced transmission at ≈ 1040-1150 cm^{-1}.

X-ray photoelectric spectroscopy (XPS) was used to determine the surface element composition of the nanoparticles. Based on the spectral data (Figure 8), the mole percent of each studied element was determined. The table 5 was generated from data reported by CW Jung[34].

The large attenuation of the iron peaks (750-1000 eV) is caused by the presence of layers of adsorbed dextran on the nanoparticle surface. Fe peaks can be seen clearly in the spectra of the uncoated sample. Jung states that the slightly more pronounced iron peaks seen in the ferumoxides (Feridex) than in the spectra of the ferumoxtran suggestive of a thinner dextran coating on Feridex.

Table 5 : Calculated surface composition based on chemical structure

Peak	E_b (eV)	Area (%)	Surface (%)	Comment
Fe	712.08	28.7	-	
$2p_{3/2}$	710.00	64.1	6.6	Fe(III)-O
	708.30	7.2	0.5	Fe(II)-O
O, 1s	533.64	2.6	1.3	RCOO/C=O
	532.48	49.3	24.2	Dextran—C-O
	-	-	-	
	531.23	11.1	5.4	
	-	-	-	
	529.82	37.0	18.2	Fe-O2-
	-	-	-	
C, 1s	288.65	3.9	1.7	RCOO/C=O
	287.45	14.0	6.1	Dextran-O-C-O
	-	-	-	
	286.05	57.7	25.2	Dextran-C-O
	284.60	24.3	10.6	Alkly C

710 eV binding energies of the Fe $2p_{3/2}$ photoelectrons are consistent with Fe^{3+} oxides (Figure 7, Table 5). There is also a weaker signal at 708 eV which is likely due to Fe^{2+} iron. The major component of the carbon 1s spectrum (286.1 eV) for the studied nanoparticles is attributable to the CHOH groups of the dextran. In principle, the reduction of x-ray peak intensities can be used to estimate the thickness (*d*) of the dextran coating. Based on the relationship:

$$d = n\,\lambda\cos\theta$$

Where λ is the photoelectron inelastic mean free path

θ is the electron takeoff angle

n is based on the photoelectron escape depth

Using a value of 3nm for λ, and 2 for *n*, a 3.3 nm thickness dextran coating in Feridex was estimated. Dextran T-10 has a mass averaged molecular weight of 9400. It is produced by Leuconostoc mesenteroides strain B512. It is 95% linear and due to multiple attachment sites to the iron oxide surface, its length of about 22 nm yields a 3.3 nm coating thickness (figure 9). This results in a predicted diameter significantly less than that determined by light scattering methods. Photon Correlation Spectroscopy (PCS) is a dynamic light scattering technique used to investigate dynamical properties of materials. The basic idea is to send in laser light with well defined properties (wavelength, polarization etc.) into a sample and investigate the properties of light scattered by the sample. With PCS the dynamical behavior, i.e. the auto correlation function, is directly obtained in the time domain. In dynamic light scattering experiments, the radius (R) of the particle is calculated from the diffusion coefficient (D) via the Stokes-Einstein equation, where *k* is the Boltzmann constant, T is the temperature, h is the solvent viscosity, and f = 6phR is the frictional coefficient for a compact sphere in a viscous medium. [35]

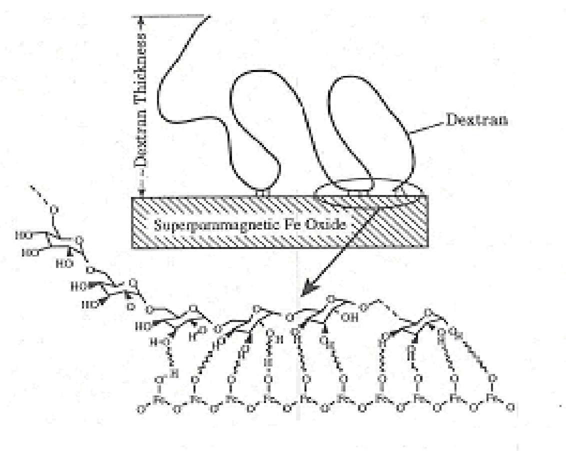

Figure 9: Model of dextran microstructure at iron oxide surface

$$D = \frac{kT}{f} = \frac{kT}{6\pi\eta R}$$

By definition then, the DLS measured radius is the radius of a hypothetical hard sphere that diffuses with the same speed as the particle under examination. This definition is somewhat problematic with regard to visualization however, since hypothetical hard spheres are non-existent. In practice, iron nanoparticles in solution are non-spherical, tend to aggregate and are dynamic (tumble), and solvated. As such, the radius calculated from the diffusional properties of a nonoparticle is indicative of the apparent size of the dynamic hydrated/solvated particle. Hence the terminology, ‘hydrodynamic’ radius. It must be stressed that aggregation results in a distribution of aggregate particle size, not individual particle size.

Static secondary ion mass spectroscopy (SSIMMS) is a very surface selective (<1 nm) method. Thus the presence of Fe-containing ions in the acquired spectra indicates that there is incomplete covering of the core iron particle by dextran. Further, the lack of dextran-Fe ionic fragments indicates the absence of a covalent bond between the dextran and iron oxide surface. Thus, the 3-5 nm dextran coating thickness reported by Jung is consistent with previous models of polymer coatings by Brant et al. [36] in which the dextran (figure 9) forms loops via focal interactions between the dextran chain and the iron oxide. The difference between the calculated dextran thickness calculated by XPS and light scattering measurements (the generally reported value for coated iron oxide particles) is due to variations in dextran hydration and conformation in aqueous solution (as is the case with light scattering measures) and solid state XPS measures. It was shown (Jung et al.[34]) that the dextran coating on Feridex is sparse and permits a greater degree of opsonification than other tested iron oxide nanoparticles.

<u>Bulk Chemical and Physical Properties of Feridex Material</u>

Superparamagnetic particles in the size range of Feridex have magnetic saturations between 5 and 90 electromagnetic units (EMU) per gram of oxide at 25ºC and lose more than 90% of their magnetism when an applied magnetic field is removed. Compared to gadolinium based contrast agents Fe compounds are more effective T1 and T2 relaxation agents. The following table is taken from the work of CW Jung et al. [37]

Table 6: Comparison of relaxivities between Feridex and Gd-DTPA

	Relaxivity $(mM\ s)^{-1}$	
Agent	**1/T1**	**1/T2**
Feridex	23.7±1.2	107±11
Gd-DTPA	4.5	5.7

Feridex provides a 5-fold increase in T1 relaxation and a nearly 18-fold increase in T2 relaxation as compared to gadolinium DTPA due to increased magnetic moment present in superparamagnetic materials.

Feridex Particle Size Distribution

The iron oxide used in the present study is in the form of a colloid with manitol and citrate. It has been previously shown that particle size is one of the determinants of macrophage uptake. However, the determination of "size" is not straightforward. Feridex contains groups of iron particles covered with low molecular weight dextran [38 39]. Polycrystalline aggregate size can be expressed in a variety of ways, depending on the characteristic of interest and the technique of determining it. The size of Feridex as well as other iron oxide particles is generally determined using commercial particle sizing instruments such as Coulter, Brookhaven, Malvern or Leeds & Northrop. All of these instruments measure particles based on the quasi-electric light scattering and work well with certified latex standards or any monodispersed particle. In more complex distributions, particularly with broad distributions of non-spherical particles (such as Feridex) these instruments may give quite different diameter values for the same sample based on the assumptions used or selection of mathematical techniques. Diameters may be expressed as [40]:

average diameter
number weighted average diameter
surface weighted average diameter
volume weighted average diameter
z-average diameter

Weighting factors applied to the numbers while averaging them include:

number
area
volume or mass
light scattering intensity

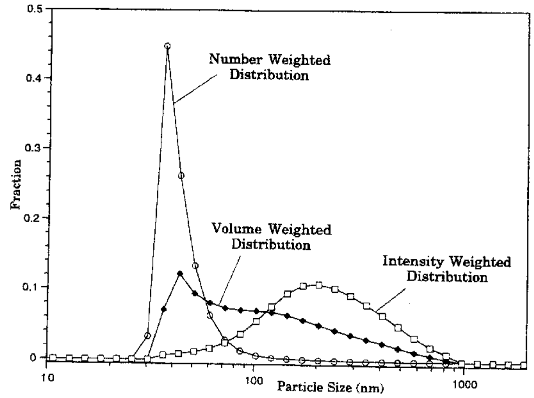

Figure 10: Particle size differences based on method of measurement

The most common method used to report particle size is that derived from light scattering techniques in which the average diameter expressed is the z-average diameter, derived as:

$$\frac{n_i d_i^6}{n_i d_i^5}$$

Because of the dependence on the sixth power of the physical diameter, it is very sensitive to larger particles and may result in significant differences between mean and mode values. The intensity of light scattered by a system of particles with diameter *d* is proportional to the number of particles *n*, the square of the particles mass m and a particle form factor P(Ø), which depends on size, scattering angle, index of refraction and wavelength. Figure 10 taken from Jung et al.[37] show the effect of size measurement method on the estimated size and size distribution of Feridex.

Dextran coated particles were developed in order to increase blood residence time before being taken up by the reticuloendothelial system (RES) including liver, spleen, lymph nodes, bone marrow and lung, as was the problem with previous larger ferromagnetic particles. Feridex, is larger than paramagnetic ions which have the problem of rapid metabolism in the target organ. For the present study, the sub-micron size is particularly important in that they can pass through the capillary network and endothelial cell spaces [41] to reach macrophages in the vascular media. However it should be understood that these particles form aggregates of multiple individual particles. This results in a wider range of effective size distribution.

Pinocytosis:

If soluble material cannot adhere to the surface of macrophages, it will be endocytosed in vitro via fluid-phase pinocytosis at the concentration that is present in the medium. If the material adheres to the cell's surface via its chemical properties (or via specific receptors [42 43 44]) it will be selectively concentrated at the macrophage surface and endocytosed by adsorptive pinocytosis [45].

Pratten et al [46] have shown that particle size, in addition to composition determines whether internalization will occur via "fluid-phase" endocytosis or phagocytosis. Particles ranging in size from 30 nm to 1100 nm were radiolabeled, and endocytotic index (microliter/10^6 cells per hour) measured with I-125 determined in the absence or presence of metabolic or cytoskeletal inhibitors. Rates of clearance (internalization) increased with increasing particle diameter. Particles of 30 nm diameter were endocytosed 10 times faster than a reference solute (polyvinylpyrrolidone, MW = 40k). Particles (polystyrene) of 100 nm diameter were endocytosed 100 times faster than the reference. It was concluded that there is no radical discontinuity between pinocytosis and phagocytic uptake, but the contribution of phagocytosis steadily increases with increasing particle size.

Using horseradish peroxidase, the nonspecific fluid-phase marker of endocytosis, Montaner et al [47] investigated the effect of T-cell cytokines IFN -γ, IL-4, IL-13 and IL-12 on fluid phase endocytosis in primary human macrophages. Mannan was used to block mannose-dependent receptor uptake. Incubation of cells with IL-4 or IL-13 resulted in an increased uptake of 200% when the mannose receptor was blocked, and 350% when it was not. This indicates a dual pathway of internalization of the horseradish peroxidase. IL-10 and IFN -

γ supressed uptake to < 25% of control. Macrophages were treated with test cytokines for 6 days and exposed to horseradish peroxidase for 60 min. Thus the normal constitutive fluid-phase uptake pathway is also regulated by macrophage activating cytokines and thus may alter uptake of iron oxide particles.

Receptor Mediated Endocytosis

The major difference with respect to phagocytic capacity and efficiency of "professional phagocytes" and the numerous other cells that have limited phagocytic capability is attributed to specialized phagocytic receptors.

Only limited work has been performed characterizing receptor-mediated endocytosis of iron oxide particles. Complement proteins present in serum, normally opsonize bacteria for phagocytosis by the C3b or C3bi receptors on macrophages. Moore et al [48] and Bogdanov [49] have shown evidence that monocrystalline iron oxide (MION) particles bind plasma proteins and are internalized by macrophages. MION particles were incubated with citrate diluted rat plasma for 4h at 37º C. Using Western blot analysis, they demonstrated that 4 major plasma proteins had been adsorbed including transferrin, fibrinogen, IgG and C3. Macrophage uptake of these proteins is via the transferrin-, Fc- , and C3- receptors respectively. They also found that the amount of surface bound dextran had a significant extent on the amount of plasma proteins bound to the iron particle. In a later study, the same group measured the macrophage uptake of opsonized, radiolabeled (I-125) MION particles in rat macrophages and glial cells. Mion was opsonized in undiluted plasma prior to incubation with isolated rat peritoneal macrophages. Serial concentrations of opsonized MION (0-25µg/ 150,000 cells) were incubated for 1h at 37 degrees. Cellular uptake in macrophages and murine glial cells (control) demonstrated preferential uptake of opsonized MION in both cell lines. Uptake of opsonized (macrophages) MION averaged 6-fold higher than non-opsonized. However in glial cells, uptake was low and not different between MION preparations. They concluded that uptake of opsonized MION by macrophages is almost solely dependent on scavenger or

CR3- receptors and cannot be explained by elevated pinocytotic uptake in macrophages, since non-opsonized MION was taken up equally in both cell lines. Although not reported, the data indicate that the receptors used to internalize opsonized MION did not show evidence of saturation over the range of tested concentrations.

In a study evaluating the macrophage uptake of cross-linked starch coated iron oxide particles (DSM, 1.0-1.8 μm). Fahlvik et al [12] used cultured murine macrophages (J774) to determine the uptake and toxicity of these particles for use as MR contrast agents in the reticuloendothelial system. These particles ranged in size from 0.1 to 1.8 μm. The J774 cell line is described as a reticulum cell sarcoma with the morphology, adherence and phagocytic properties of macrophages [50]. Cells were grown in Dulbecco's modified Eagle's medium (Gibco, USA) with 10% fetal bovine serum, benzylpenicilin (100 U/ml) and streptomycin (10 μg/ml) at 37 degrees and 5% CO_2. Uptake capacity of J774 cells was quantified by exposure to C-14 labeled iron oxide particles for up to 4h at 4 and 37 º C. Cells were incubated with either labeled DSM, hydrolyzed starch iron oxide particles (MSM) or unlabeled DSM particles. The difference between the iron oxide particles measured at 37º C and 4º C [51] was reported as the internalized fraction. The concentration of internalized, labeled particles reached a plateau by 3 hours (measurements were take at 1 hour increments). The plateau of phagocytosis (9-10 μg iron particles per 10^6 cells) was reported as similar to a report by Artursson et al.[52] in which uptake was compared between resident and activated macrophages. In the Artursson study the difference was 3 and 14μg iron particles per 10^6 cells. Fahlvik concluded that the tumor J774 cell line behaved similar to an activated macrophage cell line in regards to surface receptors and phagocytic capacity.

Differentiation Between Pinocytosis and Phagocytosis

Feature differences between these 2 routes of internalization will be used to systematically identify the route (or routes) of iron oxide internalization [53].

Pinocytosis has 3 features that may be used to distinguish it from phagocytosis. First, it takes place continuously, even in the absence of added ligands. Second, it is insensitive to the fungal metabolite cytochalasin B, which interferes with the function of actin filaments. Third, uptake by pinocytosis entails significant internalization of fluid or small particles. Phagocytosis also has unique features. First, it always requires the binding of the particle to the plasma membrane as a prelude to internalization. It should be noted that there are particles that readily bind but are only negligibly internalized. Second, particle ingestion is inhibited by cytochalasin B, implying an actin dependent mechanism. Third, the membrane of the phagosome, the initial vesicle that contains the particle, is closely apposed to the latter, so that only a small volume of fluid is taken up during phagocytosis. Combining this information with the known effects of cytokines and other exogenous agents it is expected that a potential route(s) for iron oxide particles may be elucidated.

Factors Effecting Rates of Macrophage Phagocytosis

Early atherosclerosis, primarily fatty streaks, includes primitive macrophages and T lymphocytes. Prior to activation via inflammation, *resident* macrophages are immunologically quiescent. They have low oxygen consumption, low levels of major histocompatibility complex (MHC) class II gene expression, and little or no cytokine secretion. However they are phagocytic (at a reduced level) and chemotaxic and retain some proliferative capacity. Activated macrophages are defined as those possessing specific increased functional activity. There are 2 stages of macrophage activation: "primed", with enhanced MHC expression, antigen presentation, O_2 consumption, and reduced proliferative activity. Stimulating factor(s): TNF-alpha, IFN-alpha, IFN-beta, IL-3, M-CSF TNF-alpha can "prime" a macrophage. Activated macrophages show an ability to proliferate, high O_2 consumption, maximal secretion of mediators of inflammation including: TNF-alpha, IL-1, IL-6, NO (from iNOS). The Murine J774 cell line identified in this project has been shown to behave as a constitutively activated macrophage. The macrophages that are located within the vascular wall in atherosclerosis are activated. Two aims of the present study were to determine the extent to which endogenous factors such as the cytokines Interferon-γ (IFN-γ), IL-4, and exogenous factors involved in pharmacologic therapy such as HMG Co-A reductase inhibition [54] and angiotensin converting enzyme inhibition[55] effect the rate and extent of iron oxide uptake based on their effect on other biomolecules.

The ability to detect the presence of macrophages on MR images is not directly related to the number of macrophages present per unit volume, but the number of iron oxide particles per unit volume. Therefore it is necessary to understand the effect of endogenous and exogenous factors which could affect the time course of internalization after particle administration as well as the number of particles per macrophage.

Endogenous Factors

Activated macrophages produce inflammatory cytokines, chemokines and reactive oxygen species. Transforming growth factor β1 (TGF-β1), a key cytokine for control of cell growth, extracellular matrix formation, and inflammation control, is secreted by many cells present in atherosclerotic plaque. Draude et al.[56] investigated the ability of these cytokines, at various concentrations, to influence both the expression and function of ScR-A, CD36 and LOX-1 in activated macrophages. They reported an approximately log-linear suppression effect on ScR-A and CD36 specific mRNA over increasing concentrations of TGF-β1 (2.5, 5, 10, 20, 60, 80, and 120 pM). CD36 and ScR-A mRNA levels were reduced by 20% by 20pM TGF-β1 and to 50% by 40 pM TGF -β1. Conversely, the mRNA levels of LOX-1 were significantly increased 50% by 40 pM TGF-β1. The functional relevance of mRNA up or down regulation was confirmed by incubation of cells with oxLDL which was internalized at a rate consistent with mRNA expression.

The divergent effect on receptor activity by individual cytokines were used in the present study to confirm or exclude specific receptor mediated pathways for iron oxide internalization.

Exogenous Factors

Pharmacological treatment of hypercholesterolemia has been successful in reducing clinical cardiovascular events and therefore has become a common therapy. One of the more common of this category is the class of 3-Hydroxy-3-methylgluatryl coenzyme A (HMG-CoA) reductase inhibitors. They exert an effect by blocking the conversion of HMG-CoA to mevalonate, a rate-limiting step in the biosynthesis of cholesterol. It is likely that patients undergoing evaluation for the presence of atherosclerosis may be taking this class of drugs. Thus, it is important that its effect on macrophage uptake of potential MRI atherosclerosis contrast agents (iron particles) be understood. Aikawa et al [57] recently reported that cerivatatin (an HMG-CoA reductase inhibitor) decreased the number of macrophages in cell culture in a dose dependent fashion. Bernini et al [58] investigated the mechanism of fluvastatin action on AcLDL endocytosis. Their data showed that endocytosis was down-regulated both in resident as well as activated macrophages. It was concluded that the decreased internalization of AcLDL was not related to a decreased expression of the scavenger receptor, based on data showing no decrease in cellular binding at 4º C. The effect of fluvastatin was seen to act independently on the receptor for AcLDL (although inhibition of endocytosis of other ligands was not investigated) in that native LDL degradation was seen to slightly increase when AcLDL degradation was reduced. Other members of the statin family have shown similar effects [59].

Losartan, an angiotensin II receptor antagonist, is widely prescribed as an antihypertensive medication. In addition to its blood pressure lowering effect, it has been shown to downregulate CD36 (an oxidized LDL receptor) expression by 54% [60]. This resulted in a 78% reduction in oxidixed LDL macrophage association and a 21% reduction in oxidized LDL degradation. No data exists on whether other receptor mediated or fluid-phase mechanisms of endocytosis are effected. Therefore its effect on iron oxide internalization is unknown.

Clinical Magnetic Resonance Imaging

The imaging parameters used in the present study to characterize iron oxide nanoparticles differ substantially from than those applied to patient imaging. The major differences arise from the need to account for motion and blood flow within the vessel of interest. A typical vascular exam will begin with a series of localizer images meant to identify the location and orientation of the target vessel with the patient in the supine position. Clinical scanners use a large radio-frequency coil built into the scanner bore transmit the RF pulses and a smaller coil placed on the patient to receive the MR signal . Surface coils improve signal-to-noise due to their proximity to the target but also limit the area that may be imaged. Three types of motion exist. Respiratory motion results in cyclic motion of the chest heart and great vessels. Failure to account for this motion will result in blurring and ghost artifacts, primarily along the phase encoding direction. Cardiac contraction produces 3D motion of the heart and associated great vessels. Current scanners acquire data fast enough to permit images to be acquired during a brief suspension (10-20sec) of respiration. Cardiac motion is accounted for by synchronization of acquisition to the patients' electrocardiogram (ECG). This creates an effective repetition time (TR) which is a multiple of the patients cardiac cycle length. In practice imaging efficiency is maintained by acquiring multiple anatomic locations during each cardiac cycle. Finally, overall patient movement is a minor issue as long as the acquisition period is limited to under a few minutes.

Imaging of the vessel wall must deal with blood flow within the vessel. In the proximal arteries it is pulsatile, while venous and more distal arteries display an essentially constant blood flow velocity. Blood flowing through different spatial encoding gradients will cause the signal to be incorrectly mapped to the wrong position as a ghost artifact. Refocusing gradients have been used to correct for this. Recently the majority of vascular imaging methods use a non-selective inversion pulse immediately followed by a slice selective reversion RF pulse. This results in blood prepared so as not to produce signal to flow into the imaging plane, and improve visualization of the vessel wall. A limitation of these "black-blood" sequences is that the labeled macrophages are primarily on the endothelial surface. If the region of signal loss due to Feridex is immediately adjacent to the dark vessel lumen, the region of vascular uptake may not be well appreciated.

All of these methods have the effect of changing the "weighting" of the pulse sequence. Due to the T2 shortening of the Feridex agent sensitivity to detecting the agent increases with increasing TE interval. Gradient recalled echo (GRE) sequences which use a single RF pulse followed by gradient reversal to create the echo signal are also sensitive to iron agents due to the fact that gradient rephrasing does not eliminate the dephasing effects of magnetic field inhomogeneities, such as iron particles. In practice, TE's longer than about 60 msec are sensitive to any local motion and are inherently low in SNR whether they are in a spin echo or gradient echo sequence.

Spatial resolution is limited by 2 factors, available signal and the relationship between the selected field-of-view (FOV) and the sensitive volume of the surface coil. Ideally one would like to spatial resolution that is high relative to the structure being imaged. Arterial wall thickness varies from less than 0.5 mm in the coronary arteries to about 2 –2.5 mm in the aorta. The voxel size is determined by the FOV and number of pixels in the matrix. Present clinical scanners use matrix sizes of 256^2, 512^2 and 1028^2. The cross-sectional dimensions (anterior-posterior (AP) to left-right (LR)) of phased-array surface coils is dependent on the size of the patient, usually 25 cm AP, 32 cm LR. If the selected FOV is smaller than the signal producing dimension, aliasing or "phase-wrap" artifact will incorrectly map image data extending beyond the FOV.

Combines with signal-to-noise constraints, practical resolution is presently limited to $\geq$500 microns.

Thus the lower limit of detection calculated in the present study using phantom and calculated data, is likely far lower than that which can be achieved given the constraints of actual patient imaging.

Previous Imaging Studies

While use of iron oxide particles has been used for some time for liver imaging, application in atherosclerosis is quite new. The only in vivo studies have been in rabbit models of atherosclerosis. In Watanabe Hereditable Hyperlipidemic (WHHL) rabbits, Schmitz et al.[61] used this established model of atherosclerosis in order to evaluate the effect of intravenous administration of iron oxide particles on MR images acquired using a standard clinical imager and confirm the results with post mortem histology. The particle used was a carboxydextran-coated iron oxide with an overall diameter of 25 nm. Four groups were studied: Group 1, WHHL controls: no contrast agent; group 2: 50µmole Fe/kg, with an 8-hour post contrast delay; group 3: 50 µmole Fe/kg, with a 24-hour delay; and group 4: 200 µmole Fe/kg dose with a 48-hour post contrast delay. Imaging parameters were set to produce moderate T2* weighting while maintaining the enhanced luminal blood signal attendant with standard gradient echo methods. Prior to administration of the iron agent both blood and aortic wall produced uniform "bright" signal. Aortic cross sections were acquired using 75 contiguous 2 mm slices. As expected, focal regions of signal loss were not observed in the control group. The best correlation (Spearman rank correlation coefficient of 0.78, $p=0.0007$) was reported for group 4. Using RAM-11-antimacrophage stain was used to confirm the presence and location of macrophages. Prussian blue was used to identify the location of iron particles. Iron particles were seen both associated with macrophages but also in regions of the intima devoid of macrophages. The authors concluded that increased endothelial permeability, a known functional characteristic of atherosclerosis account for this finding [62]. The percentage of particles found NOT to be associated with macrophages was not reported. It is likely that the timing from administration to analysis would affect this value.

In a study using a similar animal model but smaller iron oxide particle (18 nm) Ruehm et al.[63] evaluated the performance of ultrasmall particles of iron oxide (USPIO) as a marker of macrophage activity. This group imaged the rabbit aorta in cross section using a 3D T1 weighted pulse sequence. Images were acquired each day after administration of 1 mmole Fe/kg for 5 days. Images were analyzed for signal intensity with the aortic lumen and vessel wall. New Zealand White rabbits were imaged in the same manner and used as controls in that they do not spontaneously develop atherosclerotic disease of the aorta. Histochemical staining (Prussian blue) and EM were used to identify the location of the USPIO. Signal intensity in the lumen was reduced for the first 3 days after USPIO administration due to the T2 shortening effect of this agent at high concentration. By day 4 signal had increased and provided good contrast between aortic wall and lumen. On days 3-5, focal regions of signal loss were observed in the aortic wall of WHHL rabbits but not in controls. It was stated by the authors that gross post mortem inspection of the aortic walls of WHHL as well as control rabbits did not reveal and obvious irregularities. (the example images shown in the text did not support this statement.) Histopathology showed marked uptake of Fe particles in macrophages embedded in atherosclerotic plaque in all WHHL animals. The authors did not discuss the presence of iron particles not associated with macrophages. Electron microscopy identified myosin filaments within the USPIO containing macrophages and concluded that the macrophages were of smooth muscle cell origin. Further foam cells filled with fat molecules were found not to contain USPIO particles. No rigorous attempt was made to match regions of signal loss on MR images with histopathologically confirmed iron particles or macrophages.

Objectives and Expected Significance:

The overall objective of this project is to evaluate iron oxide particles as MRI markers of inflammation in atherosclerosis by way of their active internalization by macrophages. The specific aims are to : 1) determine the baseline time course of particle uptake in macrophage cell culture incubated with increasing concentrations if iron oxide particles. 2) Determine the effect of cytokines (IFN-γ and IL-4) on the rate an extent of iron oxide internalization. 3) Determine the effect of exogenous agents (pharmaceuticals) including HMG-CoA reductase inhibitors and angiotensin II receptor antagonists on the regulation of particle uptake. 4) Determine the effect of the mannose receptor blocker mannan. 5) Determine the effect of the cytoskeleton inhibitor cytochalasin B on SPIO uptake and 6) Determine the minimum concentration of macrophages, per unit volume, required for detection by MRI.

These results will determine the potential sensitivity and specificity of iron oxide particles in detecting atherosclerosis. Specifically, if it is determined that uptake can be significantly inhibited by specific cytokines known to be present in atherosclerotic plaque, or common drug therapy, then the absence of the contrast agent effect could not be interpreted as conclusive evidence for the lack of macrophage presence. However if there exists a level of constitutive macrophage uptake that would reach the level of MRI delectability, local stimulation of uptake induced by cytokines might be used to map macrophage activity as well as location.

Experimental Methods:

Statistical Analysis

Reported results are expressed as mean ± standard deviation. ChromaVision area for the portion of the color spectrum specific for nuclear orange and blue associated with iron within the cell cytoplasm was expressed in μm^2. Three circular regions (79206 μm^2) were analyzed in each chamber. Statistics were performed using SigmaStat version 2.1 software (SPSS Inc, Chicago, IL).

Orange and blue area within each ROI was reported as either raw area (μm^2) or percent of ROI area. To test the significance of treatment, SPIO concentration and interaction between the two on macrophage uptake of SPIO, 2-way analysis of variance was applied to the raw area data. Post hoc multiple comparisons between individual treatment and SPIO groups was performed using the Tukey Test. P-values <0.05 were considered significant. Cell density comparisons between control and treatment used a 2-tailed students *t*-test. When cell density was not the same between treatment and control blue area was corrected based on cell density and ANOVA performed on corrected values. Linear regression analysis was used to validate ChromaVision based cell density analysis against direct cell counting. This analysis was also used to determine the SPIO dose-macrophage iron uptake relationship and SPIO concentration-MRI signal relationship.

<u>Macrophage Cell Culture</u>:

The murine macrophage cell line J744A.1 is described as a reticulum cell sarcoma with the morphology, adherence and phagocytic properties of macrophages [50]. The J774 cell line has been used extensively for investigation of pinocytosis and receptor mediated phagocytosis[64,65,50]. Macrophages acquired from American Type Culture (Manassas, VA), were seeded into 75cm^2, cell culture flasks (Costar, USA) containing 20 ml's of Dulbecco's modified Eagles medium (Gibco, USA) with 10% fetal bovine serum, benzylpenicilian (100U/ml) and streptomycin (10 µg/ml) at 37º C and 5% CO_2. The macrophage concentration was determined by use of a hemocytometer (Fisher Scientific). Beginning with an initial cell colony from American Tissue Culture, additional cells were propagated in 75 cm^2 tissue culture flasks and frozen to insure a secure supply of cells from the original colony. By their nature, macrophages are uniquely adherent cells. The usual method of trypsin-EDTA and PBS are ineffective in removing adherent cells. Pieser L, et al. [66] describes the method applied to the present study. Medium was removed and cells washed with 1X PBS (x3). A detachment buffer made-up of 10-15 mM Lidocane-HCL (Sigma

Chemicals) and 10 mM EDTA in 1% PBS was added to the flask for 5-15 min followed by cyclic pipetting of buffer in order to dislodge the cells. Once cells have released from plastic flask, 10 ml of medium (including serum) was added to halt the effect of the lidocaine. Cells were centrifuged at 1500 rpm for 5 min. Cells were then resuspended in medium, counted and prepared for incubation with iron oxide and other test material. Initial dilutions of 5,000, 10,000 50,000, and 200,000 cells per 1.7 cm^2 chamber surface were incubated for 24 hours, rinsed with cold PBS to remove any non-adherent cells, then fixed with 3% gluteraldahyde.

Baseline Uptake of Iron Oxide Particles

Macrophages are highly efficient at pino and phagocytosis. Determination of baseline iron oxide "time" and "dose" relationships were performed with incubation times of 10 20, 40, 80, 240, 360 and 480 min. at concentrations of 1, 10 and 100 µL stock Feridex per ml of medium. Chamber slide systems containing either 4 or 8 wells in which the wells can be removed leaving a standard glass microscope slide were used for all experiments. Cells were cultured for 24 hrs prior to addition of iron after washing with PBS to remove any non-adherent cells. Cells were rapidly cooled to 4º C using cold PBS in order to arrest uptake. The cell membrane is not fluid enough at 4º C to permit particle internalization. Medium containing Feridex was removed, cells washed with 4º C PBS and fixed for at least 8 hours with 3% glutaraldehyde.

Establishing the Route of Internalization

In order to determine the route of particle internalization, baseline measurements will be performed using medium with and without cytochalasin B. This agent interferes with the function of actin filaments. It has been shown previously by Weiss et al [67] that phagocytosis but not pinocytosis is inhibited by this agent. The iron particle under investigation is coated with Dextran-10, which may effect its endocytotic route. To determine the role of the mannose receptor in iron uptake a group of cells were pretreated with 1.0 mg/ml mannan in standard Dulbecco’s

Modified Eagle's Medium (DMEM, American Type Culture Collection, Manassas VA) with 10% FBS. This has been shown to effectively block this receptor.[46] Opsonification is another potential route of iron particle internalization.[68,69] This route of endocytosis was examined by measuring cell-iron uptake using medium without the standard 10% FBS. HMG CoA reductase inhibitors ("statins") are know to affect LDL receptor expression and activity.[7071] This route will be examined in cells treated with different concentrations of mevinolin.

<u>Description of Histological Stains</u>

The most common application of Acridine orange (3,6-dimethylaminoacridine) is that of a fluorescent probe for biological activity in live cells. In the present study, this stain was used based on its empiric differentiation between cytoplasm and macrophage nucleus (using visible light) and its color spectrum compared to Prussian blue. In fixed cells the acridine orange dye cation stains acid components including acidic mucopolysaccharides, mast cell granules, and nucleic acids. This stain is a weak base that is readily soluble in water. Lerman [72] showed that acridine orange forms a complex between the acridine orange amino molecule with the nucleic acid base pairs. The difference in nucleic acis concentration between the cytoplasm and macrophage nucleus may account for the observed visible light color pattern. The method used includes:

Stain Solution

Aridine orange (0.1g/L of 0.5M Acetate buffer, pH 3.7@25ºC)

Method

1. Fix slide with methanol for 2 minutes and allow to air dry.
2. Flood slide with Acridine Orange Stain for 2 minutes.
3. Rinse thoroughly with tap water and allow to air dry.

The commonest method for demonstrating iron is Perls' Prussian blue stain, sometimes called Perls' acid ferrocyanide reaction. The acid ferrocyanide reaction of Perls' Prussian blue involves treatment with acid (usually hydrochloric) to release ferric ions from tissues. These are immediately captured by replacement of the cation of potassium ferrocyanide by the ferric ion, forming insoluble ferric ferrocyanide which then precipitates giving rise to the blue color. This is an extremely reliable process, and quite sensitive. Very small amounts of iron may be demonstrated microscopically. The method includes:

Solution A
Potassium ferrocyanide 2g.

Distilled water 100 mL.

Solution B
Hydrochloric acid 2 mL.

Distilled water 98 mL.

Method

1. Bring sections to distilled water.
2. Place in a freshly made equal parts mixture of solutions A and B for 20 minutes.
3. Rinse well with distilled water.
4. Dehydrate with ethanol, clear with xylene and mount with a resinous medium.

Quantification of Iron Oxide Uptake by Macrophages

Fixed cells were first stained with Acridine Orange then counter-stained with Prussian blue. These stains occupy significantly different regions of the color spectrum and can thus be analyzed without spectral "spillover". The portion of the color spectrum occupied by cytoplasmic iron stained with Prussian blue, and nuclei stained with acridine orange was defined by the band of hue, luminosity and color saturation sufficient to localize the selected color, hue combination in the desired location on multiple slides.

Figure 11: ChromaVision microscope with digital camera and automated stage.

For Acridine Orange, the values for each variable were: hue (228 high, 16 low); luminosity(145 high, 49 low); saturation(149 high, 58 low). For Prussian Blue the values applied were: hue(217 high, 28 low); luminosity(175 high, 15 low); saturation(78 high, 6 low). These values produced a narrow color “acceptance” window specific for the cells, iron and staining method. All cells were stained in exactly the same way, and the above values were used to determine the area of the slide (μm^2) automatically designated “iron” or “cell”.   Localization was further tested in slides not treated with Feridex, but treated with the 2 stains. Using a ChromaVision® automated cellular imaging system (figures 11,13) a region containing >100 cells were identified for analysis at 40x -60x magnification. The identified regions were digitized. Regions containing blue iron particles identified manually in order to "teach" the system the wavelength and variability of the Prussian blue stained particles. The same process was repeated for the orange stained nucleus and cytoplasm. The relative amount of iron particles per cell is then calculated by taking the ratio of the area (μm^2) to the total cell area (μm^2). The number of cells in the field will also be recorded. Three separate fields were analyzed within each slide chamber location and this data used for statistical comparisons.

The ChromaVision Automated Cellular Imaging system (ACIS) is an automated microscopy and computerized image processing system that can detect, count and classifies objects of interest based on color, size or shape. Specifications include an automated microscope having objectives with magnification of 4X, 10X, 20X, 40X and 60X. The microscope is interfaced to a Sony 3-Chip full color digital camera. The slide stage is computer controlled and may be moved in X, Y and Z (focus). The camera assembly is interfaced to a Windows NT 4.0 workstation equipped with a flat screen monitor having a resolution of 1280x1024 pixels. The optical resolution is listed as 0.0625 μm^2 per pixel or 160 μm x 120 μm per field-of-view. Once a color threshold (hue, luminosity and saturation) is selected, these values may be stored and cells on the current or other cell slides highlighted to show the regions meeting the selected color criteria (see figure 12).

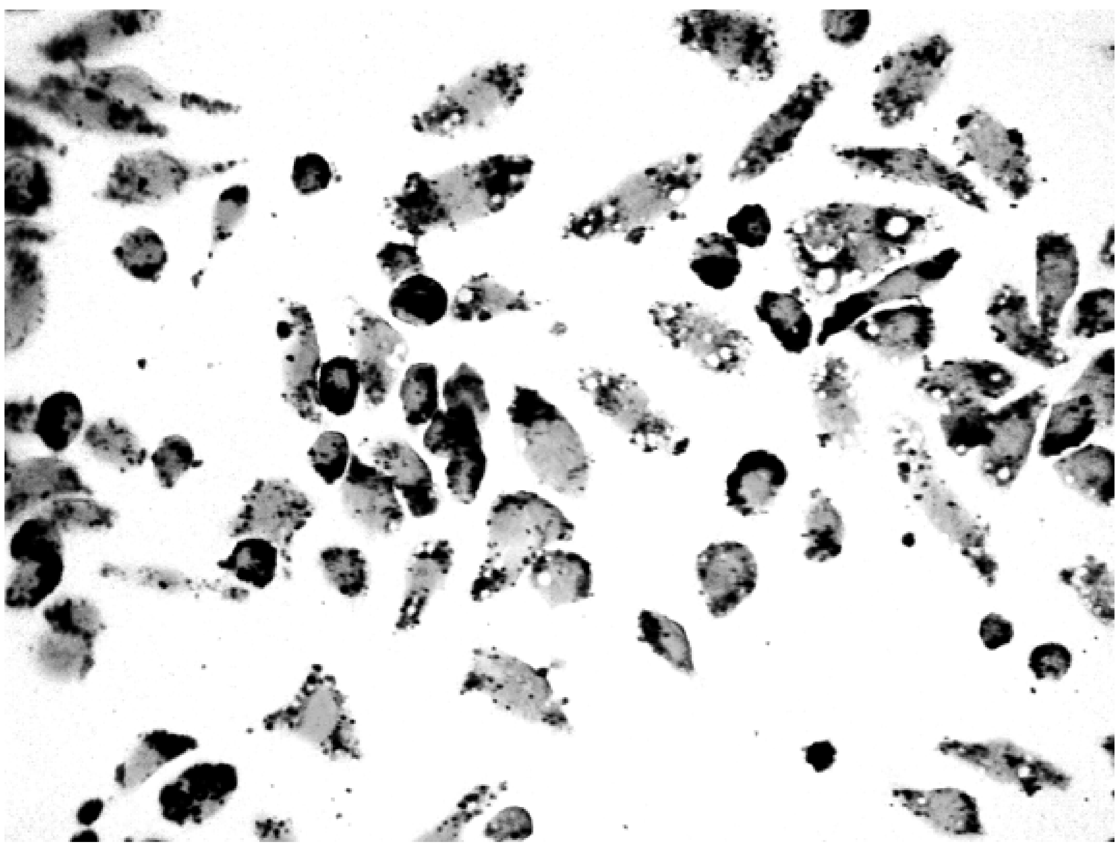

Figure 12: Grey scale representation showing regions identified as iron in black, and regions identified as cell nucleus in light grey

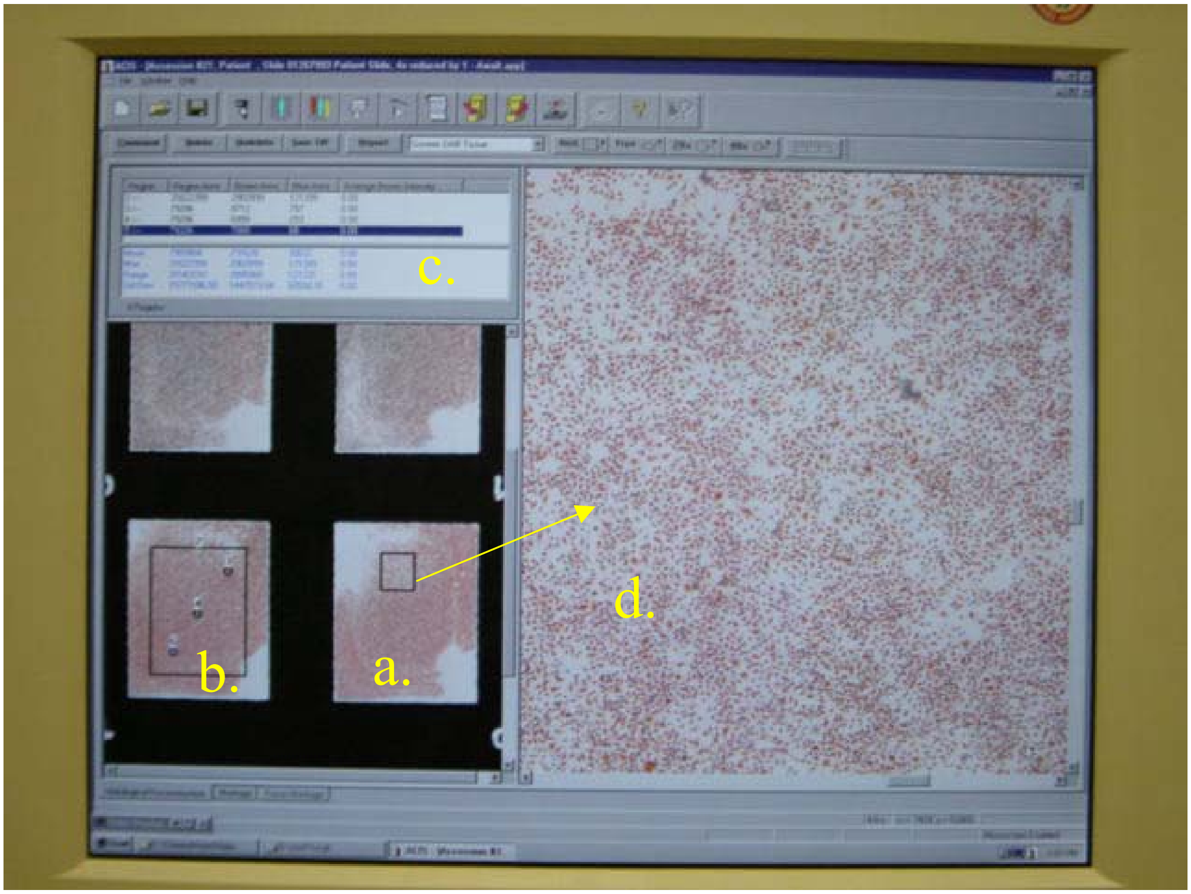

Figure 13: ChromaVision display screen. a. shows stained cells in one of 8 chambers. B. shows 3 circular ROI's used for cell density and iron uptake. c. output of orange and blue area. D. enlargement of sub-region used to evaluate staining and identify potential image artifacts.

Magnetic Resonance Relaxation Time Measurements

Measurements were performed on a GE clinical MRI at Allegheny General Hospital operating at 1.5 T. Serial dilutions of Feridex were suspended in 2% agar and placed in 50 ml centrifuge tubes. Concentrations included: 0.0 μM (control), 0.00214 μM, 0.00427 μM, 0.00855 μM. 0.0179 μM, 0.0342 μM, 0.0684 μM, 0.137 μM, 0.273 μM, 0.547 μM, 1.094 μM. According to data provided by Advanced Magnetics (the developer of Feridex) light scattering methods tend to overestimate the "actual" size of iron oxide particles.[40] Advanced Magnetics has estimated the average size of Feridex to be 20nm.[40] Based on this size it is estimated that a milliliter of Feridex contains 4.2×10^{15} dextran-coated particles.

In that there is potential for the particles to settle prior to agar solidification, cross sectional images at the top middle and bottom of the tube will be acquired and mean signal compared using ANOVA. The T1 relaxation time was quantified by calculation of nine data points generated by the inversion-recovery method including Time-to-inversion (TI) of 50, 100, 200, 400, 600, 800, 1000, 1400, and 1600 msec. The T2 relaxation time was measured from ten data points generated with a Carr-Purcell-Mieboom-Gill sequence including time to echo (TE) of 14, 25, 50, 75, 100, 200, 400, 800, 1600, and 1900 msec Field-of-view (FOV), slice thickness and matrix size will be selected to match that commonly used in clinical vascular exams. Using these data an "optimal" set of parameters was defined. In vivo imaging parameters are constrained due to the need for electrocardiogram (ECG) gating which predefines the effective repetition time (TR) as being some multiple of the cardiac cycle length. This interval of 500-1000 msec corresponds to a heart rate of between 120-60 beats-per-minute. Further excessively long TE's may result in image blurring. Therefore, based on the "ideal" in vitro parameters, potential in vivo parameters will be tested for linearity of the concentration-signal intensity relationship.

In vivo, a number of factors affect the lower limit of detection of iron oxide particles. Macrophages are not uniformly distributed within the imaged tissue. Further, macrophages are smaller than image voxels and can internalize a large number of iron particles. The effect of voxel size will be determined by acquiring images using identical parameters over a range of voxel sizes. Finally as previously stated, the effect of the iron oxide is limited to protons in their immediate vicinity. If water exchange across the macrophage membrane is slow relative to imaging speed, the number of effected protons would be reduced compared to that of an unrestricted environment. This could affect the magnitude of signal change observed. Based on imaging serial dilutions of Feridex-loaded gel, the lower limit of MRI detectability was estimated.

Results

<u>Magnetic resonance Imaging</u>

Figure 14 is a T1 weighted image of a subgroup of gel filled tubes. T1 weighting minimizes the effect of the iron agents and permits visualization of all tubes with the exception of those with the highest concentration. Signal intensity was measured in each tube over a range of Feridex concentration of 0.0 μM (tube 1), 0.002 μM (tube 2), 0.004 μM (tube 3), 0.009 μM (tube 4), 0.017 μM (tube 5), 0.034 μM (tube 6), 0.068 μM (tube 7), 0.137 μM (tube 8), 0.237 μM (tube 9), 0.547 M (tube 10), 1.09 μM (tube 11). Figure 15 plots the raw signal at each level of the gel-tube phantom for each concentration. In general, the signal was similar between levels. However it was noted that the control tube showed a trend toward greater signal at the bottom of the tube.

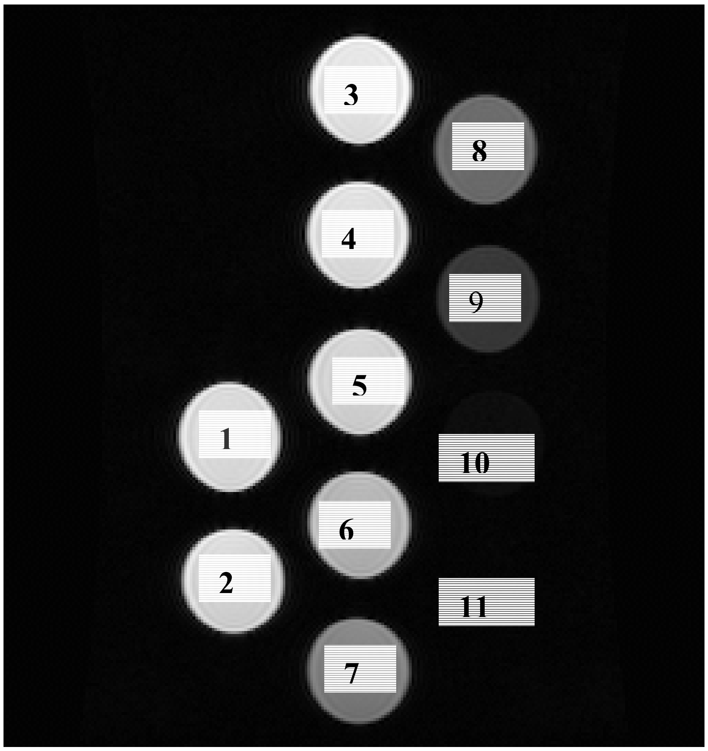

Figure 14: T1 weighted cross sectional image of tubes containing gel-Feridex material. Top left column is control, signal drops with increasing iron.

This is consistent with the "coil effect" in which the RF receiver coil is more sensitive at the surface of the coil. To correct for this effect the signal was normalized by a factor, based on signal intensity at the 3 locations in the control tube which would equalize the signal across the control tube. These data are shown in figure 16. It was concluded that the Feridex was evenly distributed within the tubes, and a single location could be used for signal analysis.

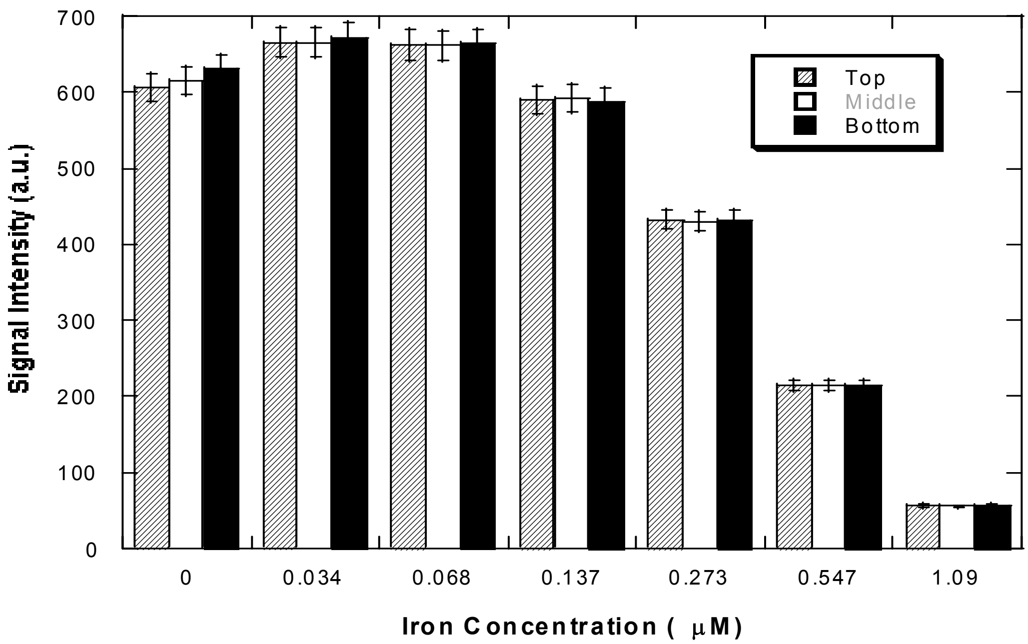

Figure 15: Plot of raw signal intensity by phantom position and iron concentration. T1-weighted image acquisition.

Figure 17 shows a representative cross-sectional spin-echo (SE) image with a TE of 50 msec. Loss of signal in all tubes of the third column and the lower rows of the second column is related to the increased iron oxide concentration and corresponding deceased T2. Figure 18 is an inversion prepared SE sequence with a time to inversion of 100 msec. The loss of signal in the center row of the center column corresponds to a TI of 700 msec which represents a gel T1 of about 1000 msec.

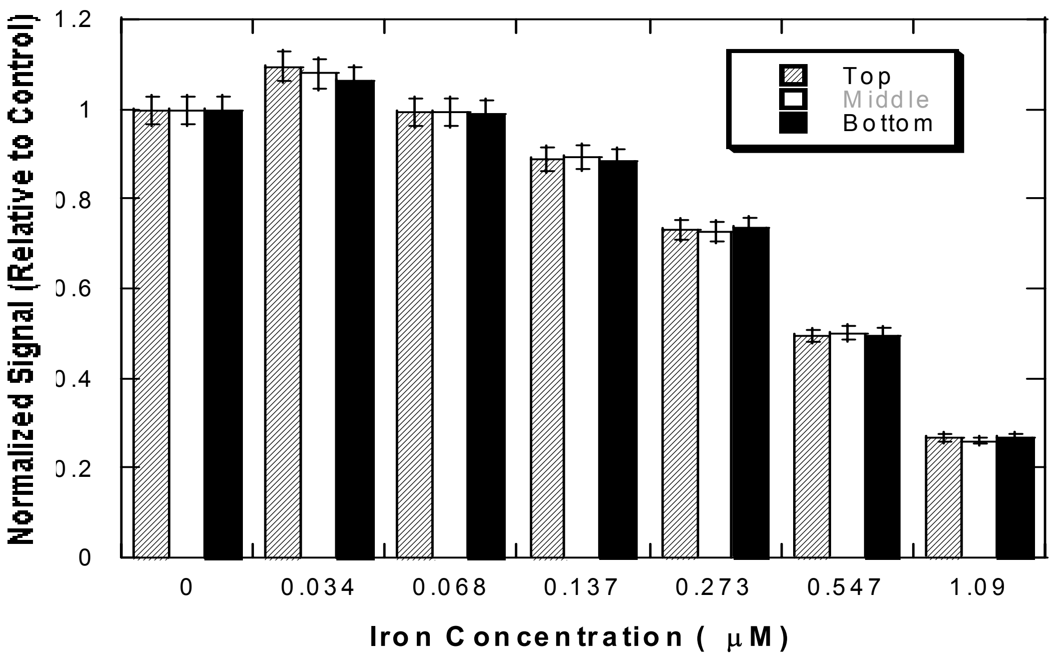

Figure 16: Signal intensity normalized to control to correct for inhomogeneity of surface coil sensitivity across tubes

In order to quantify the T2 shortening effect of increasing concentrations of iron oxide particles in the gel material, T2 was measured using the Hahn spin echo method. Figure 19 displays the relative signal for each iron concentration over

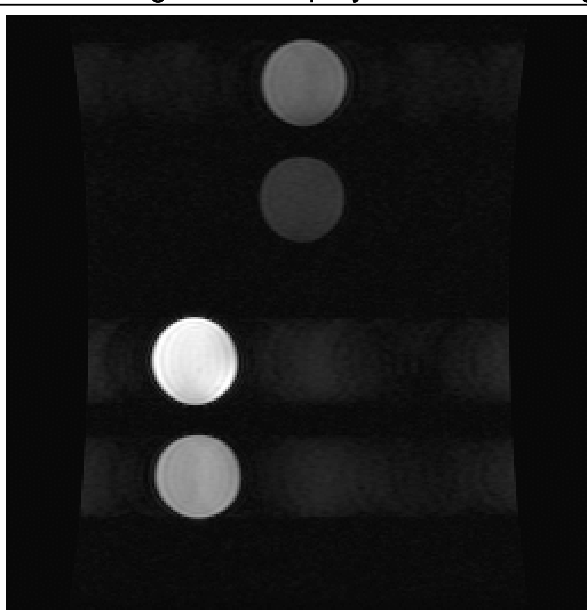

Figure 17: T2-weighted image showing greater signal loss in iron containing tubes compared with T1-weighted image (Figure 3).

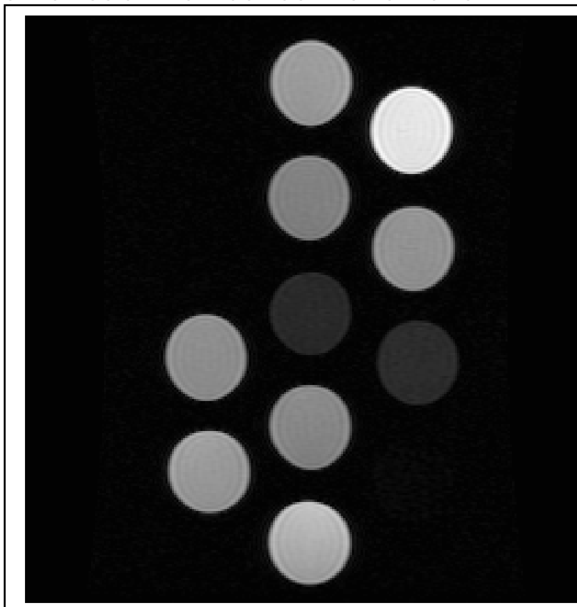

Figure 18: Spin echo image with 180 degree inversion pulse 100 msec prior to sequence.

multiple time-to-echo (TE) intervals. The vertical axis is relative signal intensity, the horizontal axis is TE in msec. It can be noted that at higher iron concentration only the early part of the curve is linear. Signal was compared to background and data points not significantly above background were not used for curve fitting or T2 determination. T2 was determined by determining the slope of the natural log of signal intensity versus TE.

To determine iron oxide dependent changes in T1, the inversion recovery method was used. Figure 20 shows the signal versus time-to-inversion (TI) for the various iron concentrations. Clinical scanners are designed to produce images and the sign of the signal data is not preserved. As can be seen in figure 20, signal for each phantom declines as the inversion time is increased, but then regrows after the zero value is reached. As is the case for most analysis, signal from tubes with high concentrations of iron oxide produce negligible signal due to the large T2 shortening effect. This could be overcome using ultra-short TE intervals, however these sequences are not available on clinical scanners.

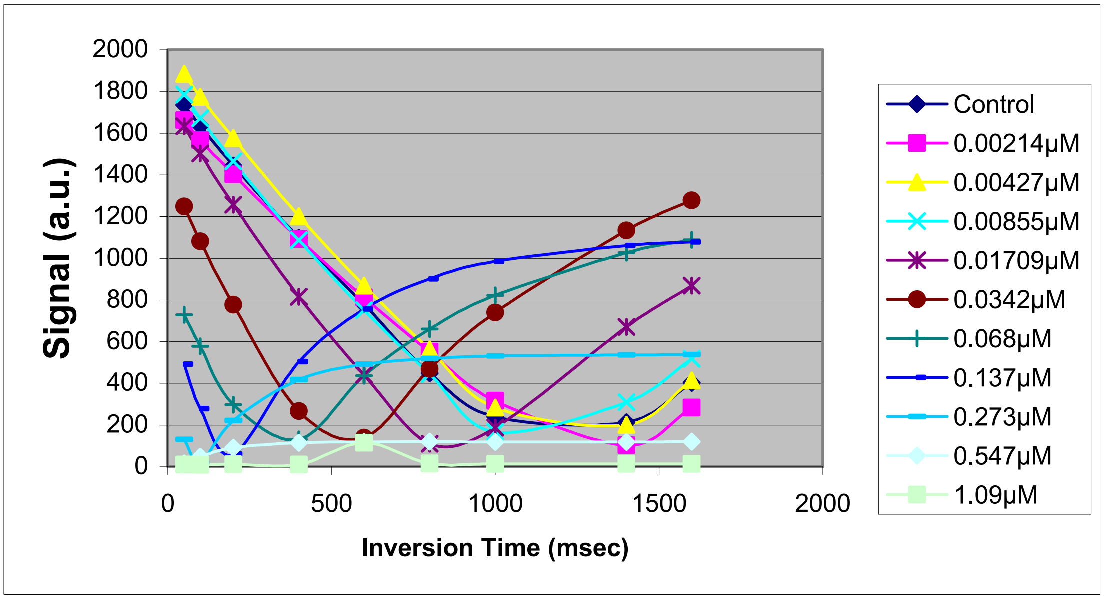

Figure 20: Signal intensity as a function of inversion time and iron concentration.

Signed values were determined by analysis of raw (pre Fourier transform) and are displayed in figure 21. The relationship between signal intensity, TI and T1 is given as:

$$Signal \propto \left[1 - 2\exp\left(-\frac{TI}{T_1}\right)\right]$$

From this relationship it can be appreciated that at the TI where signal =0.0, T1 = TI/ln 2. The linear regression was determined for each iron concentration and the exact time of minimum signal determined by setting signal to 0.0.

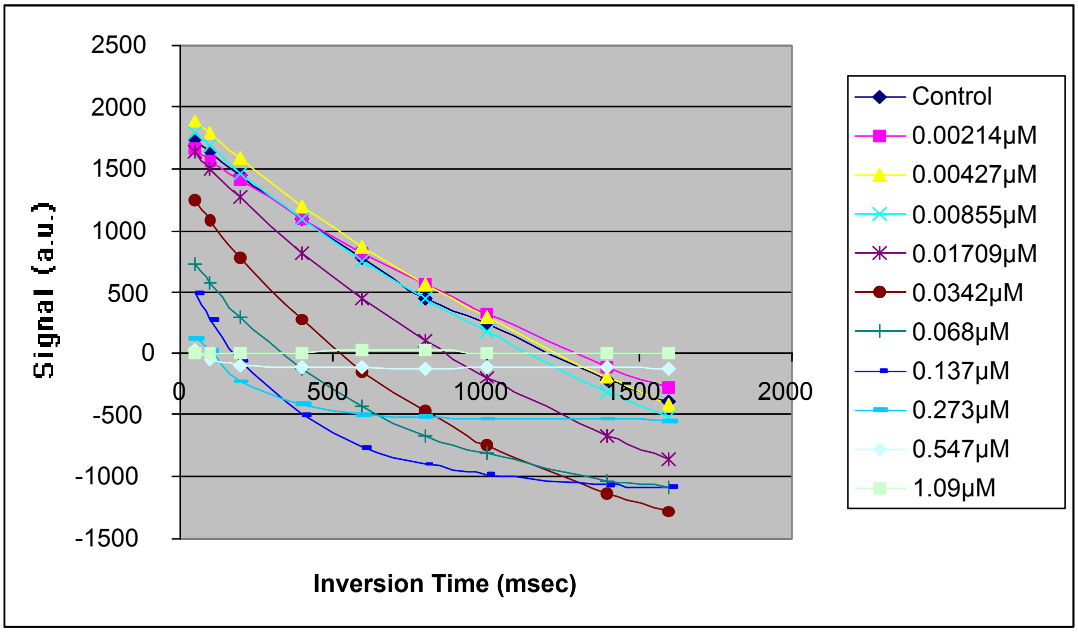

Figure 21: Plot of signed values of signal intensity. Zero-crossing is used to calculate T1 relaxation time for each iron concentration.

Figure 22 shows that at low iron concentrations (0.0 - 0.0021μM), T2 changes are more significant than T1. While at high concentrations (0.0086-0.034μM) T1 changes more rapidly than T2. In that human application will likely occur at the lower concentrations, these data would indicate that use of T2 weighted image sequences would produce more signal change, for the same change in iron concentration, than T1 weighted sequences at low iron particle concentrations.

While the T1/T2 values of the gel phantom are useful in determining the effect of iron oxide on relaxation parameters, these values are significantly greater than the 500-800 msec T1 measures in actual vascular wall. Further, the acquisition parameters used to quantify the gel's T1 and T2 are not applicable to human studies in that such studies must be synchronized to the patient’s heart cycle (700-1200 msec). Therefore the gel tubes were rescanned using conventional imaging sequences and physiological TR and TE intervals. In practice, TE's above 50-60 msec result in image blurring due to motion. Figure 22 shows the signal-iron concentration curves for a group of standard clinical acquisition sequences including standard SE with TE = 14, 25 and 50 msec.

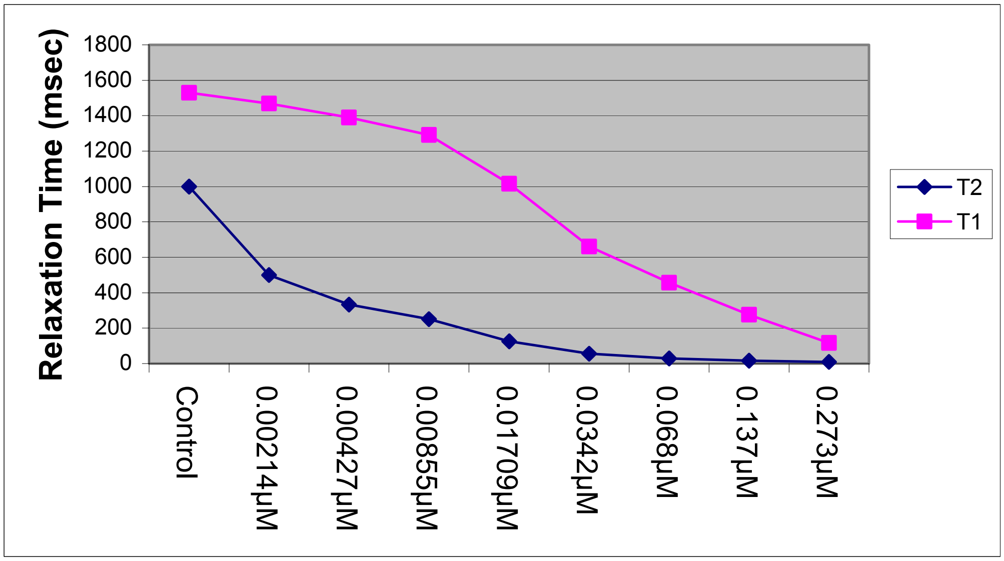

Figure 22: Summary of calculated T1 and T2 values for the tested iron particle concentrations. At lower concentrations T2 effects dominate, while at higher concentrations T1 shortening can be observed.

Fast spin echo (FSE) acquires multiple echos per heart cycle as a means of reducing acquisition time. Two, 8, and 16 echo's per cycle were tested. It should be noted that use of multiple echo's results in restriction on selection of TE. Thus T2 weighting is not equivalent between tests. An ideal contrast agent will have a predictable, if not linear signal-concentration relationship. Figure 23 shows significant non-linearity. In fact, equivalent signal is observed at multiple concentrations for a given imaging sequence. Only the most T2 (TE=96 msec) shows reasonable linearity. In order to understand this result Simulations were performed using the relationship between T1, T2, TR and TE given by: *Signal (S)* $\propto$ *[1-exp(-TR/T1)] exp(-TE/T2)*.

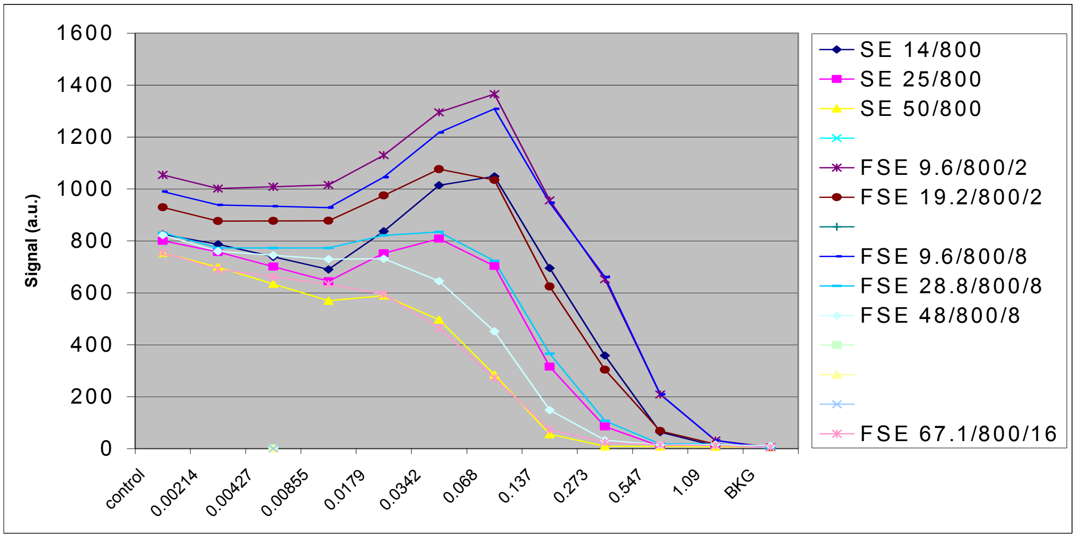

Figure 23: Signal-concentration relationship for common clinical pulse sequences. Significant non-linearity may be observed.

Figure 24 compares the signal-iron concentration relationship for four T1, T2 relaxation value pairs. The 1600/1000 predicts a similar non-linear relationship to that observed in the gel phantom study (Fig 23). As the T1/T2 values are reduced more toward that know to exist in the vessel wall (i.e. 600/200), the relationship becomes significantly more linear. In order to confirm this prediction a limited set of gel tubes were prepared including Gd-DTPA, a low molecular weight (938) agent which shortens both T1 (estimated as 505 msec) and T2. (estimated as 158 msec). Figure 25 displays the signal-concentration relationship using a TE of 60 msec and a TR of 800 msec. This confirms that the relationship between iron oxide concentration and signal change is dependent on the background T1 and T2 relaxation times. Nonlinearity exists when T1 and T2 are significantly longer than those observed in the biological system under investigation.

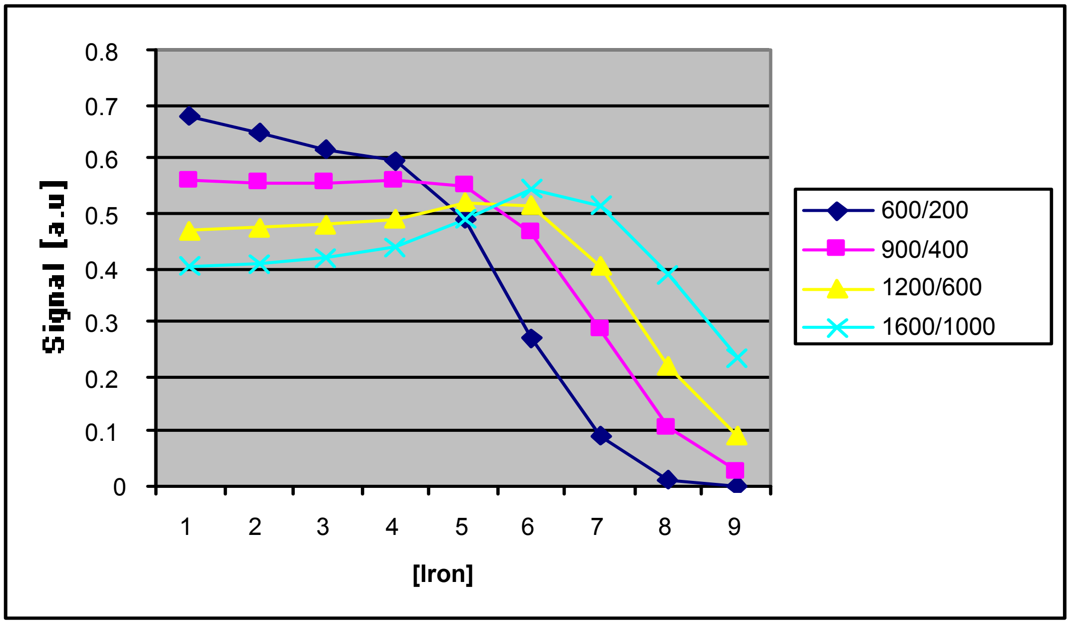

Figure 24: Simulated signal-iron concentration curves generated to determine the effect of initial T1 and T2 value on curve shape. More physiological T1 and T2 values result in a more linear relationship.

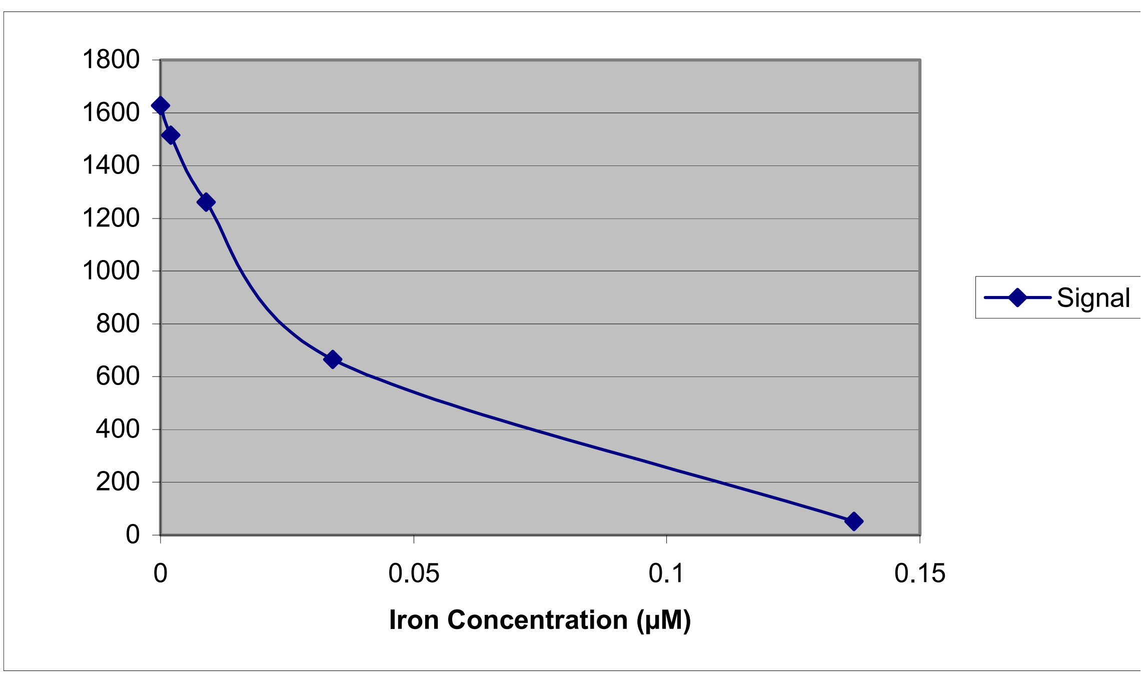

Figure 25: Experimental data showing the signal-iron concentration relationship using physiological image acquisition and phantom values. Signal-iron concentration relationship shows improved linearity.

Finally, the effect of voxel size on the signal-concentration relationship was measured using the second gel phantom set. Figure 26 shows no significant difference in signal between voxels ranging in volume from 0.34 to 2.25 mm^2. It is accepted that the iron oxide distribution used in this study was evenly distributed, with diffusion times quite unlike what may be expected in the actual vessel wall. Linear regression analysis was applied to phantom data at the physiologic T1 and T2, also using appropriate TE and TR values in order to determine the lowest concentration of iron yielding a significant signal change. The corresponding number (estimated) of iron particles that this represents per voxel will be calculated to derive an estimate of the number of macrophages required to generate this amount of iron oxide uptake.

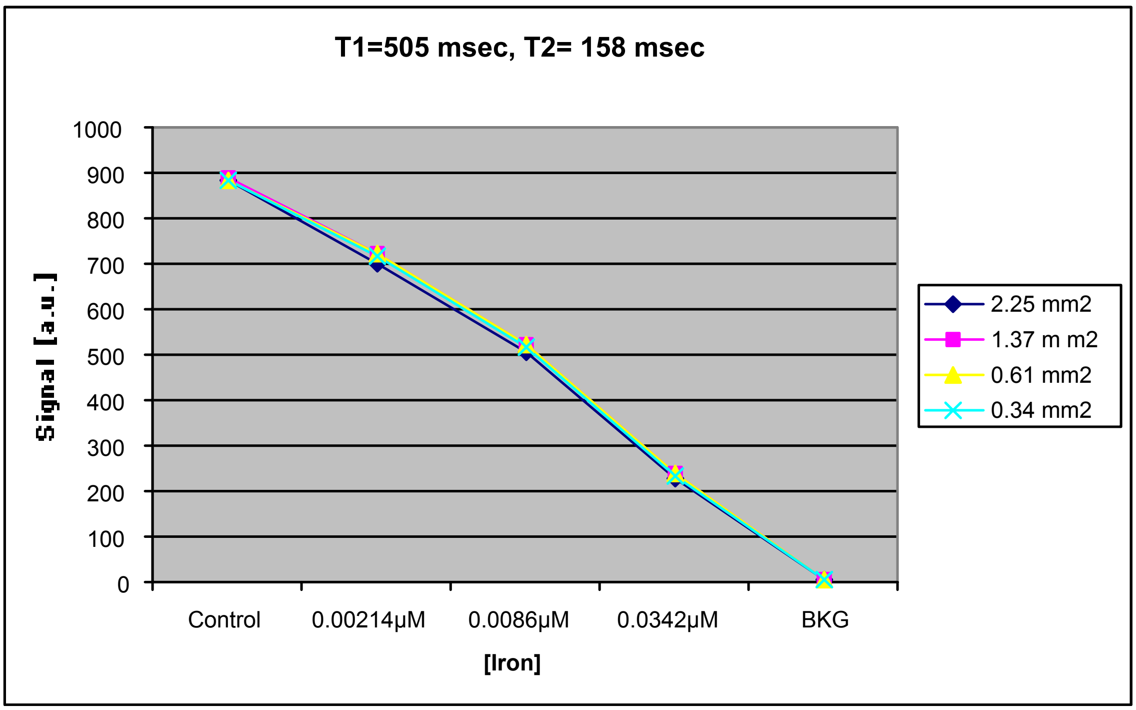

Figure 26: Effect of voxel size on signal-iron concentration relationship.

Macrophage Model

Frozen cells (J774A.1) were acquired from American Type Culture Collection (ATTC) and reconstituted in 75cm2 cell culture flasks in DMEM with 10% FBS and 1% Penicillin - Streptomycin Solution. Cells were grown to 75% confluence over a period of 3-4 days. Medium was changed daily.

Figures 27-30 are 40x digital micrographs of macrophages cultured for 24 hours at an initial concentration of approximately 5000 cells per slide chamber in DMEM with 10% FBS. Cells were then incubated at 37^{o}C in a 5% carbon dioxide atmosphere. The medium was then removed, washed with PBS to remove any non-adherent (non-viable) cells and replaced with fresh medium containing 0.0 (Fig 27), 1.0 (Fig 28), 10 (Fig 29) and 100 (Fig 30) µL of stock Feridex in 1 ml standard DMEM medium with 10% FBS. After 4 hours medium was removed, cells washed 3x with 1X PBS (4ºC) and fixed with 3% glutaraldehyde overnight. Cells were stained with Acridine orange for cytoplasm and nucleus and counter-stained with Prussian blue for iron.

The dose dependent increase in cytoplasmic iron can be observed. Arrows in figure 28 indicate small accumulations. Color based analysis available on the digital microscope was used to integrate the area of iron (see example in figure 13) and relate it to the area of the cytoplasm and nucleus. Automated cell counting will calculate the average absolute area of iron in each cell. This was used to determine differences in iron uptake in treated versus control macrophage cell groups.

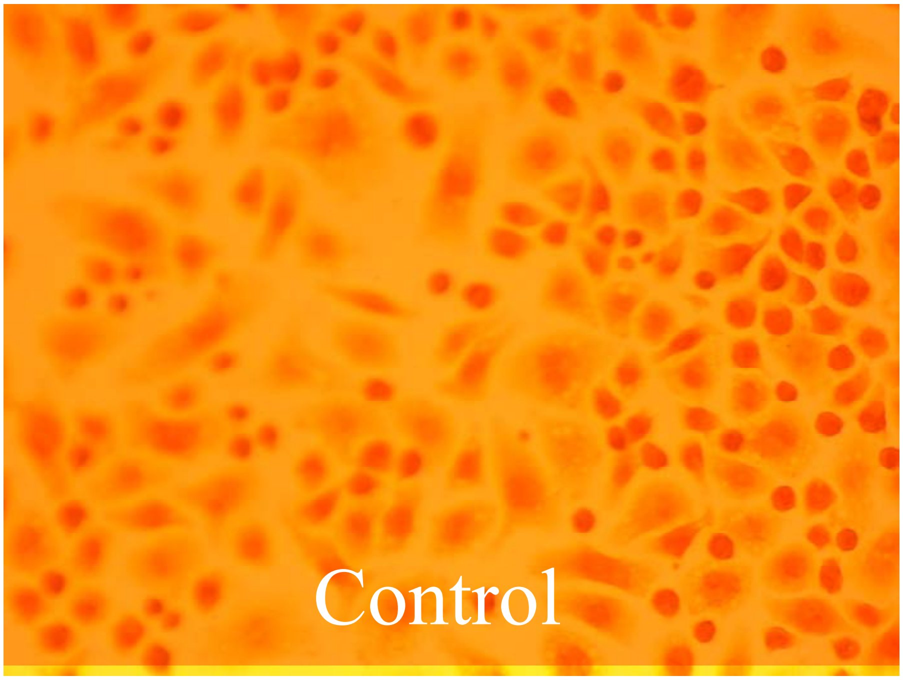

Figure 27: J774 macrophages stained with Acridine Orange and Prussian Blue. Control culture without iron particles.

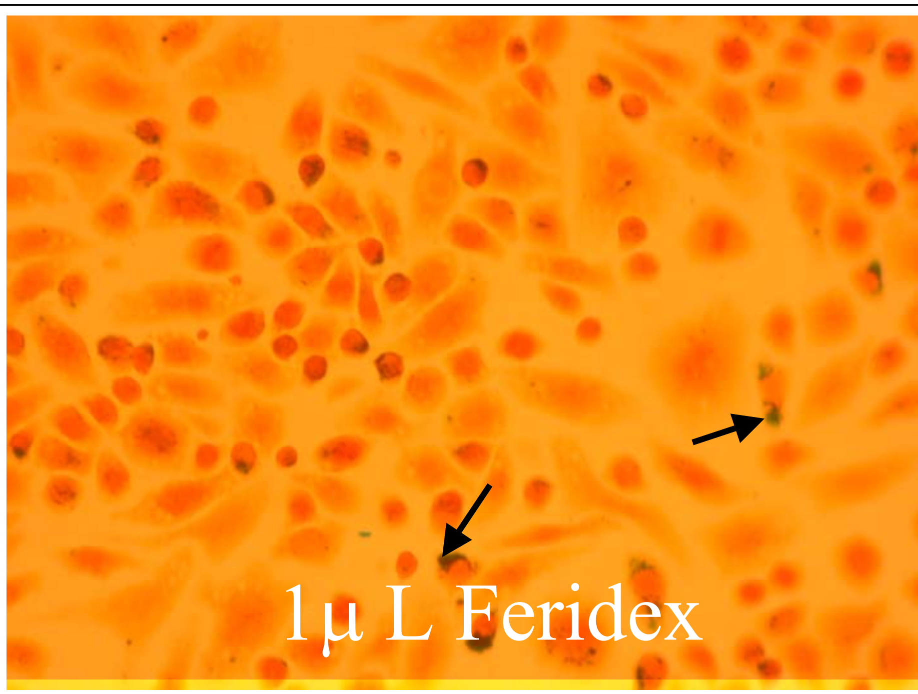

Figure 28: J774 macrophages incubated for 4 hours with 1µL/800µL then stained with Acridine Orange and Prussian Blue.

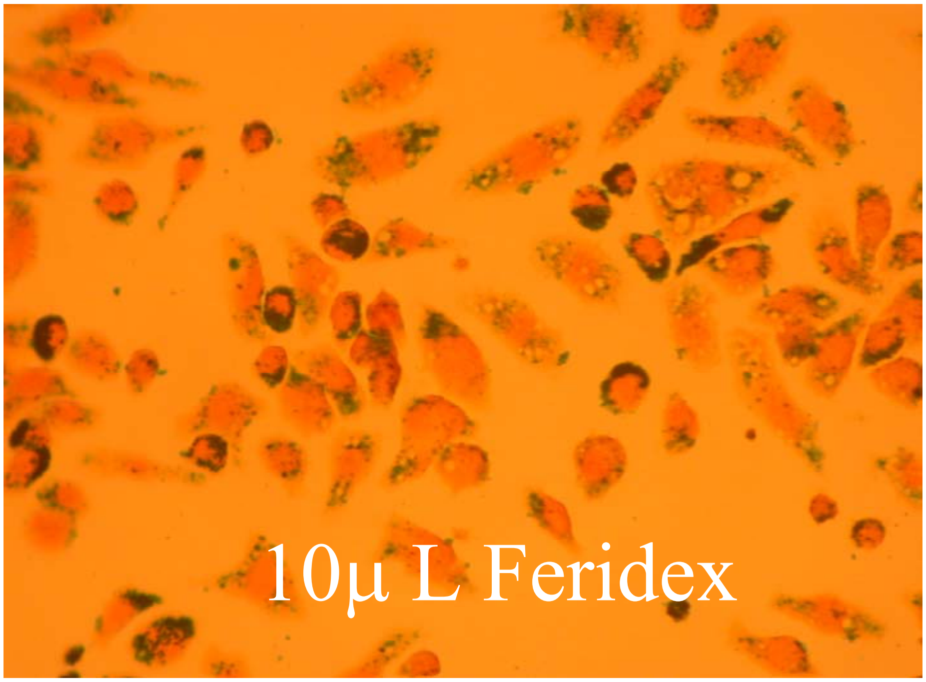

Figure 29: J774 macrophages incubated for 4 hours with 10.0 mL/800 mL then stained with Acridine Orange and Prussian Blue. Regions of cytoplasmic iron is present.

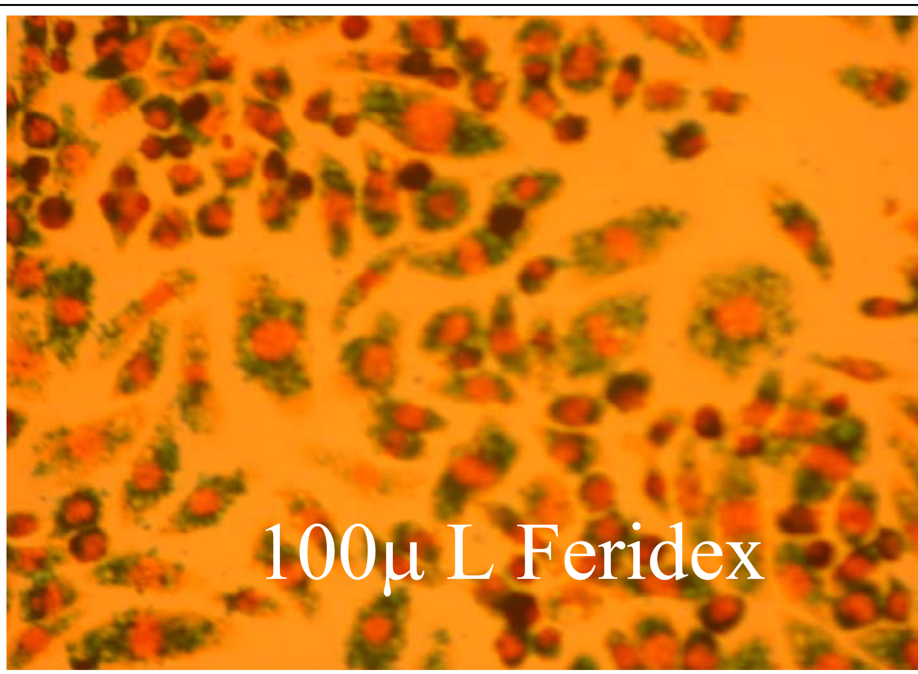

Figure 30:J774 macrophages incubated with 100μL Feridex. Cytoplasmic space is filled with iron particles.

Validation of Method used to Determine Macrophage Cell Density

Cell density was automatically estimated by creating a ratio between the area in μm^2 of the orange band of the color spectrum determined to be specific for macrophage nuclear staining using Acridine orange, to the total area scanned by the ChromaVision system. Validation was performed using Scion Image 4.0.2 a PC version of the NIH Image analysis program. In sub-regions containing between 50-300 cells (figure 31), the orange area/total are ratio was compared to direct semi-automated cell counting (figure 32). Specifically, images were filtered using an edge enhancement filter (Sobel), then converted to binary data using a manually applied threshold. A cell counting program within Scion software version 4.0.2 (Scion Corp, www.scioncorp.com) was then applied (Figure 32).

Manual editing was applied to correct for touching cells being undercounted or non-cell material resulting in an over-count. The images below are examples of the raw data (figure 31) and the Scion processed (figure 32) and numbered cells. The nuclear orange area/total area for all slides was 3.18±3.59%.

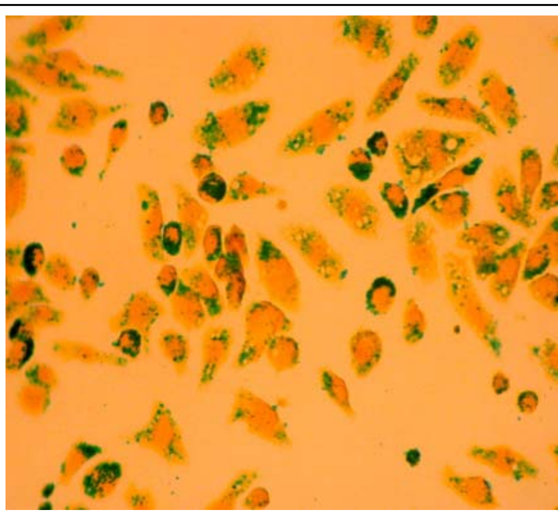

Figure 31: Sub-region of cells used for validation of automated cell density.

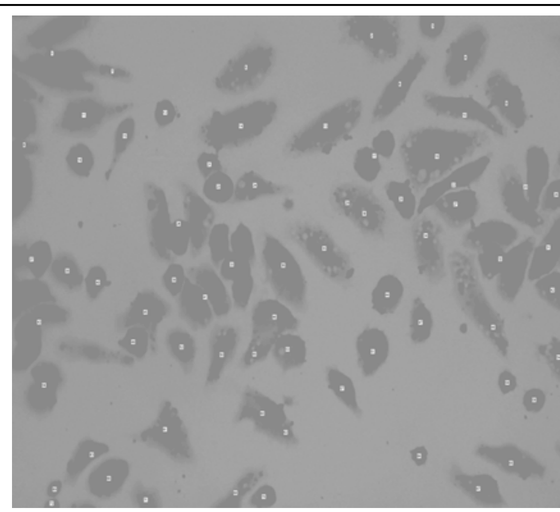

Figure 32:Processed image with cell density calculated using SCION Image software.

Linear Regression of automated cell density versus manual cell count

Cell Count = -33.303 + (11.378 * Orange Ratio (%))

N = 10.000

R = 0.992 Rsqr = 0.984 Adj Rsqr = 0.982

Standard Error of Estimate = 9.464

	Coefficient	**Std. Error**	**t**	**P**
Constant	-33.303	8.083	-4.120	0.003
Orange Ratio (%)	11.378	0.517	22.017	<0.001

Analysis of Variance:

	DF	**SS**	**MS**	**F**	**P**
Regression	1	43413.517	43413.517	484.740	<0.001
Residual	8	716.483	89.560		
Total	9	44130.000	4903.333		

Normality Test: Passed (P = 0.823)
Constant Variance Test: Passed (P = 0.081)
Power of performed test with alpha = 0.050: 1.000

It can be seen from the slope of the regression equation (Coefficient for Orange ratio) that the Orange Area Ratio as measures by the ChromaVision system provided an underestimation of the cell density compared to direct cell counting. The overall relation ship was quite linear (figure 33, $R^2 = 0.98$) and thus permits use of the regression equation as a correction factor to accurately predict actual cell density.

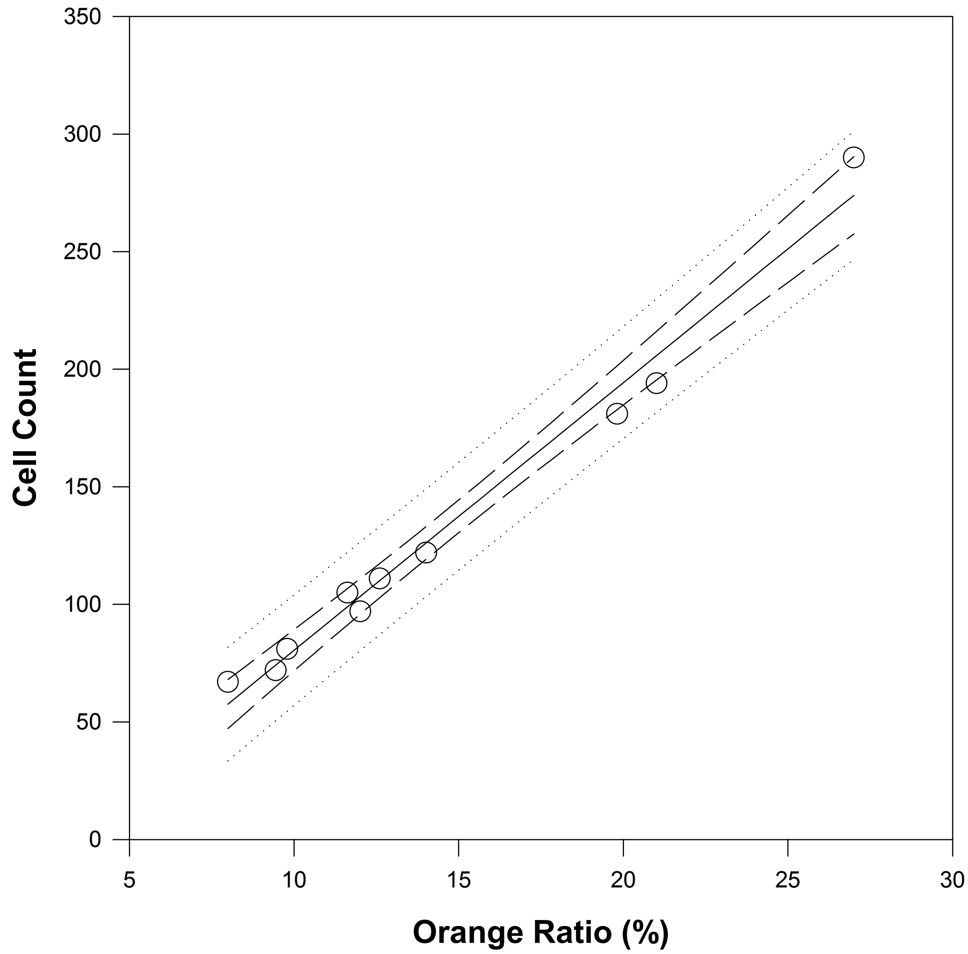

Figure 33: Regression analysis of semi-automated cell counting (SCION Image) versus fully automated area based cell density calculation (ChromaVision).

Validation of Macrophage Uptake of Iron Nanoparticles

Iron uptake was determined by calculating the ratio of area (number of pixels) of the blue part of the full color spectrum determined to be associated with Prussian blue staining of iron particles *inside* macrophages to total area analyzed. Results in treatment wells were compared to control wells incubated with the same concentration of Feridex. Results were expressed as a percent increase or decrease to control. Validation included 1. Determination of the level of “background” blue. This was the average blue area ratio in wells not treated with Feridex. 2. The relationship between iron concentration and blue area ratio over the tested iron range, and at multiple points over a lower concentration range was determined using linear regression analysis. Due to the particle size, direct comparison between blue area ratio and the number of particles is not possible as with cell number to orange area ratio. The regression analysis disclosed an underestimation of iron uptake (as measured by blue area ratio) as the iron concentration increased. This could be caused by a number of factors. First, the amount of iron taken up by cells may not be an exact measure of the amount of iron internalized. While it is known that uptake increases with increasing concentration, trans-membrane routes of internalization may become saturated resulting in the observed non-linearity. Secondly, the ChromaVision system is a 2D measure of 3D cells and cell iron. Iron particles located behind the cell nucleus or out of the focal plane could be undercounted or missed entirely. It is for these reasons that relative comparisons between control and treatment wells with the same iron concentration rather than absolute internal cell iron were used.

Uptake Characteristics in Untreated Cells

Untreated cells from all slides were pooled to permit analysis of SPIO dose uptake relationships. Figure 34 compares the calculated area associated with

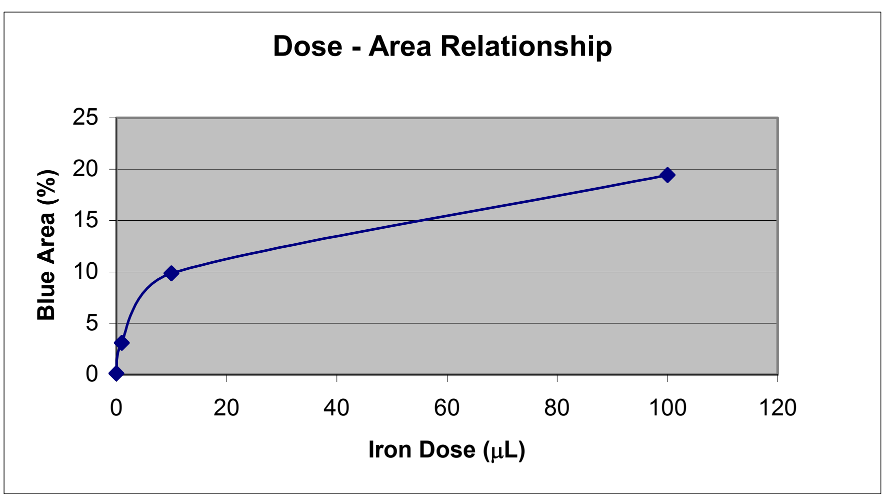

Figure 34:Plot of concentration of administered iron versus calculated "Blue" area.

Prussian Blue SPIO for control and the 3 SPIO doses. In the 22 pooled samples, the mean blue area ratio (blue area in μm^2/total sampled area in μm^2 x 100) was 19.4$\pm$7.6% at a 100 μL (1.12mg/ml) dose, 9.9 $\pm$5.6% for a 10 μL (112.0 μg/ml) dose, 3.1$\pm$5.5% at a dose of 1.0 μL (11.2 μg/ml) and 0.1$\pm$0.4% in the control wells. This last value represents the background error associated with the analysis method and will be covered in more detail in the "Validation" section. There was a strong relationship between dose and area ratio. Linear regression analysis was performed after performing a log transform of both the SPIO concentration and the area ratio values. Figure 35 is a plot of this relationship.

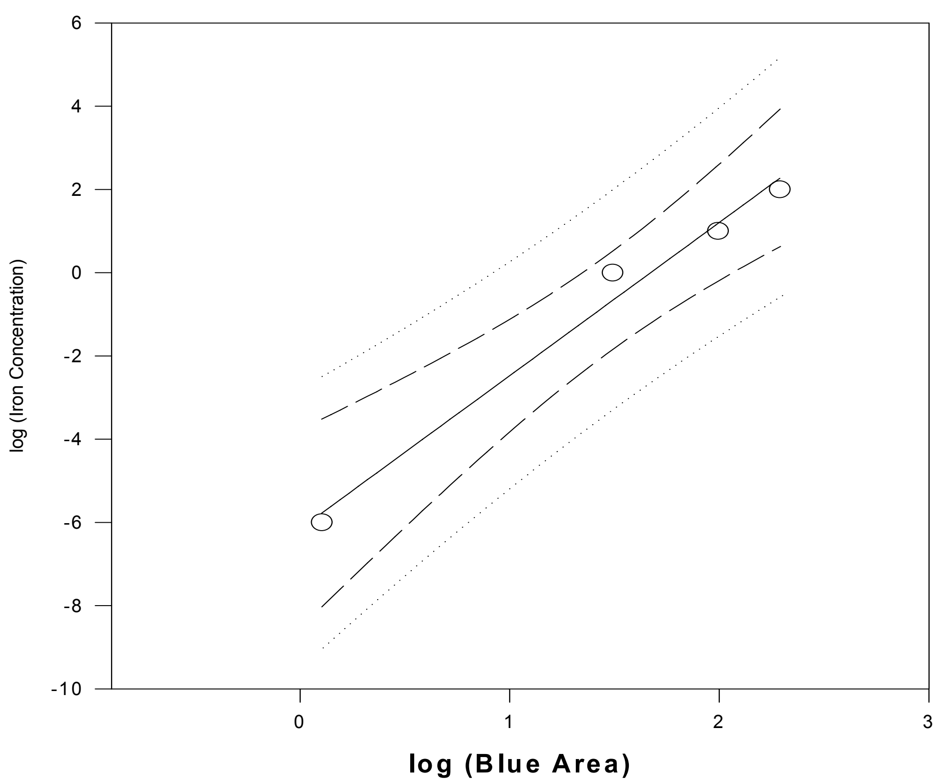

Figure 35: Iron (SPIO) concentration versus ChromaVision derived "Blue " area after log transform.

The r^2 value of this relationship is 0.92 and the regression equation: log (Iron Concentration) = -6.157 + (3.681 * log (Blue Area)). It can be seen from the slope that at higher SPIO concentrations the uptake is not in proportion to dose. This is also evident from the calculated (Area Ratio / SPIO concentration) ratio which falls from 30.9 at 1 μL to 9.8 at 10 μL to 1.9 at the highest SPIO concentration (100 μL). This is most likely due to saturation of endocytotic pathways. However, nonlinear performance of the digital image analysis system may also contribute to this effect. To better understand this relationship a group of cells were incubated with 2,4,6,8,10,12,14 and 16 μL of stock Feridex. The relationship (Figure 36) was similar to that observed over the 0-100 μL SPIO range. Again the area ratio did not increase at the same rate as the SPIO concentration. The r^2 value derived from linear regression analysis was 0.99 and the regression equation: Iron Concentration = -3.529 + (0.112 * Blue Area).

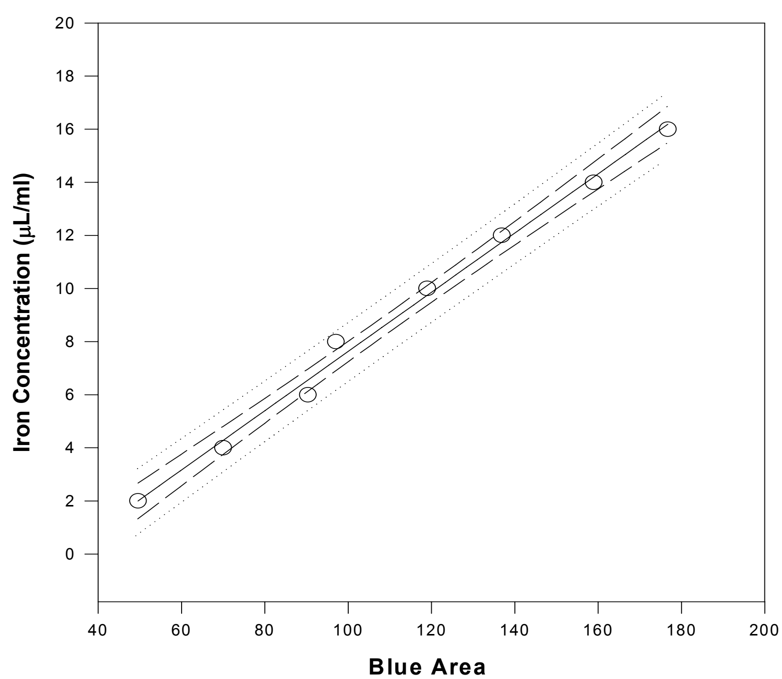

Figure 36: Iron concentration-Blue area relationship over limited "low-dose" range.

Time-Uptake Relationship

The time –uptake relationship was determined in macrophages incubated with 10μL stock Feridex solution. Cells were fixed after 5, 10, 60, 240 360 and 480 minutes of incubation. Background from untreated cells not exposed to SPIO was determined from a group of 10 samples to be 0.448±0.285 (area ratio). The area

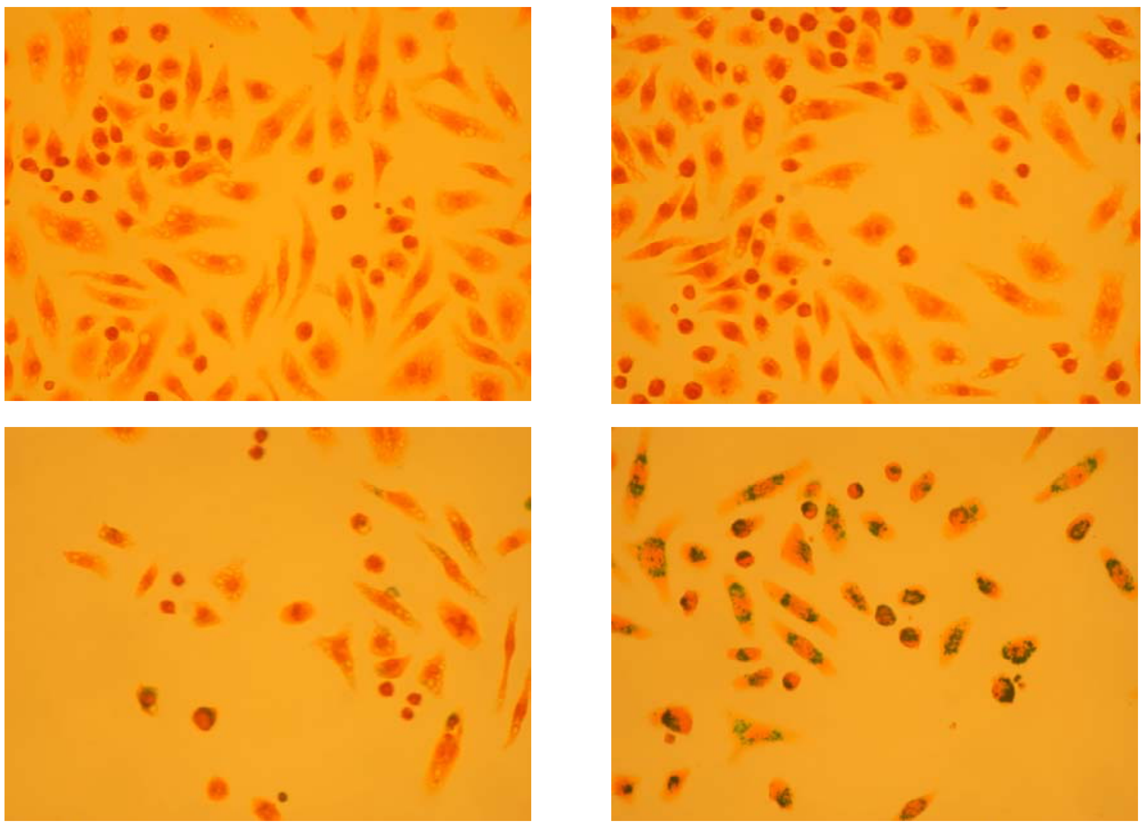

Figure 37: Examples of iron uptake after 10 μL Feridex administration. (5 min top left, 10 min top right, 1 hour bottom left, 4 hours bottom right). Progressive increase in cytoplasmic iron can be seen.

ratio measured at 5 minutes was 0.843±0.003 which was significantly greater than background (p=0.028, 2-tailed *t*-test). The area ratio peaked at 240 minutes. Uptake at 240, 360 and 480 minutes were not significantly different (p=NS, ANOVA). Therefore all uptake measurements were calculated after incubation with SPIO after 240 minutes. Figure 37 shows examples images of progressive SPIO uptake over a 4-hour period.

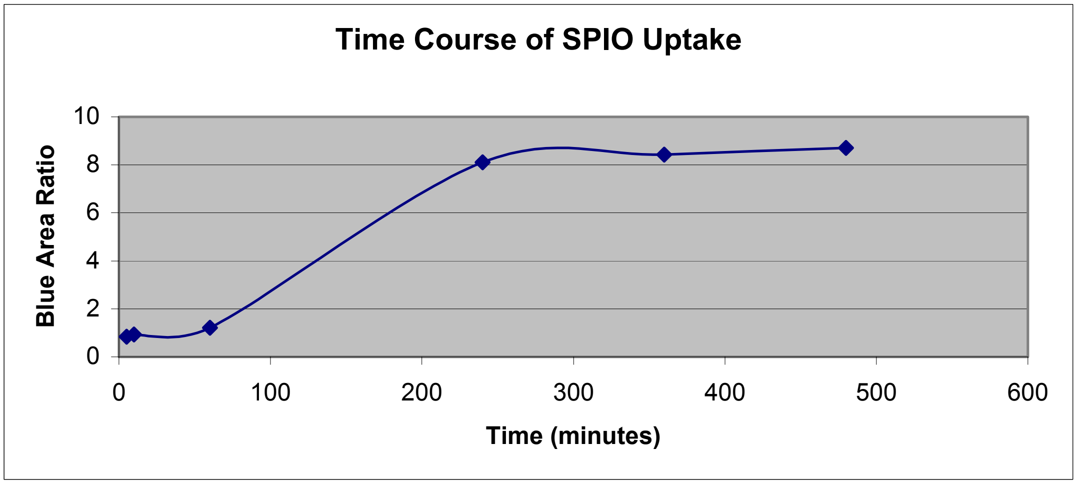

Figure 38: Plot of time-uptake relationship for cells incubated with 10 μL Feridex.

Figure 38 shows the time course of macrophage uptake of SPIO. While there was a statistically significant uptake as early as 5 minutes after SPIO administration, practically, it can be seen that substantial uptake does not occur until after 4-hours of incubation. In that these data were based on a small sample at a single dose, a more extensive evaluation looking at multiple SPIO concentrations at multiple times was undertaken.

Effect of Iron Oxide Concentration on Time-Uptake Relationship

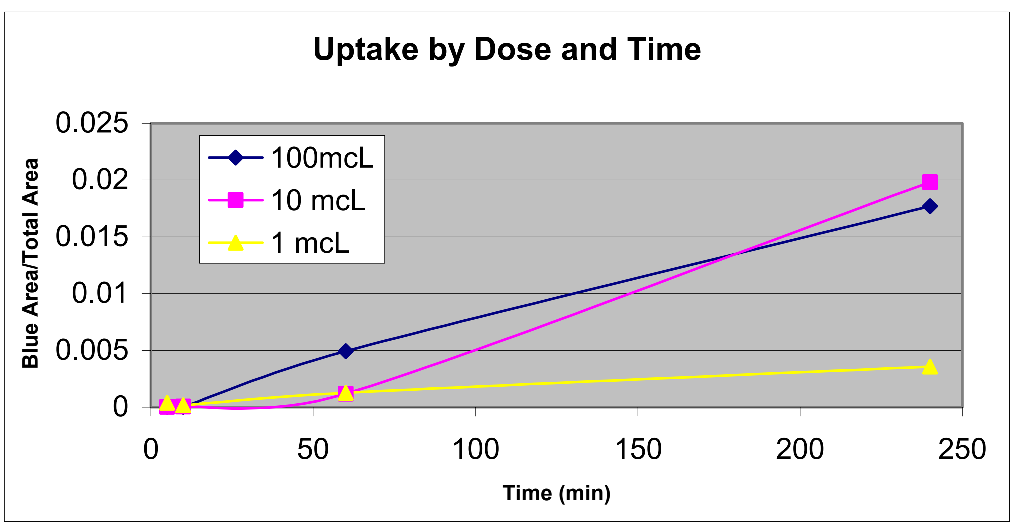

Figure 39: Effect of administered iron concentration on time-uptake relationship.

In a separate set of experiments a complete matrix of Time (5 min, 10 min, 60 and 240 min) x SPIO Dose (1.0 μL/ml, 10 μL.ml and 100 μL/ml) was performed in triplicate from the same cell culture, at the same seeding density. 2-way ANOVA was performed to evaluate the data.

Two Way Analysis of Variance (variables: Iron Dose and Time)

Source of Variation	DF	SS	MS	F	P
Time (min)	3	7139691.639	2379897.213	30.014	<0.001
Dose	2	859526.056	429763.028	5.420	0.011
Time (min) x Dose	6	2248937.278	374822.880	4.727	0.003
Residual	24	1903021.333	79292.556		
Total	35	12151176.306	347176.466		

There was no significant uptake at 5 or 10 minutes (not significantly different from background blue measured in wells stained with Prussian blue in the absence of iron oxide particles). By 1 hour blue area was significantly different from background for all iron concentration (figure 39). Further, blue area was greater at the 100μL dose versus both 1.0 and 10.0 μL levels. This interaction between dose and uptake is one that will be consistently seen with the treatment experiments. The full output of the 2-way ANOVA including interactions between dose and uptake are listed in Appendix A1.

Effect of Treatment on Macrophage Cell Density

The quantification of macrophage uptake of iron oxide particles is performed by comparing the “blue area” after Prussian blue staining between control and treatment. This method is valid only if cell density is similar between control and treatment or if statistical differences in cell density are taken into account and used to scale blue area to cell density. The table below presents the results of analysis of 3 sub-regions in control and treatment in wells in which iron oxide particles were not added. The ratio of orange area to region of interest area x100 was determined and a 2-tailed paired *t*-test performed. When there was not difference between control and treatment cell density, 2-way analysis of variance was performed using the original data. When a difference ($P<0.05$) was observed, the treatment blue area was scaled to compensate for either an increase or decrease in treatment cell density. Two-way ANOVA was performed on the scaled data and raw data for comparison.

Table 7: Analysis of cell density in control versus treatment groups.

Treatment	Control Area-Ratio	Treatment Area-Ratio	*t*-test P-value	Scale Factor
FBS	0.457+0.184	0.481+0.280	0.056	none
Mannan	1.069+1.127	0.230+0.296	0.281	none
ACEI 0.01mM	0.410+0.362	0.544+0.404	0.157	None
ACEI 0.1 mM	2.839+1.227	2.933+2.553	0.310	None
ACEI 1.0mM	3.286+3.351	5.010+7.391	0.233	none
IL-4 10 ng	26.181+4.169	24.228+3.910	0.751	none
IL-4 20 ng	19.921+2.03	22.057+1.888	0.551	none
IL-4 40 ng	23.189+1.102	18.979+5.328	0.310	none
IFN-g 10 U	0.200+0.219	0.260+0.251	0.616	none
IFN-g 100 U	15.781+2.623	17.701+3.623	0.499	none
IFN-g 500 U	8.310+3.400	7.417+1.881	0.743	none
IFN-g 1000U	5.182+2.492	5.133+1.301	0.692	none
Cytochasin D	18.054+16.136	21.505+33.285	0.879	none
HMG 1mM	5.723+4.36	5.462+4.074	0.943	none
HMG 17.5 mM	10.392+2.935	6.131+1.019	0.033	1.69

Effect of the Presence or Absence of Serum Proteins on SPIO Uptake

Source of Variation	DF	SS	MS	F	P
[iron]	3	3133692587.125	1044564195.708	481.432	<0.001
FBS	1	97433310.375	97433310.375	44.906	<0.001
[iron] x FBS	3	317465364.458	105821788.153	48.772	<0.001
Residual	16	34715270.000	2169704.375		
Total	23	3583306531.958	155795936.172		

Opsonification is known to be one mechanism by which particulate material is endocytosed by macrophages. Data from the present study showed SPIO uptake (pooled across iron dose) in macrophages incubated in the presence of 10% FBS to be 1.6 times greater than in cells incubated without FBS. Bogdanov et al.[49] using a similar dextran coated iron oxide particle showed an even greater difference. Uptake of particles opsonized by incubation with undiluted serum for 1 hour showed a 6-fold greater uptake in macrophages than in untreated particles. It is likely that incubation in pure serum achieved a higher number of opsonized particles than the use of 10% serum in the present study. It should also be noted that Bogdanov et al.[42] use gamma counting of I-125 labeled particles to quantify macrophage uptake. It is not known how results using this method compare to the image based method of the present study. In a separate publication by the same group, (Bogdanov et al.[69]), the authors presumed that iron particles opsonized to plasma proteins enter the macrophage via Fc- or CR-receptors. While this is certainly plausible based on the known selectivity of these 2 receptors, some small portion of the increase in uptake may be the result of the 25% increase in particle size (Bodanov et al.) resulting from binding to plasma proteins. In neither the present study nor that by Bogdanov was SPIO uptake completely eliminated. Thus, while opsonification reduces uptake, other endocytotic pathways must exist.

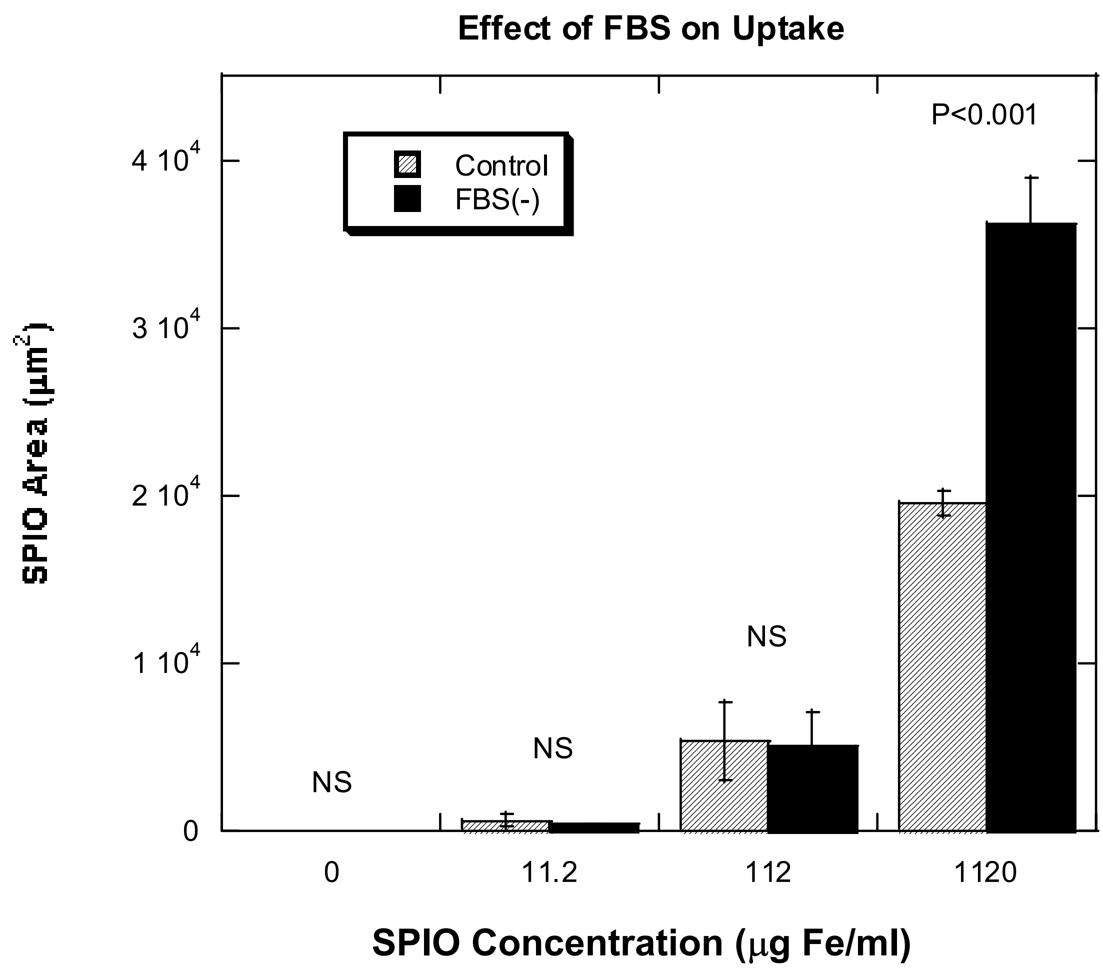

Figure 40: Effect of presence or absence of serum proteins on macrophage uptake of SPIO

Effect of Cytochalasin B on Iron Uptake

Source of Variation	DF	SS	MS	F	P
[iron]	3	4642205912.167	1547401970.722	117.310	**<0.001**

CYTO 1mcg/ml	1	53133504.167	53133504.167	4.028	**0.062**
[iron] x CYTO 1mcg/ml	3	191873468.167	63957822.722	4.849	**0.014**
Residual	16	211051657.333	13190728.583		
Total	23	5098264541.833	221663675.732		

There was a trend (P=0.062) that did not reach a significant level for treatment with cytochalasin B to reduce SPIO uptake. Based on the results from Pratten et al, that compared change in macrophage uptake of various size particles, only 100 nm latex particles and the soluble macromolecule polyvinylpyrrolidone (7 x 10^6 Da) were unaffected by cytochalasin B treatment. They showed that 300 nm particles displayed 69% of control uptake, uptake further dropped to 68% and 59% of control for 600 nm and 1100 nm latex particles respectively. It was determined that Feridex particles, aggregate in groups of particles (Jacobs[40]). Pratten et al further report that phagocytosis but not pinocytosis is substantially inhibited with 1 μg/ml cytochalasin B. Results from the present study might indicate that trans-membrane SPIO internalization occurs more by pinocytosis of individual or small groups of iron particles, or via receptor mediated pathways rather than phagocytosis of the entire aggregate. Endocytosis by means of adsorptive piocytosis, or receptor mediated means requiring interaction between individual particles and the cell surface prior to internalization would be consistent with the results observed in the present study. Complete output of the 2-way ANOVA is presented in appendix A3.

Effect of Blocking Mannose Receptors with Mannan

Source of Variation	DF	SS	MS	F	P
Mannan Block	1	5422602.667	5422602.667	1.888	0.188
[iron]	3	178080852.333	59360284.111	20.663	<0.001
Mannan Block x [iron]	3	21179777.667	7059925.889	2.458	0.100
Residual	16	45964028.667	2872751.792		
Total	23	250647261.333	10897707.014		

Addition of 1 mg/ml of mannan had no significant effect on macrophage internalization of Feridex at any tested concentration indicating that the mannose receptor does not play a significant role in endocytosis of the study particle even though it has a glucose polymer as a coating. Mannose receptors (MR) recognizes the patterns of carbohydrates that decorate the surfaces and cell walls of infectious agents. Previous studies have shown the MR to be involved in endocytosis of a wide range of materials. Montaner et al.[47] showed that horse radish peroxidase, generally used as a marker of fluid phase pinocytosis, also used the MR receptor pathway as evidenced by the effect of mannan block. Le Cabec et al.[73] showed that phagocytosis of the 6 μm polysaccharide zymosan particle was substantially inhibited after mannan treatment. The range of these 2 previous materials spans that of Feridex and excludes particle size as the factor inhibiting mannose receptor-mediated uptake.

Effect of Interleuken-4 on Macrophage Uptake of Iron Oxide

a. IL-4 at 10 ng/ml

Source of Variation	DF	SS	MS	F	P
IL-4 (10 ng/ml)	1	20276816.667	20276816.667	1.692	0.212
[iron]	3	4540930168.833	1513643389.611	126.318	<0.001
IL-4 (10 ng/ml) x [iron]	3	145048807.667	48349602.556	4.035	0.026
Residual	16	191724197.333	11982762.333		
Total	23	4897979990.500	212955651.761		

b. IL-4 (20 ng/ml)

Two Way Analysis of Variance

Source of Variation	DF	SS	MS	F	P
IL-4 (20 ng/ml)	1	93750.000	93750.000	0.00461	0.947
[iron]	3	4781933262.333	1593977754.111	78.450	<0.001
IL-4 (20 ng/ml) x [iron]	3	5172533.000	1724177.667	0.0849	0.967
Residual	16	325095190.000	20318449.375		
Total	23	5112294735.333	222273684.145		

c. IL-4 (40 ng/ml)

Two Way Analysis of Variance

Source of Variation	DF	SS	MS	F	P
IL-4 (40 ng/ml)	1	114821876.042	114821876.042	5.514	0.032
[iron]	3	5574749793.125	1858249931.042	89.239	<0.001
IL-4 (40 ng/ml) x [iron]	3	131018250.125	43672750.042	2.097	0.141
Residual	16	333171619.333	20823226.208		
Total	23	6153761538.625	267554849.505		

Iron Area Per Total Area (%)

	Control	*Treatment*
100 μL Iron:	40.29±11.17	54.94±11.11
10 μL Iron:	10.42±3.16	17.23±2.58
1 mL Iron	0.79±0.61	1.42±0.44

Interlueken-4 is produced by Th2 T-lymphocytes and its effect on macrophage activity is dependent on the presence of other cytokines. In the presence of IL-10, IL-4 acts in an immuno-regulatory manner to decrease the activity of activated macrophages. By itself, IL-4 has been shown to induce Mannose receptor expression and endocytosis in macrophages and induce an alternative form of macrophage activation[74] (Gordon, http://dunn1.path.ox.ac.uk/-cholt/sgCytoMacro.html[74]). In the present study IL-4 was studied at 10, 20 and 40 ng/ml. No effect on SPIO uptake was measured at the 2 lower concentrations. At 40 ng/ml there was a significant increase in uptake of SPIO (10198 μm^2 blue versus 14573μm^2) which expressed as percent blue of total area equates to 12.9+1.20% and 18.3+1.73% for control and IL-4 (40ng/ml) respectively (figure 41). Two-way ANOVA indicated that the treatment effect was similar at the 3 tested iron particle concentrations. There have been no previous studies

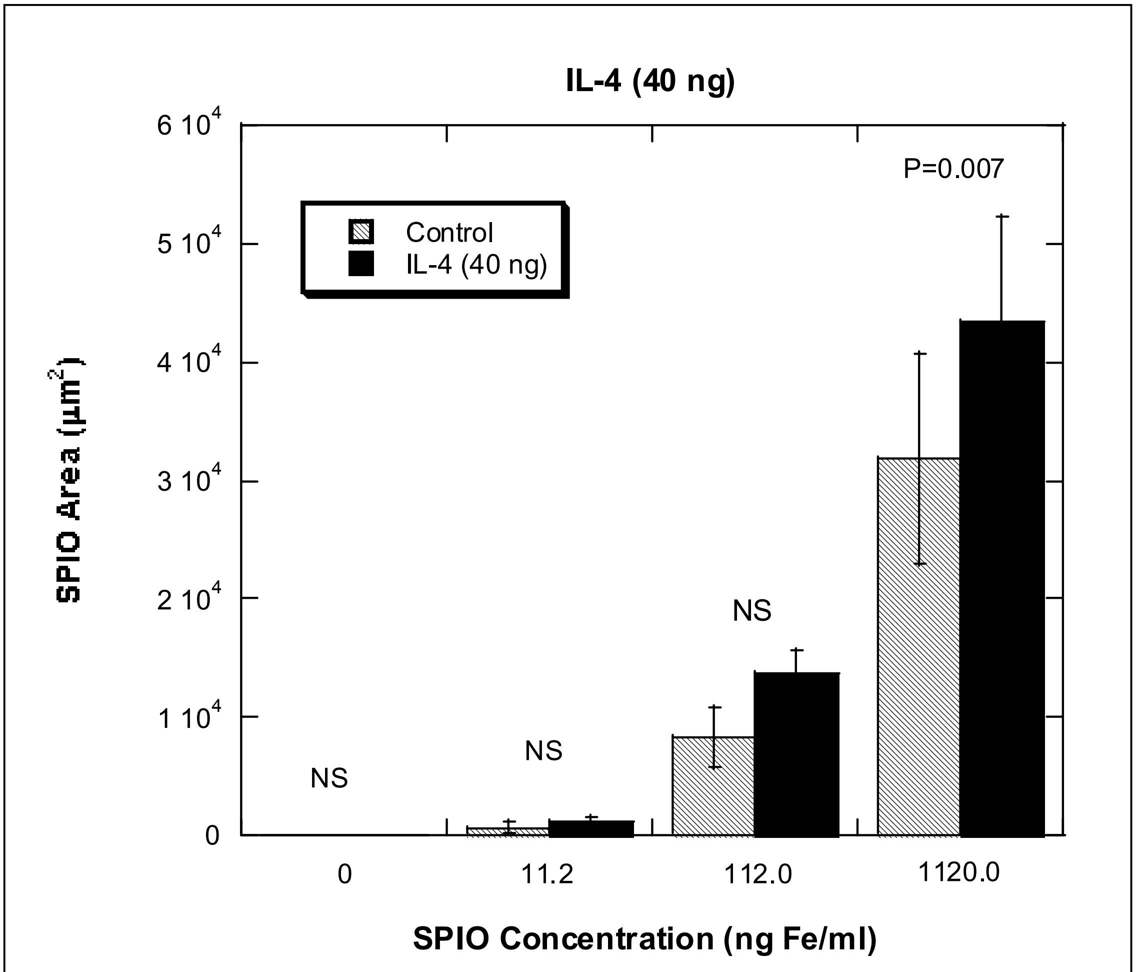

Figure 41: Effect of the cytokine IL-4 (40 ng/ml) on macrophage uptake of SPIO

investigating the effect of IL-4 treatment on macrophage uptake of iron oxide particles. Montaner et al.[47]used horseradish peroxidase (HRP) and to probe the effects of IL-4 on macrophage pinocytosis and mannose receptor endocytosis. They showed that treatment with 20 ng/ml of IL-4 resulted in a 2.8 fold increase in non-mannose receptor uptake and a 6-fold increase in mannose receptor mediated endocytosis. While the direction of change reported by Montaner et al.[40] is the same as that reported in the present study, there are a number of factors that may explain the difference in the magnitude of effect observed after IL-4 treatment. In the Montaner study. Cells were treated with IL-4 for 6 days prior to measuring cell uptake, while the present study limited treatment to 24 hours. IL-mediates uptake on a number of levels including the increase in density of tubular vesicles underneath the plasma membrane and increase gene expression of both transferring and mannose receptors. The time required for these separate events may result in less upregulation of pinocytosis and endocytosis after 1 versus 6 days of IL-4 treatment. The material tested by Montaner (HRP) showed significant macrophage uptake via the mannose receptor pathway. The present study showed no significant reduction in uptake when the mannose receptor was blocked with mannan. Finally, the Montaner study used primary human macrophages incubated with human serum. It is possible that these macrophages respond to a greater degree than murine macrophages (J774). In a study by Swanson et al[75] they showed that HRP itself stimulates pinocytosis and may have resulted in an overestimation of the direct effect of IL-4 by Montaner et al.

Effect of Human Interferon Gamma on Macrophage Uptake of Iron Oxide

a. IFN-γ at 10 U/ml

Two Way Analysis of Variance

Source of Variation	DF	SS	MS	F	P
IFN-γ (10u/ml)	1	3711493.500	3711493.500	0.346	0.565
[iron]	3	4715548409.500	1571849469.833	146.523	<0.001
IFN-γ (10u/ml) x [iron]	3	1652630.833	550876.944	0.0514	0.984
Residual	16	171642074.667	10727629.667		
Total	23	4892554608.500	212719765.587		

b. IFN-γ at 100U/ml

Two Way Analysis of Variance

Source of Variation	DF	SS	MS	F	P
IFN-γ (100u/ml)	1	2335008.167	2335008.167	0.290	0.598
[iron]	3	6917369859.500	2305789953.167	286.242	<0.001
IFN-γ (100u/ml) x [iron]	3	246260960.167	82086986.722	10.190	<0.001
Residual	16	128886100.000	8055381.250		
Total	23	7294851927.833	317167475.123		

b. IFN-γ at 500 U/ml

Two Way Analysis of Variance

Source of Variation	DF	SS	MS	F	P
IFN-γ (500u/ml)	1	4428.167	4428.167	0.000340	0.986
[iron]	3	3562854979.333	1187618326.444	91.275	<0.001
IFN-γ (500u/ml) x [iron]	3	17911468.500	5970489.500	0.459	0.715
Residual	16	208182604.000	13011412.750		
Total	23	3788953480.000	164737107.826		

c. IFN-γ at 1000U/ml

Two Way Analysis of Variance

Source of Variation	DF	SS	MS	F	P
IFN-γ	1	91057312.667	91057312.667	4.726	0.045
[iron]	3	2217676090.333	739225363.444	38.366	<0.001
IFN-γ x [iron]	3	181412470.333	60470823.444	3.138	0.055
Residual	16	308285008.000	19267813.000		
Total	23	2798430881.333	121670907.884		

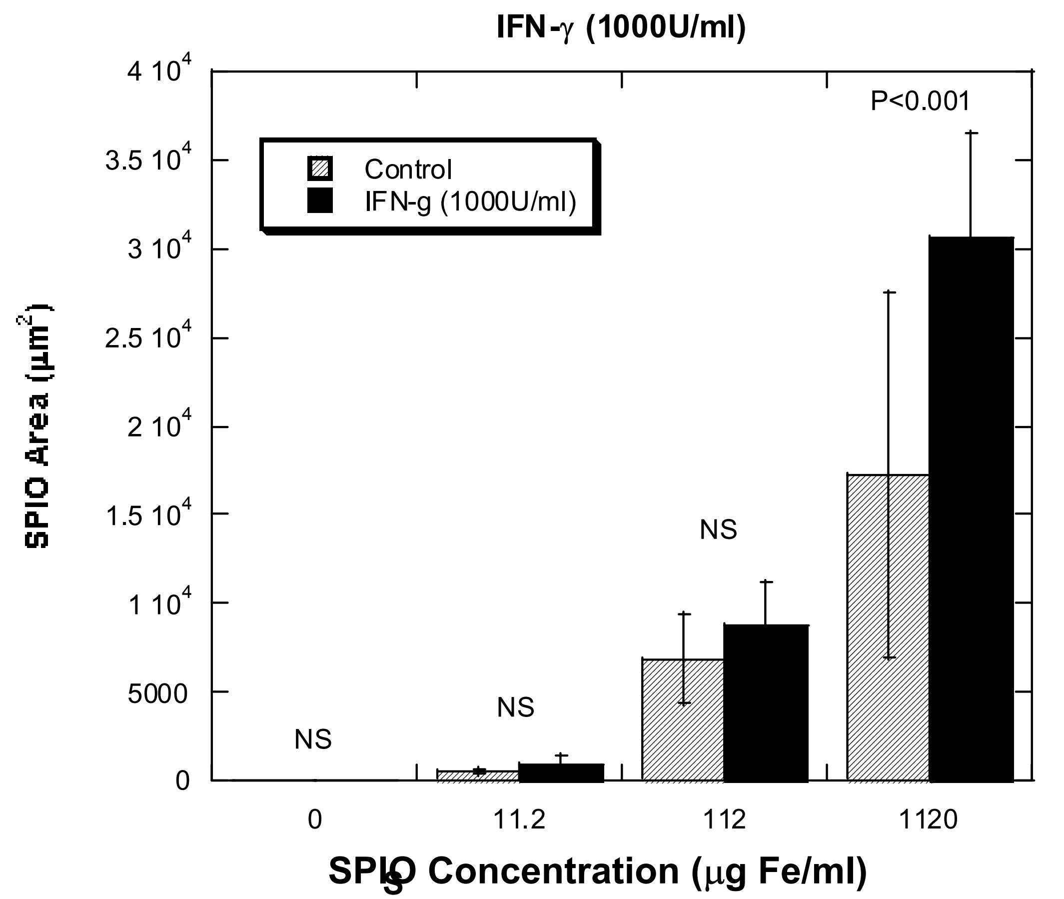

Figure 42: Effect of high dose (1000U/ml) IFN-γ on macrophage uptake of SPIO

Interferon-γ (IFN-γ), is a pleiotropic cytokine widely involved in the regulation of both innate and adaptive immune responses. The major biological activities of IFN-γ include antiviral and antiproliferative properties, macrophage activation, control of apoptosis and promotion of antigen processing, presentation and T helper type 1 (T_H1) differentiation.[76] The present study did not show any effect of IFN-γ on SPIO uptake over physiological and moderately elevated levels (10 ng/ml, 100 ng/ml and 500 ng/ml) of this cytokine. However at high dose (1000U) substantially increased SPIO uptake was observed (figure 42). This is the first study to evaluate the effect of IFN-γ on SPIO uptake. Previous studies looking at the effect of IFN-γ on macrophage function have shown it (20ng/ml) to reduce both pinocytosis and mannose receptor-mediated endocytosis of HRP in vitro.[47]

Stopeck et al.[77] reported that this low dose IFN-γ had no effect on LDL receptor activity. Taken together these reports fit with the data from the present study where IFN-γ showed no effect on SPIO internalization at comparable cytokine concentrations which would tend exclude a mannose receptor pathway (as did the mannan block data). Secondly, the lack of effect of IFN-γ (10-500 U/ml) on LDL receptor activity would permit the continued consideration of the LDL receptor pathway as a potential route for SPIO entry. The effect of high IFN-g concentration on SPIO uptake may be the result (but not proven in the present study) of secondary biomolecules. For example Inagaki et al.[78] reported that human macrophage cells produced monocyte chemoattractant protein-1 (MCP-1) increasingly as IFN-γ concentration was increased. MCP-1 is know to directly activate macrophages[79] and may explain the increased SPIO endocytosis in the present study. Finally, Schulze et al. [80] reported that the SPIO was efficiently endocytosed in C6 cells at concentrations of 4.0×10^{-10} M Fe, which the authors concluded was “several orders of magnitude below which significant uptake by fluid phase pinocytosis would occur.”

Effect of Angiotensin Converting Enzyme (ACE) Inhibition on Macrophage Uptake of Iron Oxide

a. Captopril at 0.01 mM

Two Way Analysis of Variance

Source of Variation	DF	SS	MS	F	P
CAPT 0.01mM	1	1397320.042	1397320.042	0.0919	0.766
[iron]	3	4773544524.458	1591181508.153	104.693	<0.001
CAPT 0.01mM x [iron]	3	1533378.125	511126.042	0.0336	0.991
Residual	16	243176560.000	15198535.000		
Total	23	5019651782.625	218245729.679		

b. Captopril at 0.1 mM

Two Way Analysis of Variance   Wednesday, July 12, 2000, 19:15:23

Source of Variation	DF	SS	MS	F	P
CAPT 0.1mM	1	1443541.500	1443541.500	0.373	0.550
[iron]	3	3468539248.833	1156179749.611	298.661	<0.001
CAPT 0.1mM x [iron]	3	3719204.167	1239734.722	0.320	0.811
Residual	16	61939300.000	3871206.250		
Total	23	3535641294.500	153723534.543		

c. Captopril 1.0 mM

Two Way Analysis of Variance

Source of Variation	DF	SS	MS	F	P
CAPT 1.0mM	1	1458294.000	1458294.000	0.102	0.753
[iron]	3	5002019394.167	1667339798.056	117.156	<0.001
CAPT 1.0mM x [iron]	3	7517576.333	2505858.778	0.176	0.911
Residual	16	227707774.000	14231735.875		
Total	23	5238703038.500	227769697.326		

Captopril is classified as an ACE inhibitor. ACE inhibitors block the body's production of angiotensin-converting enzymes (ACE), a chemical needed by the body to make angiotensin II, a chemical that increases blood pressure by narrowing arteries. This process leaves blood vessels more relaxed, which decreases blood pressure and increases the flow of blood and oxygen to the heart. Captopril is primarily used for treatment of high blood pressure. However its effect on macrophage function and effect on atherosclerotic progression has been established. In the present study, treatment with 0.01 mM, 0.1 mM or 1.0

mM Captopril effected neither cell density or SPIO uptake. Keider et al.[81] showed that Ang-II possesses additional atherogenic properties such as increasing the activity of the macrophage oxidized LDL receptors. Hayek et al.[82]showed that ACE treatment significantly reduced oxLDL uptake by macrophages. The present study has shown a significant reduction of SPIO uptake in HMG CoA reductase inhibitor treated cells. These data were used to implicate a role for the macrophage LDL receptor as an endocytotic SPIO uptake. However the data by Keider et. al and Hayek et al. do not necessarily contradict this hypothesis. In both of these studies, the mode of action of ACE inhibition was not directly on the macrophage receptor but rather by way of reducing elevated angiotensin II. It has been well validated that angiotensin II, particularly when elevated, stimulates lipid accumulation by increasing oxLDL receptor density (Keider et al.). It can also increase lipid peroxidation, thus increasing the concentration of lipids endocytosed via the non-concentration regulated oxLDL receptor.[83] The medium used in this study, DMEM is free from angiotensin II however, the FBS likely contains at least low levels. Thus, the lack of change in macrophage uptake of SPIO, indicates that none of the direct effects of ACE inhibition alter the pathways used by macrophages to internalize iron particles. Specifically, The known effect of ACE inhibitors on angiotensin II do not significantly alter lipid other receptors, or other modes of SPIO internalization.

Effect of HMG CoA Reductase Inhibition (Mevinolin) on Macrophage Uptake of Iron Oxide

a. Mevinolin (1.0 μM)

Two Way Analysis of Variance

Source of Variation	DF	SS	MS	F	P
HMG 1.0mcM	1	132337977.042	132337977.042	11.208	**0.004**
[iron]	3	3500330496.458	1166776832.153	98.813	<0.001
HMG 1.0mcM x	3	213200698.458	71066899.486	6.019	**0.006**

[iron]					
Residual	16	188927352.000	11807959.500		
Total	23	4034796523.958	175425935.824		

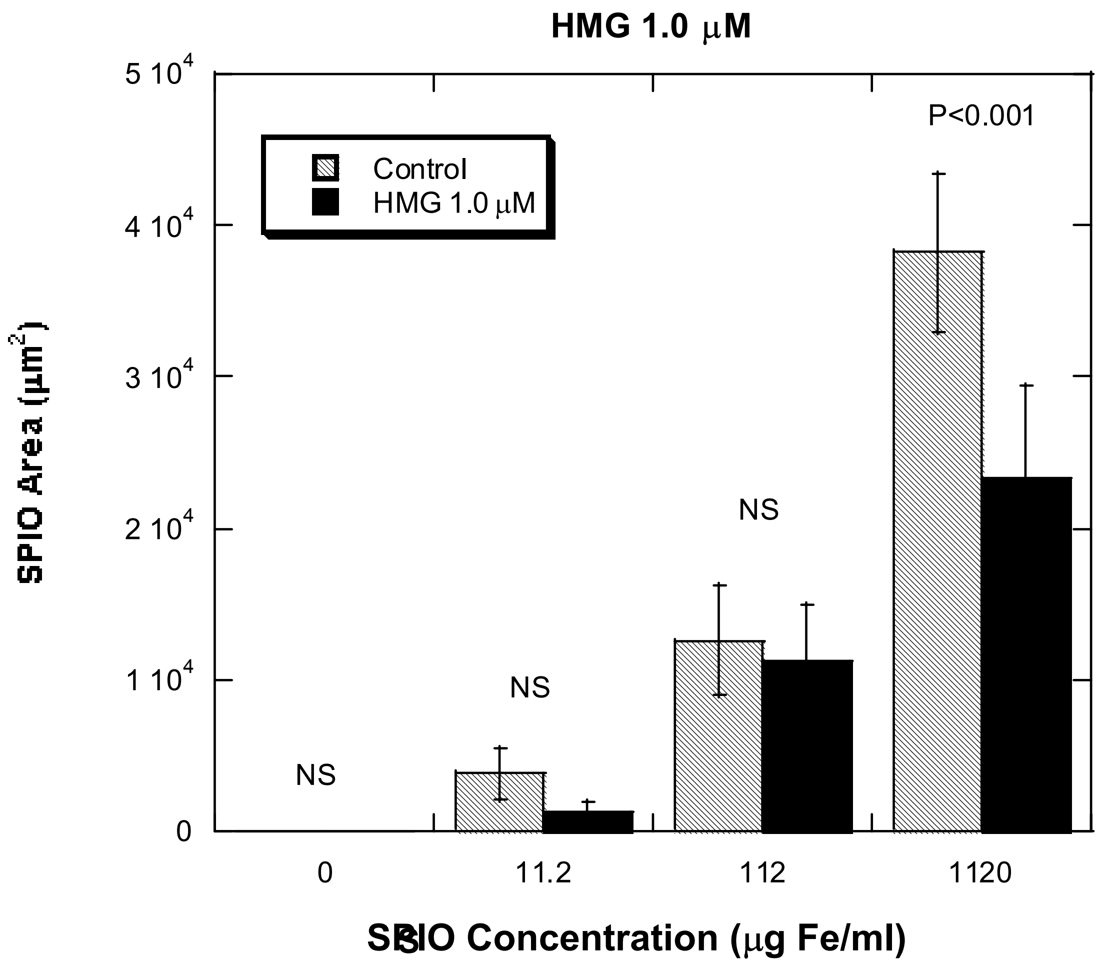

Figure 43: Effect of 1.0 μM mevinolin on macrophage uptake of SPIO

b. Mevinolin (17.5 μM)

Two Way Analysis of Variance

Source of Variation	DF	SS	MS	F	P
HMG	1	283064622.042	283064622.042	26.913	**<0.001**
[iron2]	3	2449715493.458	816571831.153	77.637	<0.001

HMG x [iron2]	3	496210450.792	165403483.597	15.726	**<0.001**
Residual	16	168285499.333	10517843.708		
Total	23	3397276065.625	147707655.027		

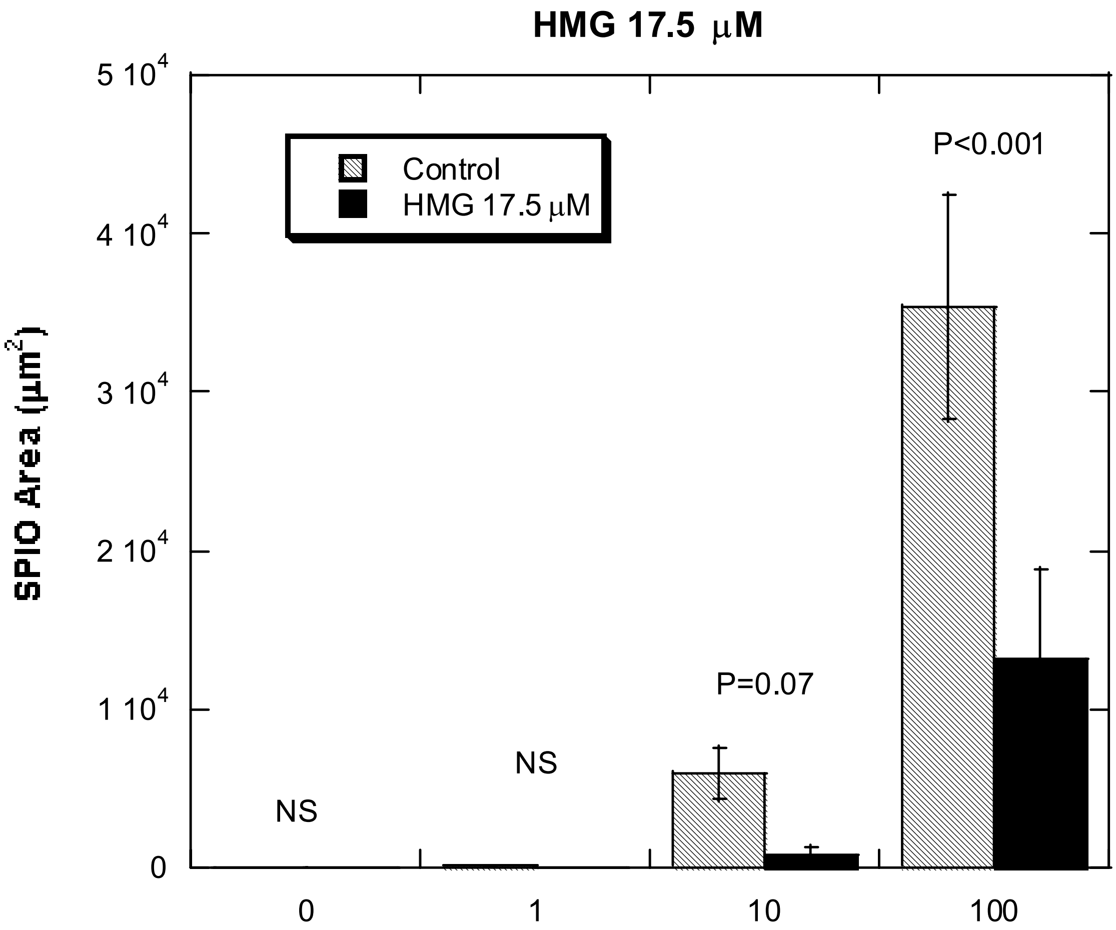

Figure 44: Effect of 17.5 μM mevinolin on macrophage uptake

c. Mevinolin at 17.5 μM Corrected

(Treatment area multiplied by 1.69 to account for reduced cell density)

Two Way Analysis of Variance

Source of Variation	DF	SS	MS	F	P
HMG	1	118368107.011	118368107.011	6.623	0.020
[iron2]	3	3471907563.896	1157302521.299	64.753	<0.001
HMG x [iron2]	3	170484041.790	56828013.930	3.180	0.053
Residual	16	285963005.284	17872687.830		
Total	23	4046722717.981	175944465.999		

Two effects were seen in macrophages treated with the HMG-CoA reductase inhibitor mevinolin. At both tested concentrations (1.0 μM and 17.5 μM) SPIO uptake was significantly diminished. At the higher HMG concentration there was also observed a lower cell density compared to control (table 7). The antiproliferative effect of statins has been well documented. Masanori et al showed a dose dependent reduction in the number of macrophage cells using the HMG-CoA inhibitor cerivastatin. Ten days of incubation of cells with as little as 0.01 mM of this agent reduced cell number compared to control. As in the present study, cell density was determined by comparison of treated to untreated cells. Thus the degree to which this difference represents anti-proliferative versus cell death could not be ascertained. A similar effect was seen by Sakai et al.[84] in macrophages stimulated to proliferate by addition of oxLDL. The present study did not observe a difference between control and HMG (1.0 μM) cells. It should be noted that Masanori treated cells for ten days prior to cell counting while the present study treated cells for 24 hours. However, incubation of cells with 17.5 μM HMG resulted in a 40% cell density compared to control.

This is the first study to document the effect of HMG treatment on macrophage uptake of iron oxide particles. Pooled across iron concentration 1.0 μM of Mevinolin resulted in a 34% decrease in SPIO uptake (figure 43), while 17.1mM statin reduced SPIO uptake 66% (figure 44) prior to correcting for the observed reduction in cell density and 42% after correction.

The effect of statins on macrophage endocytosis of oxidized LDL uptake has been well studied. Specifically, regulation the scavenger class of receptors by statins may be relevant to the present study. Zingg et al.[85] describe the 5 classes of scavenger receptors as a diverse group capable of directly binding and internalizing fatty acids, cholesterol oxLDL, HDL, LPS and indirectly aiding in endocytosis of materials as diverse as collagen, infected erythrocytes, bacteria and plastic. The size, structure and surface properties of Feridex are not dissimilar to some of these materials. Lovastatin has been shown to inhibit gene expression of the A1 scavenger receptor in human macrophages and thus reduce endocytosis of SR-A1 materials.[86] . Bellosta et al[87] showed a dose related inhibition of oxLDL uptake in macrophages treated with Fluvastatin. Uptake inhibition ranged from 14% at 0.005μM to 55% at 10.0μM. In a separate study the same group[88] determine that the HMG effect is not one of general downregulation of all endocytotic function by measuring a slight but significant increase in native LDL uptake during macrophage treatment with Simvastatin. Interpretation of data from the present study in light of previous results warrants further study to determine if scavenger receptors represent a significant endocytotic route for SPIO particles.

Discussion

Effect of Iron-Labeled Cells on MRI Signal Properties

The present study evaluated the MRI signal properties using a gel phantom loaded with increasing concentrations of the test USPIO nanoparticle. Dodd et al.[89] isolated Fischer 344 rat T cells and incubated them in culture medium with USPIO at a concentration of 2 mg Fe/10 x 10^6 cells. Using electron microscopy they confirmed that the dextran-coated USPIO particles were located in the phagocytic vacuoles. USPIO containing cells were suspended in gel at concentrations of 0.25, 1.0 and 2 x 10^6 cells/ml. Using higher resolution (50 x 50 μm) than the present study but similar scan parameters (TR = 1000 msec, TE = 30 msec) they evaluated the change in MR signal properties at 4.7 T. As in the present study overall signal intensity decreased as cell (iron) concentration increased. Their data showing that increasing TE resulted in decreased signal at the same cell (iron) concentration was in agreement to with data from the present study at 1.5T. Thus, it may be concluded that the T2 shortening effect of USPIO is similar whether the particles are intra- or extra-cellular.

Clinical Application of Feridex as a Liver Imaging Agent

The only FDA approved application of the USPIO agent (Feridex) is for detection of hepatocellular carcinoma. Administered IV, this agent is cleared from the circulation by phagocytosis of the reticuloendothelial system, including the Kupffer cells of the liver. It is the very efficient and rapid removal of feridex from the circulation which may limit its in vivo application to indirect visualization of vascular macrophages. A different product (AMI 7228) has been designed as an intravascular contrast agent, to have a longer circulation time, thus permitting grater uptake in vascular macrophages. The application for AMI 7228 is to improve blood signal for MR angiographic applications. Most focal liver lesions , particularly malignant tumors lack Kupffer cells. Therefore, the loss of signal associated with the USPIO particle is not observed in lesions resulting in retained high signal and contrast between normal and affected tissue.

In a study by Schultz et al.[90] they compared liver MRI using Feridex with CT for the detection of either primary or metastatic hepatic lesions in 57 patients. They concluded that, in this population , contrast enhanced MRI detected 76% more lesions than CT. Additionally, MRI was able to detect smaller lesions. The overall sensitivity (versus pathology in a subgroup of 22 patients) was 86% for MRI and 58% for CT ($P<0.001$). Thus by taking advantage of the cell specificity of this iron agent, the authors showed a significant improvement in diagnostic accuracy. Finally the authors calculated that MR results negated the need for biopsy in 18 patients and laproscomy in an additional 8. The calculated savings was $1901 per patient studied.

Potential Effects of Intracellular USPIO on Cell Homeostasis

Normally iron in serum is present at a concentration between 3-5 μg/ml. and is largely bound to transferrin. [91] Transferrin binds with two Fe^{3+} ions. Diferric transferrin binds to cell surface receptors and the transferrin-transferrin receptor complex is internalized in clatherin-coated vescicles. The vesicles loose their coat, fuse with endosomes and the iron is solubilized in lysosomes. USPIO, as has been shown in the present study, likely enter the cell via pinocytosis and receptor mediated endocytosis. Once inside the lysosome, the dextran coat is lost and it likely continues along the same pathway as native iron.[33]

Cellular iron homeostasis is regulated at the level of mRNA translation rather than synthesis. Iron regulatory element-binding proteins (IRP's 1 and 2) change conformation based on the cytosolic concentration of iron. When iron concentration is high, IRP-1 protein is inactivated and IRP-2 is rapidly degraded. This results in down-regulation of transferric-receptor synthesis. In the presence of low iron, the mRNA for the transferring receptor is protected from nuclease attack, permitting increased receptor mediated iron uptake.

There are a number of mechanisms by which excess cellular iron can produce damage. Low molecular weight iron can act as a catalyst in the Fenton reaction to potentiate oxygen toxicity by the generation of a wide range of free radical species, including hydroxyl radicals, $OH^{\bullet}$. For example:

$$Fe^{2+} + H_2O_2 \rightarrow Fe^{3+} + OH^{-} + OH^{\bullet}$$

Hydroxyl radicals are known to react with a wide range of cellular components including the amino acid residues and purine and pyrimidine bases of DNA, membrane lipids and can initiate lipid peroxidation. Cells differ in their sensitivity to the harmful effects of iron overload. Cells such as liver hepatocytes containing a high level of antioxidant protection are less sensitive, while neural cells will be more sensitive to iron mediated oxidative stress. Because of their role in being able to phagocytose senescent red blood cells, macrophages have developed an advanced method to balance cellular iron concentractions.

The production of NO by macrophages is a major defense mechanism used against invading organisms. Legssyer et al. [92] used dextran coated iron particles similar to the USPIO used in the present study to evaluate the effect of iron loading on the ability of macrophages to respond to infection. Through intraperitoneal injections they were able to double the iron content in alveolar macrophages. They showed that primary macrophage cultures from this mouse model stimulated with IFN-γ for 44 hrs, displayed a significant reduction in NO production. These data indicate that macrophages overloaded with iron show a diminished capacity to produce NO. It is not clear as to the actual amount of increased iron associated with a clinical dose of USPIO. Thus, while there exists the potential for iron to affect the immune macrophage response, the dose-response relationship has not been established.

Future Directions

The results of this study indicate that macrophage uptake of USPIO is regulated. However there are a number of important question beyond the scope of the in vitro model used for this study.

Question 1. Can the downregulation observed in “statin” treated cells be replicated using an in vivo animal model?

Potential approach: the Watanabe White Hyperlipidemic Rabbit is a well studied model for aortic atherosclerosis. While the developed lesions are lipidic in nature compared to the complex human lesions, they are rich in macrophages and have been used in previous USPIO studies. After approval from the Animal Care and Use Committee, I propose to study 4 groups of rabbits using the smaller USPIO agent AMI 7228. This material has a longer blood residence time which should enhance uptake of arterial macrophages. Group I will serve as a control (no statin treatment), group II will be placed on statins at a weight adjusted dose to correspond to the human dose of 20 mg/day 1 month prior to imaging. Group III will be treated at the same dose for only 2 days prior to imaging and group IV will be treated for 1 week at the same dose with statin therapy withdrawn 3 week prior to imaging. All animals will be the same age at initiation of the study and will be on identical high cholesterol diets. This design will address in vivo time required for induction of effect (if observed), the carry-over effect of treatment.

Question 2a. Does the distribution of USPIO within human carotid plaque correspond to regions associated with plaque instability based on morphology and inflammatory components?
Question 2b. Does statin treatment reduce USPIO concentration and is there an association between USPIO uptake and the presence of histological and morphological features of plaque instability?

Potential approach: Human carotid endarterectomy is still a common clinical treatment for carotid stenoses. This procedure provides a means of performing human in vivo imaging with nearly immediate post-imaging histological verification. After approval from the Human Investigation Committee, enrolled patients will be administered a clinically approved dose of Feridex or AMI 7228 (if FDA approved) and imaged the following day using a 3D high resolution T2 weighted sequence with planes oriented to cut the carotid artery in cross section from 2 cm above, to 2 cm below the carotid bifurcation. Excised specimens will be processed and stained for iron, macrophages, as well as other inflammatory and structural components. Macrophage and USPIO concentration will be estimated from histology and compared with MRI. After comparison, results from patients on statin at the time of imaging (duration limits to be established) will be compared to untreated "controls".

Conclusions

As is often the case in such studies, the resultant data raise as many new questions as they do answer. However, a number of conclusions may be drawn in the context of the experimental model. The major hypothesis that uptake of SPIO particles by macrophages is regulated by both endogenous and exogenous factors, is supported by the 3 treatment groups that resulted in modulated USPIO internalization. Specifically, the presence of serum proteins (FBS) appears to be involved in a receptor-mediated pathway. The study by Bogdanov et al.[49] speculated, but did not prove, that Fc- and/or CR-receptors were involved. Importantly, their results showing lack of enhanced uptake in C6 glioma cells supports their conclusion that enhanced pinocytosis did not explain the increased uptake.

Interleukin-4 is produced by Th2 T-lymphocytes and its effects can oppose those of IFN-gamma, which is why these two cytokines were chosen for the present study. IL-4 induces Mannose receptor expression and endocytosis in macrophages. In atherosclerotic lesions IL-4 inhibits smooth muscle cell proliferation and stimulates the production of MMP's. The enhanced USPIO internalization seen in the present study, in the presence of IL-4 (40 ng/ml), does not specifically implicate an internalization pathway, but supports the idea that a receptor-mediated pathway, rather than accelerated pinocytosis is responsible for the increased USPIO uptake.[93] This is further supported by the effect of cell treatment with mevinolin. In addition to its anti-proliferative effect on macrophages, Umetani et al.[59] showed that it directly down-regulated expression of type-1 scavenger receptor mRNA. Again this indirectly supports receptor-mediated endocytosis of USPIO.

It is important to integrate the limitations of the present study into any conclusions. The most obvious limitation is the experimental model. Cells were exposed to a single treatment agent at a time. It is well appreciated that actual atherosclerotic lesion contain a diverse group of biomolecules that often act in opposing directions. Thus, the effects seen in the present study only indicate the potential for the tested materials to modulate USPIO uptake. Further, factors such as cell density, and other macrophage cell lines could have a significant effect on macrophage phagocytic capacity.

If these results are reproduced in vivo, there are several implications for clinical imaging studies. Due to the widespread use of statins in cardiovascular disease patients, it is likely that many USPIO enhanced MRI studies will be performed and interpreted with this drug present. Lack of USPIO-associated signal loss in the vascular wall will not necessarily prove the absence of inflammatory cells such as macrophages. Further, the present data do not provide any information the effect of withdrawing statin therapy on macrophage uptake in either the short-term (life-span of the exposed macrophage) or long term, when previously statin-unexposed cells migrate into the vessel wall. Based on in vivo studies, USPIO enhanced MRI may not only be able to indirectly detect vascular inflammation but may be able to assess the effect of anti-inflammatory drug therapy.

Appendices

A1. Dose-Time Analysis

Two Way Analysis of Variance

Source of Variation	DF	SS	MS	F	P
Time (min)	3	7139691.639	2379897.213	30.014	<0.001
Dose	2	859526.056	429763.028	5.420	0.011
Time (min) x Dose	6	2248937.278	374822.880	4.727	0.003
Residual	24	1903021.333	79292.556		
Total	35	12151176.306	347176.466		

The difference in the mean values among the different levels of Time (min) is greater than would be expected by chance after allowing for effects of differences in Dose. There is a statistically significant difference (P = <0.001). To isolate which group(s) differ from the others use a multiple comparison procedure.

The difference in the mean values among the different levels of Dose is greater than would be expected by chance after allowing for effects of differences in Time (min). There is a statistically significant difference (P = 0.011). To isolate which group(s) differ from the others use a multiple comparison procedure.

The effect of different levels of Time (min) depends on what level of Dose is present. There is a statistically significant interaction between Time (min) and Dose. (P = 0.003)

Power of performed test with alpha = 0.0500: for Time (min) : 1.000
Power of performed test with alpha = 0.0500: for Dose : 0.707
Power of performed test with alpha = 0.0500: for Time (min) x Dose : 0.903

Least square means for Time (min) :

Group	Mean
240.000	1084.222
60.000	194.556
10.000	6.111
5.000	11.667

Std Err of LS Mean = 93.863

Least square means for Dose :

Group	Mean
1.000	106.417
10.000	416.833
100.000	449.167

Std Err of LS Mean = 81.288

Least square means for Time (min) x Dose :

Group	Mean
240.000 x 1.000	282.667
240.000 x 10.000	1568.333
240.000 x 100.000	1401.667
60.000 x 1.000	99.667
60.000 x 10.000	93.000
60.000 x 100.000	391.000
10.000 x 1.000	12.333
10.000 x 10.000	4.000
10.000 x 100.000	2.000
5.000 x 1.000	31.000
5.000 x 10.000	2.000
5.000 x 100.000	2.000

Std Err of LS Mean = 162.576

All Pairwise Multiple Comparison Procedures (Tukey Test):

Comparisons for factor: Time (min)

Comparison	Diff of Means	p	q	P	P<0.050
240.000 vs. 10.000	1078.111	4	11.486	<0.001	Yes
240.000 vs. 5.000	1072.556	4	11.427	<0.001	Yes
240.000 vs. 60.000	889.667	4	9.478	<0.001	Yes
60.000 vs. 10.000	188.444	4	2.008	0.500	No
60.000 vs. 5.000	182.889	4	1.948	0.525	Do Not Test
5.000 vs. 10.000	5.556	4	0.0592	1.000	Do Not Test

Comparisons for factor: Dose

Comparison	Diff of Means	p	q	P	P<0.050
100.000 vs. 1.000	342.750	3	4.216	0.017	Yes
100.000 vs. 10.000	32.333	3	0.398	0.958	No
10.000 vs. 1.000	310.417	3	3.819	0.032	Yes

Comparisons for factor: Dose within 240

Comparison	Diff of Means	p	q	P	P<0.05
10.000 vs. 1.000	1285.667	3	7.908	<0.001	Yes
10.000 vs. 100.000	166.667	3	1.025	0.751	No
100.000 vs. 1.000	1119.000	3	6.883	<0.001	Yes

Comparisons for factor: Dose within 60

Comparison	Diff of Means	p	q	P	P<0.05
100.000 vs. 10.000	298.000	3	1.833	0.411	No
100.000 vs. 1.000	291.333	3	1.792	0.427	Do Not Test
1.000 vs. 10.000	6.667	3	0.0410	1.000	Do Not Test

Comparisons for factor: Dose within 10

Comparison	Diff of Means	p	q	P	P<0.05

1.000 vs. 100.000	10.333	3	0.0636	0.999	No
1.000 vs. 10.000	8.333	3	0.0513	0.999	Do Not Test
10.000 vs. 100.000	2.000	3	0.0123	1.000	Do Not Test

Comparisons for factor: Dose within 5

Comparison	Diff of Means	p	q	P	P<0.05
1.000 vs. 100.000	29.000	3	0.178	0.991	No
1.000 vs. 10.000	29.000	3	0.178	0.991	Do Not Test
10.000 vs. 100.000	0.000	3	0.000	1.000	Do Not Test

Comparisons for factor: Time (min) within 1

Comparison	Diff of Means	p	q	P	P<0.05
240.000 vs. 10.000	270.333	4	1.663	0.648	No
240.000 vs. 5.000	251.667	4	1.548	0.696	Do Not Test
240.000 vs. 60.000	183.000	4	1.126	0.856	Do Not Test
60.000 vs. 10.000	87.333	4	0.537	0.981	Do Not Test
60.000 vs. 5.000	68.667	4	0.422	0.991	Do Not Test
5.000 vs. 10.000	18.667	4	0.115	1.000	Do Not Test

Comparisons for factor: Time (min) within 10

Comparison	Diff of Means	p	q	P	P<0.05
240.000 vs. 5.000	1566.333	4	9.634	<0.001	Yes
240.000 vs. 10.000	1564.333	4	9.622	<0.001	Yes
240.000 vs. 60.000	1475.333	4	9.075	<0.001	Yes
60.000 vs. 5.000	91.000	4	0.560	0.979	No
60.000 vs. 10.000	89.000	4	0.547	0.980	Do Not Test
10.000 vs. 5.000	2.000	4	0.0123	1.000	Do Not Test

Comparisons for factor: Time (min) within 100

Comparison	Diff of Means	p	q	P	P<0.05
240.000 vs. 5.000	1399.667	4	8.609	<0.001	Yes

240.000 vs. 10.000	1399.667	4	8.609	<0.001	Yes
240.000 vs. 60.000	1010.667	4	6.217	0.001	Yes
60.000 vs. 5.000	389.000	4	2.393	0.350	No
60.000 vs. 10.000	389.000	4	2.393	0.350	Do Not Test
10.000 vs. 5.000	0.000	4	0.000	1.000	Do Not Test

A2. Effect of the Presence or Absence of Serum Proteins on SPIO Uptake

Source of Variation	DF	SS	MS	F	P
[iron]	3	3133692587.125	1044564195.708	481.432	<0.001
FBS	1	97433310.375	97433310.375	44.906	<0.001
[iron] x FBS	3	317465364.458	105821788.153	48.772	<0.001
Residual	16	34715270.000	2169704.375		
Total	23	3583306531.958	155795936.172		

The difference in the mean values among the different levels of [iron] is greater than would be expected by chance after allowing for effects of differences in FBS. There is a statistically significant difference (P = <0.001).

The difference in the mean values among the different levels of FBS is greater than would be expected by chance after allowing for effects of differences in [iron]. There is a statistically significant difference (P = <0.001).

The effect of different levels of [iron] depends on what level of FBS is present. There is a statistically significant interaction between [iron] and FBS. (P = <0.001)

Power of performed test with alpha = 0.0500: for [iron] : 1.000

Power of performed test with alpha = 0.0500: for FBS : 1.000

Power of performed test with alpha = 0.0500: for [iron] x FBS : 1.000

Least square means for [iron] :

Group Mean

100.000 27881.667

10.000 5212.000

1.000	524.500
0.000	0.000

Std Err of LS Mean = 601.346

Least square means for FBS :

Group	Mean
1.000	10419.417
0.000	6389.667

Std Err of LS Mean = 425.216

Least square means for [iron] x FBS :

Group	Mean
100.000 x 1.000	36195.333
100.000 x 0.000	19568.000
10.000 x 1.000	5070.333
10.000 x 0.000	5353.667
1.000 x 1.000	412.000
1.000 x 0.000	637.000
0.000 x 1.000	0.000
0.000 x 0.000	0.000

Std Err of LS Mean = 850.432

All Pairwise Multiple Comparison Procedures (Tukey Test):

Comparisons for factor: [iron]

Comparison	Diff of Means	p	q	P	P<0.050
100.000 vs. 0.000	27881.667	4	46.365	<0.001	Yes
100.000 vs. 1.000	27357.167	4	45.493	<0.001	Yes
100.000 vs. 10.000	22669.667	4	37.698	<0.001	Yes
10.000 vs. 0.000	5212.000	4	8.667	<0.001	Yes

10.000 vs. 1.000	4687.500	4	7.795	<0.001	Yes
1.000 vs. 0.000	524.500	4	0.872	0.925	No

Comparisons for factor: FBS

Comparison	Diff of Means	p	q	P	P<0.050
1.000 vs. 0.000	4029.750	2	9.477	<0.001	Yes

Comparisons for factor: FBS within 100

Comparison	Diff of Means	p	q	P	P<0.05
1.000 vs. 0.000	16627.333	2	19.55	<0.001	Yes

Comparisons for factor: FBS within 10

Comparison	Diff of Means	p	q	P	P<0.05
0.000 vs. 1.000	283.333	2	0.333	0.817	No

Comparisons for factor: FBS within 1

Comparison	Diff of Means	p	q	P	P<0.05
0.000 vs. 1.000	225.000	2	0.265	0.854	No

Comparisons for factor: FBS within 0

Comparison	Diff of Means	p	q	P	P<0.05
1.000 vs. 0.000	0.000	2	0.000	1.000	No

Comparisons for factor: [iron] within 1

Comparison	Diff of Means	p	q	P	P<0.05
100.000 vs. 0.000	36195.333	4	42.561	<0.001	Yes
100.000 vs. 1.000	35783.333	4	42.077	<0.001	Yes
100.000 vs. 10.000	31125.000	4	36.599	<0.001	Yes
10.000 vs. 0.000	5070.333	4	5.962	0.003	Yes
10.000 vs. 1.000	4658.333	4	5.478	0.007	Yes
1.000 vs. 0.000	412.000	4	0.484	0.986	No

Comparisons for factor: [iron] within 0

Comparison	Diff of Means	p	q	P	P<0.05
100.000 vs. 0.000	19568.000	4	23.009	<0.001	Yes
100.000 vs. 1.000	18931.000	4	22.260	<0.001	Yes
100.000 vs. 10.000	14214.333	4	16.714	<0.001	Yes

A3. Effect of Cytochalasin B on Iron Uptake

Data source: Data 1 in Notebook

Balanced Design

Dependent Variable: Blue Area

Normality Test: Passed (P = 0.019)

Equal Variance Test: Passed (P = 0.029)

Source of Variation	DF	SS	MS	F	P
[iron]	3	4642205912.167	1547401970.722	117.310	**<0.001**
CYTO 1mcg/ml	1	53133504.167	53133504.167	4.028	**0.062**
[iron] x CYTO 1mcg/ml	3	191873468.167	63957822.722	4.849	**0.014**
Residual	16	211051657.333	13190728.583		
Total	23	5098264541.833	221663675.732		

The difference in the mean values among the different levels of [iron] is greater than would be expected by chance after allowing for effects of differences in CYTO 1mcg/ml. There is a statistically significant difference (P = <0.001). To isolate which group(s) differ from the others use a multiple comparison procedure.

The difference in the mean values among the different levels of CYTO 1mcg/ml is not great enough to exclude the possibility that the difference is just due to random sampling variability after allowing for the effects of differences in [iron]. There is not a statistically significant difference (P = 0.062).

The effect of different levels of [iron] depends on what level of CYTO 1mcg/ml is present. There is a statistically significant interaction between [iron] and CYTO 1mcg/ml. (P = 0.014)

Power of performed test with alpha = 0.0500: for [iron] : 1.000
Power of performed test with alpha = 0.0500: for CYTO 1mcg/ml : 0.360
Power of performed test with alpha = 0.0500: for [iron] x CYTO 1mcg/ml : 0.715

Least square means for [iron] :

Group	Mean
100.000	34951.500
10.000	11005.667
1.000	1877.667
0.000	21.500

Std Err of LS Mean = 1482.719

Least square means for CYTO 1mcg/ml :

Group	Mean
0.000	13452.000
1.000	10476.167

Std Err of LS Mean = 1048.440

Least square means for [iron] x CYTO 1mcg/ml :

Group	Mean
100.000 x 0.000	41322.333
100.000 x 1.000	28580.667
10.000 x 0.000	10512.000
10.000 x 1.000	11499.333
1.000 x 0.000	1930.667
1.000 x 1.000	1824.667
0.000 x 1.000	0.000

0.000 x 0.000 43.000

Std Err of LS Mean = 2096.881

All Pairwise Multiple Comparison Procedures (Tukey Test):

Comparisons for factor: [iron]

Comparison	Diff of Means	p	q	P	P<0.050
100.000 vs. 0.000	34930.000	4	23.558	<0.001	Yes
100.000 vs. 1.000	33073.833	4	22.306	<0.001	Yes
100.000 vs. 10.000	23945.833	4	16.150	<0.001	Yes
10.000 vs. 0.000	10984.167	4	7.408	<0.001	Yes
10.000 vs. 1.000	9128.000	4	6.156	0.003	Yes
1.000 vs. 0.000	1856.167	4	1.252	0.813	No

Comparisons for factor: CYTO 1mcg/ml within 100

Comparison	Diff of Means	p	q	P	P<0.05
0.000 vs. 1.000	12741.667	2	6.076	<0.001	Yes

Comparisons for factor: CYTO 1mcg/ml within 10

Comparison	Diff of Means	p	q	P	P<0.05
1.000 vs. 0.000	987.333	2	0.471	0.744	No

Comparisons for factor: CYTO 1mcg/ml within 1

Comparison	Diff of Means	p	q	P	P<0.05
0.000 vs. 1.000	106.000	2	0.0506	0.972	No

Comparisons for factor: CYTO 1mcg/ml within 0

Comparison	Diff of Means	p	q	P	P<0.05
0.000 vs. 1.000	43.000	2	0.0205	0.989	No

Comparisons for factor: [iron] within 0

Comparison	Diff of Means	p	q	P	P<0.05
100.000 vs. 0.000	41279.333	4	19.686	<0.001	Yes
100.000 vs. 1.000	39391.667	4	18.786	<0.001	Yes
100.000 vs. 10.000	30810.333	4	14.693	<0.001	Yes
10.000 vs. 0.000	10469.000	4	4.993	0.013	Yes
10.000 vs. 1.000	8581.333	4	4.092	0.047	Yes
1.000 vs. 0.000	1887.667	4	0.900	0.919	No

Comparisons for factor: [iron] within 1

Comparison	Diff of Means	p	q	P	P<0.05
100.000 vs. 0.000	28580.667	4	13.630	<0.001	Yes
100.000 vs. 1.000	26756.000	4	12.760	<0.001	Yes
100.000 vs. 10.000	17081.333	4	8.146	<0.001	Yes
10.000 vs. 0.000	11499.333	4	5.484	0.007	Yes
10.000 vs. 1.000	9674.667	4	4.614	0.023	Yes
1.000 vs. 0.000	1824.667	4	0.870	0.926	No

A4. Effect of Blocking Mannose Receptors with Mannan

Two Way Analysis of Variance

Data source: Data 1 in Notebook

Source of Variation	DF	SS	MS	F	P
Mannan Block	1	5422602.667	5422602.667	1.888	0.188
[iron]	3	178080852.333	59360284.111	20.663	<0.001
Mannan Block x [iron]	3	21179777.667	7059925.889	2.458	0.100
Residual	16	45964028.667	2872751.792		
Total	23	250647261.333	10897707.014		

The difference in the mean values among the different levels of Mannan Block is not great enough to exclude the possibility that the difference is just due to random sampling variability after allowing for the effects of differences in [iron]. There is not a statistically significant difference (P = 0.188).

The difference in the mean values among the different levels of [iron] is greater than would be expected by chance after allowing for effects of differences in Mannan Block. There is a statistically significant difference (P = <0.001). To isolate which group(s) differ from the others use a multiple comparison procedure.

The effect of different levels of Mannan Block does not depend on what level of [iron] is present. There is not a statistically significant interaction between Mannan Block and [iron]. (P = 0.100)

Power of performed test with alpha = 0.0500: for Mannan Block : 0.135

Power of performed test with alpha = 0.0500: for [iron] : 1.000

Power of performed test with alpha = 0.0500: for Mannan Block x [iron] : 0.306

Least square means for Mannan Block :

Group	Mean
0.000	1309.833
1.000	2260.500

Std Err of LS Mean = 489.281

Least square means for [iron] :

Group	Mean
100.000	6493.167
10.000	498.333
1.000	132.667
0.000	16.500

Std Err of LS Mean = 691.948

Least square means for Mannan Block x [iron] :

Group	Mean
0.000 x 100.000	4393.000
0.000 x 10.000	599.333
0.000 x 1.000	245.000
0.000 x 0.000	2.000
1.000 x 100.000	8593.333
1.000 x 10.000	397.333
1.000 x 0.000	31.000
1.000 x 1.000	20.333

Std Err of LS Mean = 978.562

All Pairwise Multiple Comparison Procedures (Tukey Test):

Comparisons for factor: [iron]

Comparison	Diff of Means	p	q	P	P<0.050
100.000 vs. 0.000	6476.667	4	9.360	<0.001	Yes
100.000 vs. 1.000	6360.500	4	9.192	<0.001	Yes
100.000 vs. 10.000	5994.833	4	8.664	<0.001	Yes
10.000 vs. 0.000	481.833	4	0.696	0.960	No
10.000 vs. 1.000	365.667	4	0.528	0.982	Do Not Test
1.000 vs. 0.000	116.167	4	0.168	0.999	Do Not Test

A result of "Do Not Test" occurs for a comparison when no significant difference is found between two means that enclose that comparison. For example, if you had four means sorted in order, and found no difference between means 4 vs. 2, then you would not test 4 vs. 3 and 3 vs. 2, but still test 4 vs. 1 and 3 vs. 1 (4 vs. 3 and 3 vs. 2 are enclosed by 4 vs. 2: 4 3 2 1). Note that not testing the enclosed means is a procedural rule, and a result of Do Not Test should be treated as if there is no significant difference between the means, even though one may appear to exist.

A5. Effect of Interleuken-4 on Macrophage Uptake of Iron Oxide

a. IL-4 at 10 ng/ml

Source of Variation	DF	SS	MS	F	P
IL-4 (10 ng/ml)	1	20276816.667	20276816.667	1.692	0.212
[iron]	3	4540930168.833	1513643389.611	126.318	<0.001
IL-4 (10 ng/ml) x [iron]	3	145048807.667	48349602.556	4.035	0.026
Residual	16	191724197.333	11982762.333		
Total	23	4897979990.500	212955651.761		

The difference in the mean values among the different levels of IL-4 (10 ng/ml) is not great enough to exclude the possibility that the difference is just due to random sampling variability after allowing for the effects of differences in [iron]. There is not a statistically significant difference (P = 0.212).

The difference in the mean values among the different levels of [iron] is greater than would be expected by chance after allowing for effects of differences in IL-4 (10 ng/ml). There is a statistically significant difference (P = <0.001). To isolate which group(s) differ from the others use a multiple comparison procedure.

The effect of different levels of IL-4 (10 ng/ml) depends on what level of [iron] is present. There is a statistically significant interaction between IL-4 (10 ng/ml) and [iron]. (P = 0.026)

Power of performed test with alpha = 0.0500: for IL-4 (10 ng/ml) : 0.116

Power of performed test with alpha = 0.0500: for [iron] : 1.000

Power of performed test with alpha = 0.0500: for IL-4 (10 ng/ml) x [iron] : 0.597

Least square means for IL-4 (10 ng/ml) :

Group	Mean
0.000	10158.583
1.000	11996.917

Std Err of LS Mean = 999.282

Least square means for [iron] :

Group	Mean
100.000	34376.500
10.000	7857.667
1.000	2049.500
0.000	27.333

Std Err of LS Mean = 1413.197

Least square means for IL-4 (10 ng/ml) x [iron] :

Group	Mean
0.000 x 100.000	29232.667
0.000 x 10.000	8703.333
0.000 x 1.000	2666.000
0.000 x 0.000	32.333
1.000 x 100.000	39520.333
1.000 x 10.000	7012.000
1.000 x 0.000	22.333
1.000 x 1.000	1433.000

Std Err of LS Mean = 1998.563

All Pairwise Multiple Comparison Procedures (Tukey Test):

Comparisons for factor: IL-4 (10 ng/ml)

Comparison	Diff of Means	p	q	P	P<0.050
1.000 vs. 0.000	1838.333	2	1.840	0.212	No

Comparisons for factor: [iron]

Comparison	Diff of Means	p	q	P	P<0.050
100.000 vs. 0.000	34349.167	4	24.306	<0.001	Yes
100.000 vs. 1.000	32327.000	4	22.875	<0.001	Yes
100.000 vs. 10.000	26518.833	4	18.765	<0.001	Yes
10.000 vs. 0.000	7830.333	4	5.541	0.006	Yes
10.000 vs. 1.000	5808.167	4	4.110	0.046	Yes
1.000 vs. 0.000	2022.167	4	1.431	0.745	No

Comparisons for factor: [iron] within 0

Comparison	Diff of Means	p	q	P	P<0.05
100.000 vs. 0.000	29200.333	4	14.611	<0.001	Yes
100.000 vs. 1.000	26566.667	4	13.293	<0.001	Yes
100.000 vs. 10.000	20529.333	4	10.272	<0.001	Yes
10.000 vs. 0.000	8671.000	4	4.339	0.034	Yes
10.000 vs. 1.000	6037.333	4	3.021	0.184	No
1.000 vs. 0.000	2633.667	4	1.318	0.789	No

Comparisons for factor: [iron] within 1

Comparison	Diff of Means	p	q	P	P<0.05
100.000 vs. 0.000	39498.000	4	19.763	<0.001	Yes
100.000 vs. 1.000	38087.333	4	19.057	<0.001	Yes
100.000 vs. 10.000	32508.333	4	16.266	<0.001	Yes
10.000 vs. 0.000	6989.667	4	3.497	0.103	No
10.000 vs. 1.000	5579.000	4	2.792	0.238	Do Not Test
1.000 vs. 0.000	1410.667	4	0.706	0.958	Do Not Test

Comparisons for factor: IL-4 (10 ng/ml) within 100

Comparison	Diff of Means	p	q	P	P<0.05
1.000 vs. 0.000	10287.667	2	5.148	0.002	Yes

Comparisons for factor: IL-4 (10 ng/ml) within 10

Comparison	Diff of Means	p	q	P	P<0.05
0.000 vs. 1.000	1691.333	2	0.846	0.558	No

Comparisons for factor: IL-4 (10 ng/ml) within 1

Comparison	Diff of Means	p	q	P	P<0.05
0.000 vs. 1.000	1233.000	2	0.617	0.669	No

A6. Effect of Interleuken-4 on Macrophage Uptake of Iron Oxide

b. IL-4 (20 ng/ml)

Two Way Analysis of Variance

Source of Variation	DF	SS	MS	F	P
IL-4 (20 ng/ml)	1	93750.000	93750.000	0.00461	0.947
[iron]	3	4781933262.333	1593977754.111	78.450	<0.001
IL-4 (20 ng/ml) x [iron]	3	5172533.000	1724177.667	0.0849	0.967
Residual	16	325095190.000	20318449.375		
Total	23	5112294735.333	222273684.145		

The difference in the mean values among the different levels of IL-4 (20 ng/ml) is not great enough to exclude the possibility that the difference is just due to random sampling variability after allowing for the effects of differences in [iron]. There is not a statistically significant difference (P = 0.947).

The difference in the mean values among the different levels of [iron] is greater than would be expected by chance after allowing for effects of differences in IL-4 (20 ng/ml). There is a statistically significant difference (P = <0.001). To isolate which group(s) differ from the others use a multiple comparison procedure.The effect of different levels of IL-4 (20 ng/ml) does not depend on what level of [iron] is present. There is not a statistically significant interaction between IL-4 (20 ng/ml) and [iron]. (P = 0.967)Power of performed test with alpha = 0.0500: for IL-4 (20 ng/ml) : 0.0500

Power of performed test with alpha = 0.0500: for [iron] : 1.000

Power of performed test with alpha = 0.0500: for IL-4 (20 ng/ml) x [iron] : 0.0500

Least square means for IL-4 (20 ng/ml) :

Group	Mean
0.000	11560.333
1.000	11435.333

Std Err of LS Mean = 1301.232

Least square means for [iron] :

Group	Mean
100.000	34974.333
10.000	10086.833
1.000	917.167
0.000	13.000

Std Err of LS Mean = 1840.220

Least square means for IL-4 (20 ng/ml) x [iron] :

Group	Mean
0.000 x 100.000	34482.667
0.000 x 10.000	10882.667
0.000 x 1.000	866.000
0.000 x 0.000	10.000
1.000 x 100.000	35466.000
1.000 x 10.000	9291.000
1.000 x 0.000	16.000
1.000 x 1.000	968.333

Std Err of LS Mean = 2602.464

All Pairwise Multiple Comparison Procedures (Tukey Test):

Comparisons for factor: IL-4 (20 ng/ml)

Comparison	Diff of Means	p	q	P	P<0.050
0.000 vs. 1.000	125.000	2	0.0961	0.947	No

Comparisons for factor: [iron]

Comparison	Diff of Means	p	q	P	P<0.050
100.000 vs. 0.000	34961.333	4	18.998	<0.001	Yes
100.000 vs. 1.000	34057.167	4	18.507	<0.001	Yes
100.000 vs. 10.000	24887.500	4	13.524	<0.001	Yes
10.000 vs. 0.000	10073.833	4	5.474	0.007	Yes
10.000 vs. 1.000	9169.667	4	4.983	0.014	Yes
1.000 vs. 0.000	904.167	4	0.491	0.985	No

A7. Effect of Interleuken-4 on Macrophage Uptake of Iron Oxide

c. IL-4 (40 ng/ml)

Two Way Analysis of Variance

Source of Variation	DF	SS	MS	F	P
IL-4 (40 ng/ml)	1	114821876.042	114821876.042	5.514	0.032
[iron]	3	5574749793.125	1858249931.042	89.239	<0.001
IL-4 (40 ng/ml) x [iron]	3	131018250.125	43672750.042	2.097	0.141
Residual	16	333171619.333	20823226.208		
Total	23	6153761538.625	267554849.505		

The difference in the mean values among the different levels of IL-4 (40 ng/ml) is greater than would be expected by chance after allowing for effects of differences in [iron]. There is a statistically significant difference (P = 0.032). To isolate which group(s) differ from the others use a multiple comparison procedure.

The difference in the mean values among the different levels of [iron] is greater than would be expected by chance after allowing for effects of differences in IL-4 (40 ng/ml). There is a statistically significant difference (P = <0.001). To isolate which group(s) differ from the others use a multiple comparison procedure.

The effect of different levels of IL-4 (40 ng/ml) does not depend on what level of [iron] is present. There is not a statistically significant interaction between IL-4 (20 ng/ml) and [iron]. (P = 0.141)

Power of performed test with alpha = 0.0500: for IL-4 (40 ng/ml) : 0.508

Power of performed test with alpha = 0.0500: for [iron] : 1.000

Power of performed test with alpha = 0.0500: for IL-4 (40 ng/ml) x [iron] : 0.236

Least square means for IL-4 (40 ng/ml) :

Group	Mean
0.000	10198.833
1.000	14573.417

Std Err of LS Mean = 1317.296

Least square means for [iron] :

Group	Mean
100.000	37711.833
10.000	10947.333
1.000	873.333
0.000	12.000

Std Err of LS Mean = 1862.938

Least square means for IL-4 (40 ng/ml) x [iron] :

Group	Mean
0.000 x 100.000	31911.667
0.000 x 10.000	8251.333
0.000 x 1.000	622.333
1.000 x 100.000	43512.000
1.000 x 10.000	13643.333
1.000 x 1.000	1124.333
1.000 x 0.000	14.000

Std Err of LS Mean = 2634.592

All Pairwise Multiple Comparison Procedures (Tukey Test):

Comparisons for factor: IL-4 (40 ng/ml)

Comparison	Diff of Means	p	q	P	P<0.050
1.000 vs. 0.000	4374.583	2	3.321	0.032	Yes

Comparisons for factor: [iron]

Comparison	Diff of Means	p	q	P	P<0.050
100.000 vs. 0.000	37699.833	4	20.237	<0.001	Yes
100.000 vs. 1.000	36838.500	4	19.774	<0.001	Yes
100.000 vs. 10.000	26764.500	4	14.367	<0.001	Yes
10.000 vs. 0.000	10935.333	4	5.870	0.004	Yes
10.000 vs. 1.000	10074.000	4	5.408	0.007	Yes
1.000 vs. 0.000	861.333	4	0.462	0.988	No

1.000 x 10.000	13643.333	1.000 x 1.000	1124.333
1.000 x 0.000	14.000		

Std Err of LS Mean = 2634.592

All Pairwise Multiple Comparison Procedures (Tukey Test):

Comparisons for factor: IL-4 (40 ng/ml)

Comparison	Diff of Means	p	q	P	P<0.050
1.000 vs. 0.000	4374.583	2	3.321	0.032	Yes

Comparisons for factor: [iron]

Comparison	Diff of Means	p	q	P	P<0.050
100.000 vs. 0.000	37699.833	4	20.237	<0.001	Yes
100.000 vs. 1.000	36838.500	4	19.774	<0.001	Yes
100.000 vs. 10.000	26764.500	4	14.367	<0.001	Yes
10.000 vs. 0.000	10935.333	4	5.870	0.004	Yes
10.000 vs. 1.000	10074.000	4	5.408	0.007	Yes
1.000 vs. 0.000	861.333	4	0.462	0.988	No

Comparisons for factor: [iron] within 0

Comparison	Diff of Means	p	q	P	P<0.05
100.000 vs. 0.000	31901.667	4	12.109	<0.001	Yes
100.000 vs. 1.000	31289.333	4	11.876	<0.001	Yes
100.000 vs. 10.000	23660.333	4	8.981	<0.001	Yes
10.000 vs. 0.000	8241.333	4	3.128	0.162	No
10.000 vs. 1.000	7629.000	4	2.896	0.212	Do Not Test
1.000 vs. 0.000	612.333	4	0.232	0.998	Do Not Test

Comparisons for factor: [iron] within 1

Comparison	Diff of Means	p	q	P	P<0.05
100.000 vs. 0.000	43498.000	4	16.510	<0.001	Yes
100.000 vs. 1.000	42387.667	4	16.089	<0.001	Yes
100.000 vs. 10.000	29868.667	4	11.337	<0.001	Yes
10.000 vs. 0.000	13629.333	4	5.173	0.010	Yes
10.000 vs. 1.000	12519.000	4	4.752	0.019	Yes
1.000 vs. 0.000	1110.333	4	0.421	0.991	No

Comparisons for factor: IL-4 (40 ng/ml) within 100

Comparison	Diff of Means	p	q	P	P<0.05
1.000 vs. 0.000	11600.333	2	4.403	0.007	Yes

Comparisons for factor: IL-4 (40 ng/ml) within 10

Comparison	Diff of Means	p	q	P	P<0.05
1.000 vs. 0.000	5392.000	2	2.047	0.167	No

Comparisons for factor: IL-4 (40 ng/ml) within 1

Comparison	Diff of Means	p	q	P	P<0.05
1.000 vs. 0.000	502.000	2	0.191	0.895	No

A8. Effect of Human Interferon Gamma on Macrophage Uptake of Iron Oxide

a. IFN-γ at 10 U/ml

Two Way Analysis of Variance

Source of Variation	DF	SS	MS	F	P
IFN-γ (10u/ml)	1	3711493.500	3711493.500	0.346	0.565
[iron]	3	4715548409.500	1571849469.833	146.523	<0.001
IFN-γ (10u/ml) x [iron]	3	1652630.833	550876.944	0.0514	0.984
Residual	16	171642074.667	10727629.667		
Total	23	4892554608.500	212719765.587		

The difference in the mean values among the different levels of IFN-g (10u/ml) is not great enough to exclude the possibility that the difference is just due to random sampling variability after allowing for the effects of differences in [iron]. There is not a statistically significant difference (P = 0.565).

The difference in the mean values among the different levels of [iron] is greater than would be expected by chance after allowing for effects of differences in IFN-γ (10u/ml). There is a statistically significant difference (P = <0.001). To isolate which group(s) differ from the others use a multiple comparison procedure.

The effect of different levels of IFN-γ (10u/ml) does not depend on what level of [iron] is present. There is not a statistically significant interaction between IFN-g (10u/ml) and [iron]. (P = 0.984)

Power of performed test with alpha = 0.0500: for IFN-g (10u/ml) : 0.0500
Power of performed test with alpha = 0.0500: for [iron] : 1.000
Power of performed test with alpha = 0.0500: for IFN-g (10u/ml) x [iron] : 0.0500

Least square means for IFN-γ (10u/ml) :

Group	Mean
0.000	11087.500
1.000	11874.000

Std Err of LS Mean = 945.499

Least square means for [iron] :

Group	Mean
100.000	34979.667
10.000	9329.667
1.000	1592.167
0.000	21.500

Std Err of LS Mean = 1337.138

Least square means for IFN-γ (10u/ml) x [iron] :

Group	Mean
0.000 x 100.000	34630.667
0.000 x 10.000	8618.000
0.000 x 1.000	1076.667
0.000 x 0.000	24.667
1.000 x 100.000	35328.667
1.000 x 10.000	10041.333
1.000 x 1.000	2107.667
1.000 x 0.000	18.333

Std Err of LS Mean = 1890.999

All Pairwise Multiple Comparison Procedures (Tukey Test):

Comparisons for factor: [iron]

Comparison	Diff of Means	p	q	P	P<0.050
100.000 vs. 0.000	34958.167	4	26.144	<0.001	Yes
100.000 vs. 1.000	33387.500	4	24.969	<0.001	Yes
100.000 vs. 10.000	25650.000	4	19.183	<0.001	Yes
10.000 vs. 0.000	9308.167	4	6.961	<0.001	Yes
10.000 vs. 1.000	7737.500	4	5.787	0.004	Yes
1.000 vs. 0.000	1570.667	4	1.175	0.839	No

A9. Effect of Human Interferon Gamma on Macrophage Uptake of Iron Oxide

b. IFN-γ at 500 U/ml

Two Way Analysis of Variance

Source of Variation	DF	SS	MS	F	P
IFN-γ (500u/ml)	1	4428.167	4428.167	0.000340	0.986
[iron]	3	3562854979.333	1187618326.444	91.275	<0.001
IFN-γ (500u/ml) x [iron]	3	17911468.500	5970489.500	0.459	0.715
Residual	16	208182604.000	13011412.750		
Total	23	3788953480.000	164737107.826		

The difference in the mean values among the different levels of IFN-γ (500u/ml) is not great enough to exclude the possibility that the difference is just due to random sampling variability after allowing for the effects of differences in [iron]. There is not a statistically significant difference (P = 0.986).

The difference in the mean values among the different levels of [iron] is greater than would be expected by chance after allowing for effects of differences in IFN-γ (500u/ml). There is a statistically significant difference (P = <0.001). To isolate which group(s) differ from the others use a multiple comparison procedure.

The effect of different levels of IFN-γ (500u/ml) does not depend on what level of [iron] is present. There is not a statistically significant interaction between IFN-γ (500u/ml) and [iron]. (P = 0.715)

Power of performed test with alpha = 0.0500: for IFN-γ (500u/ml) : 0.0500
Power of performed test with alpha = 0.0500: for [iron] : 1.000

Power of performed test with alpha = 0.0500: for IFN-γ (500u/ml) x [iron] : 0.0500

Least square means for IFN-γ (500u/ml) :

Group	Mean
0.000	11550.083
1.000	11522.917

Std Err of LS Mean = 1041.290

Least square means for [iron] :

Group	Mean
100.000	30172.333
10.000	14631.667
1.000	1310.000
0.000	32.000

Std Err of LS Mean = 1472.606

Least square means for IFN-γ (500u/ml) x [iron] :

Group	Mean
0.000 x 100.000	31553.667
0.000 x 10.000	13655.667
0.000 x 1.000	956.000
0.000 x 0.000	35.000
1.000 x 100.000	28791.000
1.000 x 10.000	15607.667
1.000 x 1.000	1664.000
1.000 x 0.000	29.000

Std Err of LS Mean = 2082.580

All Pairwise Multiple Comparison Procedures (Tukey Test):

Comparisons for factor: [iron]

Comparison	Diff of Means	p	q	P	P<0.050
100.000 vs. 0.000	30140.333	4	20.467	<0.001	Yes
100.000 vs. 1.000	28862.333	4	19.599	<0.001	Yes
100.000 vs. 10.000	15540.667	4	10.553	<0.001	Yes
10.000 vs. 0.000	14599.667	4	9.914	<0.001	Yes
10.000 vs. 1.000	13321.667	4	9.046	<0.001	Yes
1.000 vs. 0.000	1278.000	4	0.868	0.926	No

A10. Effect of Human Interferon Gamma on Macrophage Uptake of Iron Oxide

b. IFN-γ at 500 U/ml

Two Way Analysis of Variance

Source of Variation	DF	SS	MS	F	P
IFN-γ (500u/ml)	1	4428.167	4428.167	0.000340	0.986
[iron]	3	3562854979.333	1187618326.444	91.275	<0.001
IFN-γ (500u/ml) x [iron]	3	17911468.500	5970489.500	0.459	0.715
Residual	16	208182604.000	13011412.750		
Total	23	3788953480.000	164737107.826		

The difference in the mean values among the different levels of IFN-γ (500u/ml) is not great enough to exclude the possibility that the difference is just due to random sampling variability after allowing for the effects of differences in [iron]. There is not a statistically significant difference (P = 0.986).

The difference in the mean values among the different levels of [iron] is greater than would be expected by chance after allowing for effects of differences in IFN-γ (500u/ml). There is a statistically significant difference (P = <0.001). To isolate which group(s) differ from the others use a multiple comparison procedure.

The effect of different levels of IFN-γ (500u/ml) does not depend on what level of [iron] is present. There is not a statistically significant interaction between IFN-γ (500u/ml) and [iron]. (P = 0.715)

Power of performed test with alpha = 0.0500: for IFN-γ (500u/ml) : 0.0500
Power of performed test with alpha = 0.0500: for [iron] : 1.000

Power of performed test with alpha = 0.0500: for IFN-γ (500u/ml) x [iron] : 0.0500

Least square means for IFN-γ (500u/ml) :

Group	Mean
0.000	11550.083
1.000	11522.917

Std Err of LS Mean = 1041.290

Least square means for [iron] :

Group	Mean
100.000	30172.333
10.000	14631.667
1.000	1310.000
0.000	32.000

Std Err of LS Mean = 1472.606

Least square means for IFN-γ (500u/ml) x [iron] :

Group	Mean
0.000 x 100.000	31553.667
0.000 x 10.000	13655.667
0.000 x 1.000	956.000
0.000 x 0.000	35.000
1.000 x 100.000	28791.000
1.000 x 10.000	15607.667
1.000 x 1.000	1664.000
1.000 x 0.000	29.000

Std Err of LS Mean = 2082.580

All Pairwise Multiple Comparison Procedures (Tukey Test):

Comparisons for factor: [iron]

Comparison	Diff of Means	p	q	P	P<0.050
100.000 vs. 0.000	30140.333	4	20.467	<0.001	Yes
100.000 vs. 1.000	28862.333	4	19.599	<0.001	Yes
100.000 vs. 10.000	15540.667	4	10.553	<0.001	Yes
10.000 vs. 0.000	14599.667	4	9.914	<0.001	Yes
10.000 vs. 1.000	13321.667	4	9.046	<0.001	Yes
1.000 vs. 0.000	1278.000	4	0.868	0.926	No

A11. Effect of Human Interferon Gamma on Macrophage Uptake of Iron Oxide

c. IFN-γ at 1000U/ml

Two Way Analysis of Variance

Source of Variation	DF	SS	MS	F	P
IFN-γ	1	91057312.667	91057312.667	4.726	0.045
[iron]	3	2217676090.333	739225363.444	38.366	<0.001
IFN-γ x [iron]	3	181412470.333	60470823.444	3.138	0.055
Residual	16	308285008.000	19267813.000		
Total	23	2798430881.333	121670907.884		

The difference in the mean values among the different levels of IFN-γ is greater than would be expected by chance after allowing for effects of differences in [iron]. There is a statistically significant difference (P = 0.045). To isolate which group(s) differ from the others use a multiple comparison procedure.

The difference in the mean values among the different levels of [iron] is greater than would be expected by chance after allowing for effects of differences in IFN-γ. There is a statistically significant difference (P = <0.001). To isolate which group(s) differ from the others use a multiple comparison procedure.

The effect of different levels of IFN-γ does not depend on what level of [iron] is present. There is not a statistically significant interaction between IFN-g and [iron]. (P = 0.055)

Power of performed test with alpha = 0.0500: for IFN-γ : 0.432
Power of performed test with alpha = 0.0500: for [iron] : 1.000
Power of performed test with alpha = 0.0500: for IFN-γ x [iron] : 0.438

Least square means for IFN-γ :

Group	Mean
0.000	6149.500
1.000	10045.167

Std Err of LS Mean = 1267.143

Least square means for [iron] :

Group	Mean
100.000	23893.167
10.000	7777.333
1.000	713.833
0.000	5.000

Std Err of LS Mean = 1792.011

Least square means for IFN-γ x [iron] :

Group	Mean
0.000 x 100.000	17220.333
0.000 x 10.000	6857.667
0.000 x 1.000	516.000
0.000 x 0.000	4.000
1.000 x 100.000	30566.000
1.000 x 10.000	8697.000
1.000 x 1.000	911.667
1.000 x 0.000	6.000

Std Err of LS Mean = 2534.286

All Pairwise Multiple Comparison Procedures (Tukey Test):

Comparisons for factor: IFN-γ

Comparison	Diff of Means	p	q	P	P<0.050
1.000 vs. 0.000	3895.667	2	3.074	0.045	Yes

Comparisons for factor: [iron]

Comparison	Diff of Means	p	q	P	P<0.050
100.000 vs. 0.000	23888.167	4	13.330	<0.001	Yes
100.000 vs. 1.000	23179.333	4	12.935	<0.001	Yes
100.000 vs. 10.000	16115.833	4	8.993	<0.001	Yes
10.000 vs. 0.000	7772.333	4	4.337	0.034	Yes
10.000 vs. 1.000	7063.500	4	3.942	0.058	No
1.000 vs. 0.000	708.833	4	0.396	0.992	No

1.000 x 1.000	911.667	1.000 x 0.000	6.000

Std Err of LS Mean = 2534.286

All Pairwise Multiple Comparison Procedures (Tukey Test):

Comparisons for factor: IFN-g

Comparison	Diff of Means	p	q	P	P<0.050
1.000 vs. 0.000	3895.667	2	3.074	0.045	Yes

Comparisons for factor: [iron]

Comparison	Diff of Means	p	q	P	P<0.050
100.000 vs. 0.000	23888.167	4	13.330	<0.001	Yes
100.000 vs. 1.000	23179.333	4	12.935	<0.001	Yes
100.000 vs. 10.000	16115.833	4	8.993	<0.001	Yes
10.000 vs. 0.000	7772.333	4	4.337	0.034	Yes
10.000 vs. 1.000	7063.500	4	3.942	0.058	No
1.000 vs. 0.000	708.833	4	0.396	0.992	No

Comparisons for factor: [iron] within 0

Comparison	Diff of Means	p	q	P	P<0.05
100.000 vs. 0.000	17216.333	4	6.793	0.001	Yes
100.000 vs. 1.000	16704.333	4	6.591	0.001	Yes
100.000 vs. 10.000	10362.667	4	4.089	0.047	Yes
10.000 vs. 0.000	6853.667	4	2.704	0.262	No
10.000 vs. 1.000	6341.667	4	2.502	0.323	Do Not Test
1.000 vs. 0.000	512.000	4	0.202	0.999	Do Not Test

Comparisons for factor: [iron] within 1

Comparison	Diff of Means	p	q	P	P<0.05
100.000 vs. 0.000	30560.000	4	12.059	<0.001	Yes
100.000 vs. 1.000	29654.333	4	11.701	<0.001	Yes

100.000 vs. 10.000	21869.000	4	8.629	<0.001	Yes
10.000 vs. 0.000	8691.000	4	3.429	0.112	No
10.000 vs. 1.000	7785.333	4	3.072	0.173	Do Not Test
1.000 vs. 0.000	905.667	4	0.357	0.994	Do Not Test

Comparisons for factor: IFN-g within 100

Comparison	Diff of Means	p	q	P	P<0.05
1.000 vs. 0.000	13345.667	2	5.266	0.002	Yes

Comparisons for factor: IFN-g within 10

Comparison	Diff of Means	p	q	P	P<0.05
1.000 vs. 0.000	1839.333	2	0.726	0.615	No

Comparisons for factor: IFN-g within 1

Comparison	Diff of Means	p	q	P	P<0.05
1.000 vs. 0.000	395.667	2	0.156	0.914	No

A12. Effect of Angiotensin Converting Enzyme (ACE) Inhibition on Macrophage Uptake of Iron Oxide

a. Captopril at 0.01 mM

Two Way Analysis of Variance

Source of Variation	DF	SS	MS	F	P
CAPT 0.01mM	1	1397320.042	1397320.042	0.0919	0.766
[iron]	3	4773544524.458	1591181508.153	104.693	<0.001
CAPT 0.01mM x [iron]	3	1533378.125	511126.042	0.0336	0.991
Residual	16	243176560.000	15198535.000		
Total	23	5019651782.625	218245729.679		

The difference in the mean values among the different levels of CAPT 0.01mM is not great enough to exclude the possibility that the difference is just due to random sampling variability after allowing for the effects of differences in [iron]. There is not a statistically significant difference (P = 0.766).

The difference in the mean values among the different levels of [iron] is greater than would be expected by chance after allowing for effects of differences in CAPT 0.01mM. There is a statistically significant difference (P = <0.001). To isolate which group(s) differ from the others use a multiple comparison procedure.

The effect of different levels of CAPT 0.01mM does not depend on what level of [iron] is present. There is not a statistically significant interaction between CAPT 0.01mM and [iron]. (P = 0.991)

Power of performed test with alpha = 0.0500: for CAPT 0.01mM : 0.0500

Power of performed test with alpha = 0.0500: for [iron] : 1.000

Power of performed test with alpha = 0.0500: for CAPT 0.01mM x [iron] : 0.0500

Least square means for CAPT 0.01mM :

Group	Mean
0.000	13690.417
1.000	13207.833

Std Err of LS Mean = 1125.409

Least square means for [iron] :

Group	Mean
100.000	35143.000
10.000	16752.500
1.000	1851.333
0.000	49.667

Std Err of LS Mean = 1591.568

Least square means for CAPT 0.01mM x [iron] :

Group	Mean
0.000 x 100.000	35655.333
0.000 x 10.000	16697.333
0.000 x 1.000	2322.000
0.000 x 0.000	87.000
1.000 x 100.000	34630.667
1.000 x 10.000	16807.667
1.000 x 1.000	1380.667
1.000 x 0.000	12.333

Std Err of LS Mean = 2250.817

All Pairwise Multiple Comparison Procedures (Tukey Test):

Comparisons for factor: [iron]

Comparison	Diff of Means	p	q	P	P<0.050
100.000 vs. 0.000	35093.333	4	22.050	<0.001	Yes
100.000 vs. 1.000	33291.667	4	20.918	<0.001	Yes
100.000 vs. 10.000	18390.500	4	11.555	<0.001	Yes
10.000 vs. 0.000	16702.833	4	10.495	<0.001	Yes
10.000 vs. 1.000	14901.167	4	9.363	<0.001	Yes
1.000 vs. 0.000	1801.667	4	1.132	0.853	No

A13. Effect of Angiotensin Converting Enzyme (ACE) Inhibition on Macrophage Uptake of Iron Oxide

b. Captopril at 0.1 mM

Two Way Analysis of Variance Wednesday, July 12, 2000, 19:15:23

Source of Variation	DF	SS	MS	F	P
CAPT 0.1mM	1	1443541.500	1443541.500	0.373	0.550
[iron]	3	3468539248.833	1156179749.611	298.661	<0.001
CAPT 0.1mM x [iron]	3	3719204.167	1239734.722	0.320	0.811
Residual	16	61939300.000	3871206.250		
Total	23	3535641294.500	153723534.543		

The difference in the mean values among the different levels of CAPT 0.1mM is not great enough to exclude the possibility that the difference is just due to random sampling variability after allowing for the effects of differences in [iron]. There is not a statistically significant difference (P = 0.550).

The difference in the mean values among the different levels of [iron] is greater than would be expected by chance after allowing for effects of differences in CAPT 0.1mM. There is a statistically significant difference (P = <0.001). To isolate which group(s) differ from the others use a multiple comparison procedure.

The effect of different levels of CAPT 0.1mM does not depend on what level of [iron] is present. There is not a statistically significant interaction between CAPT 0.1mM and [iron]. (P = 0.811)

Power of performed test with alpha = 0.0500: for CAPT 0.1mM : 0.0500

Power of performed test with alpha = 0.0500: for [iron] : 1.000

Power of performed test with alpha = 0.0500: for CAPT 0.1mM x [iron] : 0.0500

Least square means for CAPT 0.1mM :

Group	Mean
0.000	10965.000
1.000	10474.500

Std Err of LS Mean = 567.979

Least square means for [iron] :

Group	Mean
100.000	30124.333
10.000	11325.500
1.000	1414.000
0.000	15.167

Std Err of LS Mean = 803.244

Least square means for CAPT 0.1mM x [iron] :

Group	Mean
0.000 x 100.000	30880.667
0.000 x 10.000	11797.333
0.000 x 1.000	1157.667
0.000 x 0.000	24.333
1.000 x 100.000	29368.000
1.000 x 10.000	10853.667
1.000 x 1.000	1670.333
1.000 x 0.000	6.000

Std Err of LS Mean = 1135.959

All Pairwise Multiple Comparison Procedures (Tukey Test):

Comparisons for factor: [iron]

Comparison	Diff of Means	p	q	P	P<0.050
100.000 vs. 0.000	30109.167	4	37.484	<0.001	Yes
100.000 vs. 1.000	28710.333	4	35.743	<0.001	Yes
100.000 vs. 10.000	18798.833	4	23.404	<0.001	Yes
10.000 vs. 0.000	11310.333	4	14.081	<0.001	Yes
10.000 vs. 1.000	9911.500	4	12.339	<0.001	Yes
1.000 vs. 0.000	1398.833	4	1.741	0.617	No

A14. Effect of Angiotensin Converting Enzyme (ACE) Inhibition on Macrophage Uptake of Iron Oxide

c. Captopril 1.0 mM

Two Way Analysis of Variance

Source of Variation	DF	SS	MS	F	P
CAPT 1.0mM	1	1458294.000	1458294.000	0.102	0.753
[iron]	3	5002019394.167	1667339798.056	117.156	<0.001
CAPT 1.0mM x [iron]	3	7517576.333	2505858.778	0.176	0.911
Residual	16	227707774.000	14231735.875		
Total	23	5238703038.500	227769697.326		

The difference in the mean values among the different levels of CAPT 1.0mM is not great enough to exclude the possibility that the difference is just due to random sampling variability after allowing for the effects of differences in [iron]. There is not a statistically significant difference ($P = 0.753$).

The difference in the mean values among the different levels of [iron] is greater than would be expected by chance after allowing for effects of differences in CAPT 1.0mM. There is a statistically significant difference ($P = <0.001$). To isolate which group(s) differ from the others use a multiple comparison procedure.

The effect of different levels of CAPT 1.0mM does not depend on what level of [iron] is present. There is not a statistically significant interaction between CAPT 1.0mM and [iron]. ($P = 0.911$)

Power of performed test with alpha = 0.0500: for CAPT 1.0mM : 0.0500

Power of performed test with alpha = 0.0500: for [iron] : 1.000

Power of performed test with alpha = 0.0500: for CAPT 1.0mM x [iron] : 0.0500

Least square means for CAPT 1.0mM :

Group	Mean
0.000	11979.750
1.000	12472.750

Std Err of LS Mean = 1089.026

Least square means for [iron] :

Group	Mean
100.000	36200.333
10.000	10851.333
1.000	1838.167
0.000	15.167

Std Err of LS Mean = 1540.116

Least square means for CAPT 1.0mM x [iron] :

Group	Mean
0.000 x 100.000	35884.667
0.000 x 10.000	9749.333
0.000 x 1.000	2264.667
0.000 x 0.000	20.333

A15. Effect of HMG CoA Reductase Inhibition (Mevinolin) on Macrophage Uptake of Iron Oxide

b. Mevinolin (1.0 μM)

Two Way Analysis of Variance

Source of Variation	DF	SS	MS	F	P
HMG 1.0mcM	1	132337977.042	132337977.042	11.208	0.004
[iron]	3	3500330496.458	1166776832.153	98.813	<0.001
HMG 1.0mcM x [iron]	3	213200698.458	71066899.486	6.019	0.006
Residual	16	188927352.000	11807959.500		
Total	23	4034796523.958	175425935.824		

The difference in the mean values among the different levels of HMG 1.0mcM is greater than would be expected by chance after allowing for effects of differences in [iron]. There is a statistically significant difference (P = 0.004). To isolate which group(s) differ from the others use a multiple comparison procedure.

The difference in the mean values among the different levels of [iron] is greater than would be expected by chance after allowing for effects of differences in HMG 1.0mcM. There is a statistically significant difference (P = <0.001). To isolate which group(s) differ from the others use a multiple comparison procedure.

The effect of different levels of HMG 1.0mcM depends on what level of [iron] is present. There is a statistically significant interaction between HMG 1.0mcM and [iron]. (P = 0.006)

Power of performed test with alpha = 0.0500: for HMG 1.0mcM : 0.865
Power of performed test with alpha = 0.0500: for [iron] : 1.000
Power of performed test with alpha = 0.0500: for HMG 1.0mcM x [iron] : 0.837

Least square means for HMG 1.0mcM :

Group	Mean
0.000	13650.000
1.000	8953.583

Std Err of LS Mean = 991.966

Least square means for [iron] :

Group	Mean
100.000	30767.167
10.000	11882.667
1.000	2548.333
0.000	9.000

Std Err of LS Mean = 1402.852

Least square means for HMG 1.0mcM x [iron] :

Group	Mean
0.000 x 100.000	38220.333
0.000 x 10.000	12564.000
0.000 x 1.000	3803.667
0.000 x 0.000	12.000
1.000 x 100.000	23314.000
1.000 x 10.000	11201.333
1.000 x 1.000	1293.000
1.000 x 0.000	6.000

Std Err of LS Mean = 1983.932

All Pairwise Multiple Comparison Procedures (Tukey Test):

Comparisons for factor: HMG 1.0mcM

Comparison	Diff of Means	p	q	P	P<0.050
0.000 vs. 1.000	4696.417	2	4.734	0.004	Yes

Comparisons for factor: [iron]

Comparison	Diff of Means	p	q	P	P<0.050
100.000 vs. 0.000	30758.167	4	21.925	<0.001	Yes
100.000 vs. 1.000	28218.833	4	20.115	<0.001	Yes
100.000 vs. 10.000	18884.500	4	13.462	<0.001	Yes
10.000 vs. 0.000	11873.667	4	8.464	<0.001	Yes
10.000 vs. 1.000	9334.333	4	6.654	0.001	Yes
1.000 vs. 0.000	2539.333	4	1.810	0.588	No

Comparisons for factor: [iron] within 0

Comparison	Diff of Means	p	q	P	P<0.05
100.000 vs. 0.000	38208.333	4	19.259	<0.001	Yes
100.000 vs. 1.000	34416.667	4	17.348	<0.001	Yes
100.000 vs. 10.000	25656.333	4	12.932	<0.001	Yes
10.000 vs. 0.000	12552.000	4	6.327	0.002	Yes
10.000 vs. 1.000	8760.333	4	4.416	0.030	Yes
1.000 vs. 0.000	3791.667	4	1.911	0.546	No

Comparisons for factor: [iron] within 1

Comparison	Diff of Means	p	q	P	P<0.05
100.000 vs. 0.000	23308.000	4	11.748	<0.001	Yes
100.000 vs. 1.000	22021.000	4	11.100	<0.001	Yes
100.000 vs. 10.000	12112.667	4	6.105	0.003	Yes
10.000 vs. 0.000	11195.333	4	5.643	0.005	Yes
10.000 vs. 1.000	9908.333	4	4.994	0.013	Yes
1.000 vs. 0.000	1287.000	4	0.649	0.967	No

Comparisons for factor: HMG 1.0mcM within 100

Comparison	Diff of Means	p	q	P	P<0.05
0.000 vs. 1.000	14906.333	2	7.514	<0.001	Yes

Comparisons for factor: HMG 1.0mcM within 10

Comparison	Diff of Means	p	q	P	P<0.05
0.000 vs. 1.000	1362.667	2	0.687	0.634	No

Comparisons for factor: HMG 1.0mcM within 1

Comparison	Diff of Means	p	q	P	P<0.05
0.000 vs. 1.000	2510.667	2	1.266	0.384	No

Comparisons for factor: HMG 1.0mcM within 0

Comparison	Diff of Means	p	q	P	P<0.05
0.000 vs. 1.000	6.000	2	0.00302	0.998	No

A16. Effect of HMG CoA Reductase Inhibition (Mevinolin) on Macrophage Uptake of Iron Oxide

b. Mevinolin (17.5 μM)

Two Way Analysis of Variance

Source of Variation	DF	SS	MS	F	P
HMG	1	283064622.042	283064622.042	26.913	<0.001
[iron2]	3	2449715493.458	816571831.153	77.637	<0.001
HMG x [iron2]	3	496210450.792	165403483.597	15.726	<0.001
Residual	16	168285499.333	10517843.708		
Total	23	3397276065.625	147707655.027		

The difference in the mean values among the different levels of HMG is greater than would be expected by chance after allowing for effects of differences in [iron2]. There is a statistically significant difference (P = <0.001). To isolate which group(s) differ from the others use a multiple comparison procedure.

The difference in the mean values among the different levels of [iron2] is greater than would be expected by chance after allowing for effects of differences in HMG. There is a statistically significant difference (P = <0.001). To isolate which group(s) differ from the others use a multiple comparison procedure.

The effect of different levels of HMG depends on what level of [iron2] is present. There is a statistically significant interaction between HMG and [iron2]. (P = <0.001)

Power of performed test with alpha = 0.0500: for HMG : 0.999
Power of performed test with alpha = 0.0500: for [iron2] : 1.000
Power of performed test with alpha = 0.0500: for HMG x [iron2] : 1.000

Least square means for HMG :

Group	Mean
0.000	10385.917

1.000	3517.333

Std Err of LS Mean = 936.209

Least square means for [iron2] :

Group	Mean
100.000	24288.000
10.000	3416.167
1.000	95.333
0.000	7.000

Std Err of LS Mean = 1323.999

Least square means for HMG x [iron2] :

Group	Mean
0.000 x 100.000	35391.000
0.000 x 10.000	5985.000
0.000 x 1.000	155.667
0.000 x 0.000	12.000
1.000 x 100.000	13185.000
1.000 x 10.000	847.333
1.000 x 1.000	35.000
1.000 x 0.000	2.000

Std Err of LS Mean = 1872.418

All Pairwise Multiple Comparison Procedures (Tukey Test):

Comparisons for factor: HMG

Comparison	Diff of Means	p	q	P	P<0.050
0.000 vs. 1.000	6868.583	2	7.337	<0.001	Yes

Comparisons for factor: [iron2]

Comparison	Diff of Means	p	q	P	P<0.050
100.000 vs. 0.000	24281.000	4	18.339	<0.001	Yes
100.000 vs. 1.000	24192.667	4	18.272	<0.001	Yes
100.000 vs. 10.000	20871.833	4	15.764	<0.001	Yes
10.000 vs. 0.000	3409.167	4	2.575	0.300	No
10.000 vs. 1.000	3320.833	4	2.508	0.321	Do Not Test
1.000 vs. 0.000	88.333	4	0.0667	1.000	Do Not Test

Comparisons for factor: [iron2] within 0

Comparison	Diff of Means	p	q	P	P<0.05
100.000 vs. 0.000	35379.000	4	18.895	<0.001	Yes
100.000 vs. 1.000	35235.333	4	18.818	<0.001	Yes
100.000 vs. 10.000	29406.000	4	15.705	<0.001	Yes

10.000 vs. 0.000	5973.000	4	3.190	0.151	No
10.000 vs. 1.000	5829.333	4	3.113	0.165	Do Not Test
1.000 vs. 0.000	143.667	4	0.0767	1.000	Do Not Test

Comparisons for factor: [iron2] within 1

Comparison	Diff of Means	p	q	P	P<0.05
100.000 vs. 0.000	13183.000	4	7.041	<0.001	Yes
100.000 vs. 1.000	13150.000	4	7.023	<0.001	Yes
100.000 vs. 10.000	12337.667	4	6.589	0.001	Yes
10.000 vs. 0.000	845.333	4	0.451	0.988	No
10.000 vs. 1.000	812.333	4	0.434	0.990	Do Not Test
1.000 vs. 0.000	33.000	4	0.0176	1.000	Do Not Test

Comparisons for factor: HMG within 100

Comparison	Diff of Means	p	q	P	P<0.05
0.000 vs. 1.000	22206.000	2	11.860	<0.001	Yes

Comparisons for factor: HMG within 10

Comparison	Diff of Means	p	q	P	P<0.05
0.000 vs. 1.000	5137.667	2	2.744	0.070	No

Comparisons for factor: HMG within 1

Comparison	Diff of Means	p	q	P	P<0.05
0.000 vs. 1.000	120.667	2	0.0644	0.964	No

Comparisons for factor: HMG within 0

Comparison	Diff of Means	p	q	P	P<0.05
0.000 vs. 1.000	10.000	2	0.00534	0.997	No

A17. Effect of HMG CoA Reductase Inhibition (Mevinolin) on Macrophage Uptake of Iron Oxide

c. Mevinolin (17.5 μM) Data corrected for cell density

Two Way Analysis of Variance

Source of Variation	DF	SS	MS	F	P
HMG	1	118368107.011	118368107.011	6.623	0.020
[iron2]	3	3471907563.896	1157302521.299	64.753	<0.001
HMG x [iron2]	3	170484041.790	56828013.930	3.180	0.053
Residual	16	285963005.284	17872687.830		
Total	23	4046722717.981	175944465.999		

The difference in the mean values among the different levels of HMG is greater than would be expected by chance after allowing for effects of differences in [iron2]. There is a statistically significant difference (P = 0.020). To isolate which group(s) differ from the others use a multiple comparison procedure.

The difference in the mean values among the different levels of [iron2] is greater than would be expected by chance after allowing for effects of differences in HMG. There is a statistically significant difference (P = <0.001). To isolate which group(s) differ from the others use a multiple comparison procedure.

The effect of different levels of HMG does not depend on what level of [iron2] is present. There is not a statistically significant interaction between HMG and [iron2]. (P = 0.053)

Power of performed test with alpha = 0.0500: for HMG : 0.604

Power of performed test with alpha = 0.0500: for [iron2] : 1.000

Power of performed test with alpha = 0.0500: for HMG x [iron2] : 0.446

Least square means for HMG :

Group	Mean
0.000	10385.917
1.000	5944.293

Std Err of LS Mean = 1220.406

Least square means for [iron2] :

Group	Mean
100.000	28836.825
10.000	3708.497
0.000	7.690
1.000	107.408

Std Err of LS Mean = 1725.915

Least square means for HMG x [iron2] :

Group	Mean
0.000 x 100.000	35391.000
0.000 x 10.000	5985.000
0.000 x 0.000	12.000
0.000 x 1.000	155.667
1.000 x 100.000	22282.650
1.000 x 10.000	1431.993
1.000 x 0.000	3.380
1.000 x 1.000	59.150
1.000 x 0.000	3.380
1.000 x 1.000	59.150

Std Err of LS Mean = 2440.812

All Pairwise Multiple Comparison Procedures (Tukey Test):

Comparisons for factor: HMG 17.5 □M (corrected for cell density)

Comparison	Diff of Means	p	q	P	P<0.050
0.000 vs. 1.000	4441.623	2	3.639	0.021	Yes

Comparisons for factor: [iron2]

Comparison	Diff of Means	p	q	P	P<0.050
100.000 vs. 0.000	28829.135	4	16.704	<0.001	Yes
100.000 vs. 1.000	28729.417	4	16.646	<0.001	Yes
100.000 vs. 10.000	25128.328	4	14.559	<0.001	Yes
10.000 vs. 0.000	3700.807	4	2.144	0.451	No
10.000 vs. 1.000	3601.088	4	2.086	0.474	Do Not Test
1.000 vs. 0.000	99.718	4	0.0578	1.000	Do Not Test

Comparisons for factor: [iron2] within 0

Comparison	Diff of Means	p	q	P	P<0.05
100.000 vs. 0.000	35379.000	4	14.495	<0.001	Yes
100.000 vs. 1.000	35235.333	4	14.436	<0.001	Yes
100.000 vs. 10.000	29406.000	4	12.048	<0.001	Yes
10.000 vs. 0.000	5973.000	4	2.447	0.341	No
10.000 vs. 1.000	5829.333	4	2.388	0.361	Do Not Test
1.000 vs. 0.000	143.667	4	0.0589	1.000	Do Not Test

Comparisons for factor: [iron2] within 1

Comparison	Diff of Means	p	q	P	P<0.05
100.000 vs. 0.000	22279.270	4	9.128	<0.001	Yes
100.000 vs. 1.000	22223.500	4	9.105	<0.001	Yes
100.000 vs. 10.000	20850.657	4	8.543	<0.001	Yes
10.000 vs. 0.000	1428.613	4	0.585	0.975	No
10.000 vs. 1.000	1372.843	4	0.562	0.978	Do Not Test
1.000 vs. 0.000	55.770	4	0.0228	1.000	Do Not Test

Comparisons for factor: HMG within 100

Comparison	Diff of Means	p	q	P	P<0.05
0.000 vs. 1.000	13108.350	2	5.370	0.002	Yes

Comparisons for factor: HMG within 10

Comparison	Diff of Means	p	q	P	P<0.05
0.000 vs. 1.000	4553.007	2	1.865	0.206	No

Comparisons for factor: HMG within 0

Comparison	Diff of Means	p	q	P	P<0.05
0.000 vs. 1.000	8.620	2	0.00353	0.998	No

Cited References

[1] Ross R. Atherosclerosis-an inflammatory disease. N Engl J Med ;340:115-126,1999.

[2] Libby P, Ross R, Cytokines and growth regulatory molecules. In: Fuster V, Ross R, Topol E, eds. Atherosclerosis and Coronary Artery Disease. Philadelphia, Pa: Lippincott-Raven; 585-594,1996.

[3] Hansson GK, Regulation of immune mechanisms in atherosclerosis. Ann N Y Acad Sci.;947:157-65, 2001.

[4] Gotto AM. Insights on treating an over-the-counter-type subgroup: data from the Air Force/Texas Coronary Atherosclerosis Prevention Study Population. Am J Cardiol;85(12A):8E-14E, 2000.

[5] Hironosuke S, Masanori A, Hill CC, Weiss D, Taylor WR, Libby P, Lee RT. Biomechanical strain induces class A scavenger receptor expression in human monocyte/macrophages and THP-1 cells: a potential mechanism of increased atherosclerosis in hypertension. Circulation,104:109-114,2001.

[6] Davies PF, Polacek DC, Shi C, Helmke BP. The convergence of haemodynamics, genomics, and endothelial structure in studies of the focal origin of atherosclerosis. Biorheology;39(3-4):299-306, 2002.

[7] Libby P, Ridker PM, Maseri A. Inflammation and Atherosclerosis. Circulation;105:1135-1143, 2002.

[8] Luster, A.D. Chemokines – chemotactic cytokines that mediate inflammation. N Engl J Med 338, 436-445, 1998.

[9] Reape TJ, Groot PH. Chemokines and atherosclerosis. Atherosclerosis;147(2):213-25, 1999.

[10] Flanagan AM, Lader CS. Update on the biologic effects of macrophage colony-stimulating factor. Curr Opin Hematol;5(3):181-5, 1998.

[11] Fisher B, von Knethen A, Brune B. Dualism of oxidized lipoproteins in provoking and attenuating the oxidative burst in macrophages: role of peroxisome proliferator-activated receptor-gamma. J Immunol;168:2828-34, 2002.

[12] Stary HC. Lipid and macrophage accumulations in arteries of children and the development of atherosclerosis. AJCN. 72:1297S-1306S, 2000.

[13] Stary HC, Chandler AB, Glagov S, Guyton JR, Insull W Jr, Rosenfeld ME, Schaffer SA Schwartz CJ, Wagner WD, Wissler RW. A definition of initial, fatty streak, and intermediate lesions of atherosclerosis: a report from the Committee on vascular lesions of the Council on Atherosclerosis, American heart Association. Artioscler Thromb; 14:840-856, 1994.

[14] Stary HC, Chandler AB, Dinsmore RE, Fuster V, Glagov S, Insull W Jr, Rosenfeld ME, Schwartz CJ, wagner WD, Wissler RW. A definition of advanced types of atherosclerotic lesions and a histological classification of atherosclerosis: a report from the Committee on vascular lesions of the Council on Atherosclerosis, American heart Association. Artioscler Thromb; 15:1512-1531, 1995.

[15] Hansson GK, Libby P, Schonbeck U, Yan ZQ. Innate and adaptive immunity in the pathogenesis of atherosclerosis. Circ Res 23;91(4):281-91, 2002.

[16] Galis ZS et al. Increased expression of matrix metalloprotienases and matrix degradingactivity in vulnerable regions of human atherosclerotic plaques. J Clin Invest. ;94:2493-2503, 1994.

[17] Price SJ, Greaves DR, Watkins H. Identification of novel, functional genetic variants in the human matrix metalloprotienase-2 gene: role of Sp1 in allele-specific transcriptional regulation. J Biol Chem.;276:7549-7558, 2001.

[18] Carmeliet P, Collen D. Transgenic mouse models in angiogenisis and cardiovascular disease. J Pathol.;190:387-405, 2000.

[19] Weiss L. editor, Cell and Tissue Biology: A textbook of histology. Urban & Schwarzenberg Publisher, Baltimore, 1988.

[20] Buys SS, Kaplan J. Effect of phagocytosis on receptor distribution and endocytoyic activity in macrophages. J Cell Physiol.;131:442-9,1987.

[21] Peisor L, Gordon S. The function of scavenger receptors expressed by macrophages and their role in the regulation of inflammation. Microbes Infect;3:149-159,2001.

[22] L. Peiser, P.J. Gough, T. Kodama and S. Gordon. Macrophage class A scavenger receptor-mediated phagocytosis of E. Coli: Role of cell heterogeneity, microbial strain and culture conditions in vitro. Inf. & Immunity 68: (4) 1953-1963, 2000.

[23] Goldstein JL e al. Binding site on macrophages that mediates uptake and degradation of acyetylated low density lipoprotein, producing massive cholesterol deposition. Proc Natl Acad Sci;76:333-337, 1979.

[24] Endocytosis. Edited by Ira Pastan and Mark C. Willingham, Plenum Press, N.Y., 1985.

[25] Castonguay LA, Treasurywala AM, Caulfield TJ, Jaeger EP, Keller KE. Prediction of q-values and conformations of gadolinium chelates for magnetic resonance imaging. Bioconjugate Chem;10:958-964, 1999.

[26] Brasch CB. Principales of MRI contrast enhancement. From "medical magnetic resonance", editors: Budinger TF and Margulis AR. , Society of Magnetic Resonance, 1988.

[27] Bloembergen N, Purcell EM, Pound RV. Relaxation effects in nuclear magnetic resonance absorption. Phys Rev; 73:679-710, 1948.

[28] Bean CP, Livingston JD. Superparamagnetism. J Appl Physiol;30:120S,1959.

[29] Feridex® Package insert. Berlex laboratoies, Wayne NJ, 19xx.

[30] Wang Y-XJ, Hussain SM, Krestin GP. Superparamagnetic iron oxide contrast agents: physiochemical characteristics and applications in MR imaging. Eur radiol;11:2319-2331, 2001.

[20] Weissleder R, Stark D, Engelstad BL et al. Superparamagnetic iron oxide: Pharmacokinetics and toxicity. AJR;152:167-173, 1989.

[32] Mukherjee S, Ghosh RN, Maxfield FR. Endocytosis. Physiol Rev; Physiol Rev;77(3):759-803, 1997.

[33] Skotland T, Sontum PC, Oulie I. In vitro stability analysis as a model for metabolism of ferromagnetic particles, a contrast agent for magnetic resonance imaging. J Pharm Biomed Anal;28:323-329, 2002.

[34] Jung CW. Surface properties of superparamagnetic iron oxide MR contrast agents: Ferumoxides, ferumoxtran, ferumoxsil. J Mag Reson Imaging;13:675-691, 1995.

[35] Protein solutions website: http://www.protein-solutions.com/psi_books/psi_books.htm

[36] Brant DA, Burton BA. The configurational statistics of pullulan and some related glucans. ACS. Symp. Ser. (Solution Properties of Polysaccharides) 150:81-99;1981.

[37] Jung CW, Jacobs P. Physical and chemical properties of superparamagnetic iron oxide MR contrast agents: ferumoxides, ferumoxtran, ferumoxsil. Magn. Reson. Imaging;13:661-674, 1995.

[38] Gunther WHH, Fujii DK, Keller KE, Black CDV, Desai VC, Beeber M, Wellons J, Fahlvik AK, Naevested A. Superparamagnetic contrast media coated with starch and polyalkylene oxides. United States Patent # 6,123,920, 2000.

[39] Palmacci S, Josephson. 1993. Synthesis of polysaccharide covered superparamagnetic oxide colloids (example1). U.S. Patent 5,262,176. 16 November 1993.

[40] Jacobs P. particle sizing, definition and overview. Unpublished white paper, Advanced Magnetics, Inc., 2000.

[41] Guretzki HJ, Gerbitz KD, Olgemoller B, Schleicher E. Atherogenic levels of low density lipoprotein alter the permeability and composition of the endothelial barrier. Atherosclerosis;107:15-24, 1994.

[42] Van berkel TJ, Van Eck M, Herijgers N, Fluiter K, Nion S. Scavenger receptor classes A and B. their roles in atherosclerosis and the metabolism of modified LDL and HDL. Ann NY Acad Sci;902:113-126,2000.

[43] Shirai H, Murakami T, Yamada Y, Doi T, Hamakubo T, Kodama. Structure and function of type I and II macrophage scavenger receptors. Mech Ageing Dev;111:107-121,1999.

[44] Zingg J-M, Ricciarelli R, Azzi . Scavenger receptor regulation and atherosclerosis. Biofactors ;11:189-2000.

[45] Van Es LA, Daha MR. Factors influencing the endocytosis of immune complexes. Adv Nephrol Necker Hosp;13:341-367, 1984.

[46] Pratten MK, Lloyd JB. Pinocytosis and phagocytosis: the effect of size of a particle substrate on its mode of capture by rat peritoneal macrophages cultured in vitro. Biochim Biophys Acta ; 881:307-313, 1986.

[47] Montainer LJ, da Silva RP, Sun J, Sutterwala S, Hollinshead M, Vaux D, Gordon S. Type 1 and type 2 cytokine regulation of macrophage endocytosis: differential activation by IL-4/IL-13 as opposed to IFN-γ or IL-10. J Immunol;162:4606-4613, 1999.

[48] Moore A, Weisslender R, Bogdanov A. Uptake of dextran-coated monocrystalline iron oxides in tumor cells and macrophages. J Magn reson Imaging;7:1140-1145, 1997.

[49] Bogdanov A, Papisov M, Weisslender R, Shen T, Brady TJ. Opsonization of dextran-stabilized iron oxides with plasma proteins. Society of magnetic resonance in Medicine, Book of abstracts,;1:864, 1992.

[50] Ralph P, Prichard J, Cohn M. Reticulum cell sarcoma. An effector cell in antibody-dependent cell-mediated immunity. J Immunol, 114:898-905, 1975.

[51] Faghihi-Shirazi M, Aronson NN, Dean RT. Temperature dependence of certain integrated membrane functions in macrophages. J Cell Sci;57:115-127, 1982.

[52] Artursson P, Arro E, Edman P, Ericsson JLE, Sjoholm I. Biodegradable microspheres. V: stimulation of macrophages with microparticles made of various polysacchaeides. J Pharm Sci;76:127-133, 1987.

[53] Aderem A, Underhill DM. Mechanism of phagocytosis in macrophages. AR Immunol;17:593-623,1999.

[54] Paoletti R, Bellosta S, Bernini F. Pharmacological control of phagocytic function: inhibition of cholesterol accumulation. Ann NY Acad Sci;15:322-329,1997.

[55] Kowala MC, Grove RI, Aberg G. Inhibitors of angiotensin converting enzyme decrease early atherosclerosis in hyperlipidemic hamsters. Fosinopril reduces plasma cholesterol and captopril inhibits macrophage-foam cell accumulation independently of blood pressure and plasma lipids. Atherosclerosis;108:61-72, 1994.

[56] Draude G, Lorenz RL. TGF-β downregulates CD36 and scavenger receptor A but upregulates LOX-1 in human macrophages. AJP;278:H1042-H1048, 2000.

[57] Aikawa M, Rabkin E, Sugiyama S, Voglic SJ, Fukumoto Y, Furukawa Y, Shiomi M, Schoen FJ, Libby P. An HMG-CoA reductase inhibitor, cervastatin, supresses growth of macrophages expressing matrix metalloproteinases and tissue factor in vivo and in vitro. Circulation;103:276-283, 2001.

[58] Bernini F, Scurati N, Bonfadini G, Fumagalli R. HMG-CoA reductase inhibitors reduce acetyl LDL endocytosis in mouse peritoneal macrophages. Arterioscler Thromb; 15:1352-1358, 1995.

[59] Umetani N, Kanayama Y, Okamura M, Negoro N, Takeda T. Lovastatin inhibits gene expression of type-I scavenger receptor in THP-1 human macrophages. Biochem Biophys Acta;1303:199-206,1996.

[60] Heyek T, Aviram M, Heinrich R, Sakhnini E, keidar S. Losartan inhibits cellular uptake of oxidized LDL by monocyte-macrophages from hypercholesterolemic patients. Biochem Biophys res Commun ;273:417-420,2000.

[61] Schmitz SA, Coupland SE, Gust R, Winterhalten S, Wagner S, Kresse M, Semmler W, Wolf K-J. Superparamagnetic iron oxide-enhanced MRI of atherosclerotic plaques in Watanabe Hereditable Hyperlipidemic Rrabbits. Invest Radiol;35:460-471,2000.

[62] Guretzki HJ, Gerbitz KD, Olgemoller B, Schleicher E. Atherogenic levels of low density lipoprotein alter the permeability and composition of the endothelial barrier. Atherosclerosis;107:15-24, 1994.

[63] Ruehm SG, Corot C, Vogt P, Kilb S, Debatin JF. Magnetic resonance imaging of atherosclerotic plaque with ultrasmall superparamagnetic particles of iron oxide in hyperlipidemic rabbits. Circulation;103:415-422, 2001.

[64] Fahlvik AK, Artursson P, Edman P. Magnetic starch microspheres: interactions of a microsphere MR contrast medium with macrophages in vitro. International Journal of Phamaceutics;65:249-259,1990.

[65] Buys SS, Kaplan J. Effect of phagocytosis on receptor distribution and endocytoyic activity in macrophages. J Cell Physiol. 1987;131:442-9.

[66] Paulnock DM editor, Macrophages: a practical approach. University of Wisconsin Medical School, 2000.

[67] Weiss L. editor, Cell and Tissue Biology: A textbook of histology. Urban & Schwarzenberg Publisher, Baltimore, 1988.

[68] Bogdanov A, Papisov, Weisslender R, Shen T, Brady TJ. (Abstract) 11th Annual Society of Magnetic Resonance in medicine Meeting, 1;864, 1992.

[69] Bogdanova A, Nossiff N, Bogdanov A, Brady TJ. Weisslender R. (Abstract) Proceedings of the Society of Magnetic Resonance, 2;931, 1994.

[70] Van berkel TJ, Van Eck M, Herijgers N, Fluiter K, Nion S. Scavenger receptor classes A and B. their roles in atherosclerosis and the metabolism of modified LDL and HDL. Ann NY Acad Sci;902:113-126,2000.

[71] Shirai H, Murakami T, Yamada Y, Doi T, Hamakubo T, Kodama. Structure and function of type I and II macrophage scavenger receptors. Mech Ageing Dev;111:107-121,1999.

[72] Lerman LS. Spectral properties of acridine orange in complexes with nucleic acids. J Molec Biol;3:18-31, 1961.

[64] Cabec V, Cols C, Maridonneau-Parini I. Nonopsonic phagocytosis of zymosan and mycobacterium kansasii by CR3 (CD11b/CD18) involves distinct molecular

determinants and is not coupled with NADPH oxidase activation. Infect Immun;68:4736-4745, 2000.

[74] Gordon, http://dunn1.path.ox.ac.uk/-cholt/sgCytoMacro.html

[75] Swanson B, Yirinec B, Silverstein S. Phorbol esters and horse radish peroxidase stimulates pinocytosis and redirect the flow of pinocytosed fluid in macrophages. J. Cell Biol.;100:851, 1985.

[76] Boehm, U., Klamp, T., Groot, M. & Howard, J.C. Cellular responses to interferon-γ. *Annu. Rev*. Immunol*.* 15, 749-795, 1997.

[77] Stopeck AT, Nicholson AC, Mancini FP, Hajjar DP. Cytokine regulation of low density lipoprotein receptor gene transcription. Jbiol Chem;268:17489-17494,1993.

[78] Inagaki Y, Yamagishi S, Amano S, Okamoto T, Koga K, Makita Z. Interferon-g-induced apoptosis and activation of THP-1 macrophages. Life Sci;71:2499-2580, 2002.

[79] Ikeda U, Matsui K, Murakami Y, Shimada K. Monocyte chemoattractant protein-1 and coronary artery disease. Clin Cardiol;25:143-147, 2002.

[80] Schulze E, Ferrucci JT, Poss K, Lapointe L, Bogdanova A, Weissleder R. Cellular uptake and trafficking of a prototypical magnetic iron oxide label in vitro. Invest Radiol; 30:604-10,1995.

[81] Keider S. Angiotensin, LDL peroxidation and atherosclerosis. Life Sci;63(1):1-11, 1998.

[82] Hayek T, Kaplan M, Raz A, Keidar A, Coleman R Aviram M. Ramipril administration to atherosclerotic mice reduces oxidized low-density lipoprotein uptake by their macrophages and blocks the progression of atherosclerosis. Atherosclerosis;161:65-74, 2002.

[83] Warnholtz A, Nickening G, Schultz E, Marcharzina R, Brasen JH, Skatchov M et al. Increased NADH-oxidase mediated super-oxide production in the earlt stages of atherosclerosis:evidences for involvement of the rennin-angiotensin system. Circulation;20:2027-2033, 1999.

[84] Sakai M, Kobori S, Miyazaki A, Horiuchi S. Macrophage proliferation in atherosclerosis. Curr Opin Lipidol;11:503-9,2000.

[85] Zingg J-M, Ricciarelli R, Azzi A. Scanenger receptor regulation and atherosclerosis. Biofactors;11:189-200, 2000.

[86] Umetani N, Kanayama Y, Okamura M, Negoro N, Takeda T. Lovastatin inhibits gene expression of type-1 scavenger receptor in THP-1 human macrophages. Biochim. Biophys. Acta;1303:199-206, 1996.

[87] Bellosta S, Ferri N, Arnaboldi L, Bernini F, Paoletti R, Corsini A. Pleitropic effects of statins in atherosclerosis and diabetes. Diabetes Care;23;B72-B78, 2000.

[88] Bernini F, Scurati N, Bonfadini G, Fumagalli R. HMG-CoA reductase inhibitors reduce acetyl LDL endocytosis in mouse peritoneal macrophages. Arterioscler. Thromb. ;15:1352-1358, 1995.

[89] Dodd SJ, Williams M, Suhan JP, Willams DS, Koretsky AP, Ho C. Detection of single mammalian cells by high-resolution magnetic resonance imaging. Biophysical J;76:103-109,1999.

[90] Schultz JF, Bell JD, Goldstein RM, Kuhn JA, McCarty TM. Hepatic tumor imaging using iron oxide MRI: Comparison with computed tomography, clinical imact, and cost analysis. Ann Surg Oncol;6:691-698, 1999.

[91] Crichton RR, Wilmet S, Legssyer R, Ward RJ. Molecular and cellular mechanisms of iron homeostasis and toxicity in mammalian cells. J Inorg Biochem;91:9-18, 2002.

[92] Legssyer R, Ward R, Crichton J, Boeleart J. Effect of chronic chloroquine administration on iron loading in the liver and reticuloendothelial system and on oxidative responses by the alveolar macrophages. J Biochem Pharmacol;57:907-911, 1999.

[93] Higuchi S, Tanimato A, Arima N, Xu H, Murata Y, Hamada T, Makisima K, Sasaguri Y. Effects of histamine and interleukin-4 synthesized in the arterial intima on phagocytosis by monocytes/macrophages in relation to atherosclerosis. FEBS Letters;505:217-222, 2001.